THE REGULATION AND FUNCTION OF MAJOR HISTOCOMPATIBILITY COMPLEX II ON LUNG TYPE II ALVEOLAR CELLS

Sushila Ann Toulmin

A DISSERTATION

in

Immunology

Presented to the Faculties of the University of Pennsylvania

in

Partial Fulfillment of the Requirements for the

Degree of Doctor of Philosophy

2020

Supervisor of Dissertation

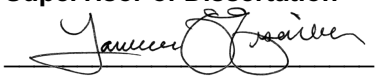

Laurence C. Eisenlohr, V.M.D., Ph.D.

Professor of Pathology and Laboratory Medicine

Graduate Group Chairperson

David Michael Allman, Ph.D.

Professor of Pathology and Laboratory Medicine

Dissertation Committee

Scott E. Hensley, Ph.D., Associate Professor of Microbiology

Carolina B. Lopez, Ph.D., Professor of Molecular Microbiology

Sunny Shin, Ph.D., Associate Professor of Microbiology

G. Scott Worthen, M.D., Professor of Pediatrics

ACKNOWLEDGMENTS

The work in this dissertation was only made possible by the contributions of countless others, who provided me with invaluable personal support and scientific guidance over the years.

First and foremost, I would like to thank my family, whose support from across the country and world has always been a constant grounding force. In particular, I would like to express my most sincere and heartfelt gratitude to my parents; without their lifelong unconditional love and support, this thesis would never have been possible. I am especially grateful to my mum, Pragna, for all of her pride in me and my work, and for being an incredible example of strength and resilience. I am also extremely thankful to my sister Asha, for always being there for me so completely in the way only a sister can, during my lowest lows and my highest highs. Thank you also to my sister Alice, for always reminding me to be good to myself in the midst of all of the hard work. And a special thank you to Tómas Andersen, for his love and support throughout medical and graduate school, and for always believing in me and encouraging me to keep going when I didn't think I could.

I am also deeply grateful for the support and friendship of my colleagues over the years. To my 2014 entering MSTP/IGG classmates Ruth, Emma, and Samir, thank you for genuinely understanding all of the ins and outs of this journey. In particular, to Ruth, thank you for our countless early morning science/life/exercise sessions that helped me keep perspective throughout. To the fantastic members of Eisenlohr laboratory, you are truly a special group; thank you for making lab such a warm place and for being a second family to me. In particular, I am deeply indebted to Chaitali Bhadiadra, who single handedly made all of the *in vivo* studies possible,

and whose energy and empathy fueled me at a time when I needed it most. I am also extremely thankful for the friendship and mentorship of Mike Hogan, whose intelligence and enthusiasm for research were an infectious and invaluable part of my scientific training in the lab.

Innumerable people within the Penn immunology, virology, and lung biology communities helped me to think about and gain a deeper understanding of this work. In particular, I am grateful to Andrew Paris and Scott Worthen, for helping me get started in the lung world, and for providing valuable insight throughout.

I am also so fortunate to have had numerous mentor figures who have contributed greatly to my scientific development. I am grateful to my thesis committee members for their invaluable feedback and encouragement over the last three years. I would like to especially thank Scott Hensley, whose continued support and mentorship since my first lab rotation at Penn has made a profound impact on my training. I am also deeply grateful to Steve Migueles, for inspiring me to become a physician-scientist, and for his guidance and friendship during my time at the NIH and beyond.

Lastly, I cannot imagine having navigated this work without the incredible mentorship of Ike Eisenlohr. To Ike, thank you for sharing your scientific philosophy and so much of your time with me, and for your endlessly bright outlook that invariably outshone my gloomy one. Thank you for your enthusiasm for this work, your constant encouragement, and for calling me out when I needed it while always having my back. You are a fantastic scientist and a truly good human being, and I am so lucky to have learned from you.

ABSTRACT

THE REGULATION AND FUNCTION OF MAJOR HISTOCOMPATIBILITY COMPLEX II ON LUNG TYPE II ALVEOLAR CELLS

Sushila A. Toulmin

Laurence C. Eisenlohr

$CD4^+$ T cells are critical regulators of adaptive immune responses. $CD4^+$ T cell activation is initiated and shaped by $CD4^+$ T cell receptor (TCR) recognition of cognate peptide/major histocompatibility complex II (MHCII) complexes on the surface of antigen presenting cells (APCs). MHCII presentation of antigenic peptides has historically been viewed as a property restricted to a subset of immune cells deemed "professional" APCs – dendritic cells, macrophages, and B cells – that constitutively express MHCII. However, recently it has been demonstrated that various other immune and non-immune cell types can express MHCII, and that these "atypical" APCs make essential contributions to the regulation of $CD4^+$ T cell responses in the periphery. In the distal lung, type II alveolar cells (AT2s), epithelial cells whose main functions are to produce surfactant and facilitate lung regeneration, have also been reported to express MHCII at homeostasis. However, the contribution of AT2 MHCII to lung adaptive immune responses, and the factors driving its expression, are unknown. Here we explore both the regulation and function of MHCII on AT2s. First, we demonstrate that AT2s constitutively express high levels of MHCII in a manner that does not require induction by inflammatory stimuli, making them unique among all other previously studied non-immune cells. Using mouse models, we also

demonstrate that AT2 MHCII participates in lung immune responses *in vivo.* At homeostasis, aged mice lacking AT2 MHCII have lower frequencies of lung T cells with an antigen-experienced phenotype. Furthermore, following respiratory viral infection, the absence of AT2 MHCII results in increased morbidity and mortality. In both of these settings, the contribution of AT2 MHCII is moderate. Consistent with this more modest impact, we find that AT2s demonstrate a globally limited capacity to present antigen via MHCII. We propose that the combination of high MHCII expression with restrained MHCII antigen presentation enables AT2s to contribute to lung immune responses in a more measured fashion, preventing excessive inflammation that would be damaging to the delicate gas-exchange lung parenchyma.

TABLE OF CONTENTS

ACKNOWLEDGMENTS II

ABSTRACT IV

LIST OF TABLES VIII

LIST OF FIGURES IX

LIST OF KEY ABBREVIATIONS XII

CHAPTER 1: GENERAL INTRODUCTION 1

1.1 Introduction to the immune system 1

1.2 T cell responses in antiviral adaptive immunity 3

1.3 The T cell – APC interaction 4

1.4 Pathways of MHCII antigen processing and presentation 5

1.5 The regulation of MHCII expression 8

1.6 The professional APCs and the requirements of an APC 10

1.7 Non-professional MHCII-expressing APCs 14

1.8 Functions of type II alveolar cells in lung physiology 17

1.9 The lower respiratory tract immune system 19

1.10 Type II alveolar cells in lung innate and adaptive immune responses 21

1.11 Goals for the thesis 24

CHAPTER 2: TYPE II ALVEOLAR CELLS CONSTITUTIVELY EXPRESS MAJOR HISTOCOMPATIBILITY COMPLEX II INDEPENDENT OF CONVENTIONAL INFLAMMATORY MEDIATORS 26

2.1 Introduction 27

2.2 Results 29

2.3 Discussion 39

CHAPTER 3: TYPE II ALVEOLAR CELL MAJOR HISTOCOMPATIBILITY COMPLEX II CONTRIBUTES MODESTLY TO LUNG T CELL HOMEOSTASIS AND PROTECTION DURING RESPIRATORY VIRAL INFECTION..... 43

3.1 Introduction 44

3.2 Results 46

3.3 Discussion 62

CHAPTER 4: TYPE II ALVEOLAR CELLS EXHIBIT RESTRAINED MAJOR HISTOCOMPATIBILITY COMPLEX II ANTIGEN PRESENTATION..... 72

4.1 Introduction 73

4.2 Results 74

4.3 Discussion 82

CHAPTER 5: DISCUSSION AND FUTURE DIRECTIONS..... 86

5.1 Constitutive MHCII expression paired with restrained antigen presentation: a model for AT2 MHCII function tailored to the unique requirements of the lung 88

5.2 Possible contributors to poor MHCII antigen presentation by AT2s..... 89

5.3 Drivers of constitutive MHCII expression by AT2s 92

5.4 Polarity of MHCII expression by AT2s 94

5.5 The possibility of novel functions of MHCII on AT2s..... 95

5.6 The potential role of AT2 MHCII in other immune settings 97

5.7 Concluding remarks: why do AT2s express MHCII?..... 105

CHAPTER 6: MATERIALS AND METHODS 107

REFERENCES 128

LIST OF TABLES

CHAPTER 3

Table 3.1: Mixed-effects model analysis results for weight loss after IAV infection. . 61

Table 3.2: Mixed-effects model analysis results for weight loss after SeV infection. 61

CHAPTER 5

Table 5.1: MHCII and invariant chain transcripts are among the most highly abundant in AT2s. 96

CHAPTER 6

Table 6.1: Flow cytometry antibodies used for all studies..... 127

LIST OF FIGURES

CHAPTER 1

Figure 1.1: Invariant chain deficient mouse DCs express MHCII..... 12

CHAPTER 2

Figure 2.1: Mouse and human AT2s express MHCII at homeostasis..... 29

Figure 2.2: AT2s express high levels of MHCII similar to professional APCs..... 30

Figure 2.3: AT2s synthesize their own MHCII transcript and protein..... 30

Figure 2.4: AT2 MHCII expression is driven by CIITA pIV..... 31

Figure 2.5: AT2 MHCII expression does not require canonical IFNγ inflammation... 32

Figure 2.6: AT2s express MHCII independent of a variety of broad innate and adaptive inflammatory mediators..... 33

Figure 2.7: AT2s are capable of extracellular antigen uptake and degradation..... 34

Figure 2.8: AT2s express invariant chain protein..... 35

Figure 2.9: AT2s express functional H2M protein..... 36

Figure 2.10: AT2s express exclusively H2Mβ1 transcripts, not H2Mβ2, at homeostasis..... 37

Figure 2.11: AT2s express noncanonical costimulatory molecule ICAM-1, but not CD80 or CD86..... 38

Figure 2.12: APCs differentially express H2Mβ1 and H2Mβ2..... 42

CHAPTER 3

Figure 3.1: $SPC^{\Delta Ab1}$ mice demonstrate specific deletion of MHCII on AT2s..... 46

Figure 3.2: Mice of the $Ab1^{fl/fl}$ background demonstrate lower expression of MHCII in some professional APCs, independent of Cre..... 47

Figure 3.3: 14-month-old $SPC^{\Delta Ab1}$ mice demonstrate disrupted lung T cell homeostasis..... 49

Figure 3.4: 14-month-old $SPC^{\Delta Ab1}$ mice demonstrate relatively normal T cell homeostasis in the spleen..... 50

Figure 3.5: 14-month-old $SPC^{\Delta Ab1}$ mice exhibit normal numbers and frequencies of immune cells in the lung..... 51

Figure 3.6: 7-month-old SPC$^{\Delta Ab1}$ mice demonstrate normal T cell homeostasis in the lung. 52
Figure 3.7: 7-month-old SPC$^{\Delta Ab1}$ mice demonstrate normal T cell homeostasis in the spleen. 53
Figure 3.8: 7-month-old SPC$^{\Delta Ab1}$ mice exhibit normal numbers and frequencies of immune cells in the lung. 54
Figure 3.9: 9-month-old SPC$^{\Delta Ab1}$ mice demonstrate healthy lung histology with no inflammatory infiltrates. 55
Figure 3.10: Loss of AT2 MHCII does not affect regenerative capacity. 56
Figure 3.11: Loss of AT2 MHCII results in greater weight loss and reduced survival after respiratory viral infection. 57
Figure 3.12: Differences in weight loss and survival between Ab1$^{fl/fl}$ and SPC$^{\Delta Ab1}$ mice were subject to experiment to experiment variation. 58
Figure 3.13: Loss of AT2 MHCII does not affect lung virus titers after respiratory viral infection. 59
Figure 3.14: Loss of AT2 MHCII does not alter frequencies of LAG3^{+} T cells after influenza virus infection. 60
Figure 3.15: Ab1$^{fl/fl}$ control mice exhibit worse weight loss and disease and delayed viral clearance compared to SPC^{Cre} control mice after virus infection. 70

CHAPTER 4

Figure 4.1: AT2s exhibit a globally restricted capacity to present individual influenza virus epitopes via MHCII *in vitro*. 75
Figure 4.2: AT2s are robustly infected with influenza virus *in vitro*. 76
Figure 4.3: *In vivo*-infected AT2s exhibit poor presentation of influenza virus epitopes to polyclonal CD4^{+} T cells via MHCII. 77
Figure 4.4: AT2s are robustly infected with influenza virus *in vivo*. 78
Figure 4.5: AT2 MHCII presentation capacity is enhanced in the setting of inflammation but remains limited. 79
Figure 4.6: Expression of I-A^{b}, I-E^{d}, and H2M in AT2s increases after *in vivo* treatment with IFN-γ, but does not explain poor MHCII presentation. 81

CHAPTER 5

Figure 5.1: AT2s express proteases associated with antigen processing and presentation. 90
Figure 5.2: AT2s upregulate MHCII expression after birth. 93
Figure 5.3: Homeostatic AT2 MHCII expression is conserved across multiple mouse strains but is absent in A/J mice. 100
Figure 5.4: SPC$^{\Delta Ah1}$ mice exhibit cellular signs of increased allergic phenotype compared to Ab1$^{fl/fl}$ control mice in an inhaled ova allergy model. 103

CHAPTER 6

Figure 6.1: Murine AT2s gating strategies. 114
Figure 6.2: Human AT2s gating strategy. 114

LIST OF KEY ABBREVIATIONS

$Ab1^{fl/fl}$	$H2\text{-}Ab1^{fl/fl}$ mice
APC	Antigen presenting cell
AT1	Type I alveolar cell
AT2	Type II alveolar cell
B6	C57Bl/6 mice
CIITA	Class II transactivator
CLIP	Class II-associated invariant chain peptide
DC	Dendritic cell
EC	Endothelial cell
Flu	Influenza virus
HA	Hemagglutinin
HSC	Hematopoietic stem cell
IAV PR8	Influenza A virus strain PR8
IEC	Intestinal epithelial cell
IFNAR	Interferon α/β receptor
IFNγ	Interferon γ
IFNγR	Interferon γ receptor
LNSC	Lymph node stromal cell
IL2	Interleukin 2
ILC3	Type 3 innate lymphoid cell
LB	Lamellar body
MHCI	Major histocompatibility complex I
MHCII	Major histocompatibility complex II
$MHCII^{-/-}$	MHCII-deficient mice
NA	Neuraminidase
NP	Nucleoprotein
Ova	Ovalbumin protein
pIV	CIITA promoter IV
SeV 52	Sendai virus strain 52
$SPC^{\Delta Ab1}$	SPC-Cre-ERT2$^{+/-}$ x $H2\text{-}Ab1^{fl/fl}$ mice
SPC^{Cre}	SPC-Cre-ERT2$^{+/-}$ mice
TCR	T cell receptor
TEC	Thymic epithelial cell
Tfh	T follicular helper cell
Th	T helper cell
TNFα	Tumor necrosis factor α
Treg	Regulatory T cell
Trm	Tissue resident memory cell
WT	Wild-type

CHAPTER 1:

GENERAL INTRODUCTION

1.1 Introduction to the immune system

The mammalian immune system is composed of an extensive network of cells, as well as intracellular, cell-surface, and secreted molecules. Exquisitely precise coordination of all of these factors is required for the appropriate recognition of foreign substances and the execution of robust, yet regulated, defenses against them. Both the failure to identify harmful substances and the inappropriate recognition of harmless or host-derived molecules as foreign can result in disease; similarly, effector responses that are inadequate, as well as responses that are too strong and uncontrolled, can both be damaging. The immune system must therefore constantly maintain a fine balance and does so by integrating multiple layers of countless cellular and molecular inputs.

Immune responses can be broadly classified into two main classes: innate and adaptive [1]. Innate immune responses are initiated quickly, within hours of exposure a harmful stimulus. They are classically associated with barrier sites of continuous pathogen exposure, such as the skin, lung, or gut, and they are targeted against broadly conserved pathogen or tissue damage associated motifs. In contrast, adaptive immune responses are slower, developing over the course of days, but are much more precisely targeted against the specific offending infectious agent. Adaptive immune responses are also unique in that they generate immunological memory, such that upon re-exposure to the same specific pathogen, responses will be faster and more robust. During host responses to many infections,

such as viruses, both innate and adaptive immune responses represent sequential and integrated phases of host defense. This dissertation primarily addresses the adaptive component of antiviral host immune responses.

By far the most well studied cell types involved in the orchestration of adaptive immune responses are conventional immune cells, which are derived from hematopoietic stem cells (HSCs) in the bone marrow. Out of the many different hematopoietic immune cell types, this dissertation explores the functions of the classical antigen-presenting cells (APCs), which include dendritic cells (DCs), B cells, and macrophages, and their interactions with one of the main adaptive immune cell lineages, $CD4^+$ T cells.

The contributions of all other cell types, ie: those that are not derived from HSCs, to adaptive immune responses are far less well understood. One notable exception is thymic epithelial cells (TECs), nonhematopoietic cells of the thymus that have been well studied for their critical function in T cell development. Otherwise, the role that other “non-immune” cells of the body, such as those that compose functional organs and tissues, may play in adaptive immune responses has historically not been the subject of extensive investigation. In this thesis I focus on the contribution of one particular non-immune cell type, the lung type II alveolar cell (AT2), to antiviral adaptive immune responses in the lower respiratory tract.

1.2 T cell responses in antiviral adaptive immunity

T cells and B cells represent the two main arms of adaptive immune effector responses. Here, I detail the general functions of T cells, with particular attention to the $CD4^+$ T cell lineage.

$CD4^+$ T "helper" (Th) cells play a central role in coordinating essentially all adaptive immune responses. Their main effector functions are to secrete instructive cytokines and to provide stimulatory signals to potentiate and alter the functions of other immune cell types. $CD4^+$ T cells can adopt a number of different helper phenotypes that are each optimal for a distinct immune context. Major $CD4^+$ Th phenotypes include Th1 that predominates during viral infections, Th2 during allergic and helminth responses,Th17 during responses to extracellular pathogens, as well as T follicular helper (Tfh) cells that are specialized for B cell help and regulatory T (Treg) cells that contribute to immunosuppressive responses [2]. During lung viral infections, $CD4^+$ T cells mainly adopt a type 1 (Th1) phenotype that enhances the antiviral immune response. These cells secrete effector cytokines (IFN-γ, TNF-α, IL-2), help B cells to produce high-affinity neutralizing antibodies, enhance $CD8^+$ T cell cytolysis of infected cells and memory formation, and in some cases are directly cytolytic [3]. In these cases, a different $CD4^+$ T cell phenotype-driven response, such as Th2, worsens disease by enhancing immunopathology in the lung [4, 5]; thus, the development of appropriate Th function is critical. The mechanisms governing $CD4^+$ T cell activation and differentiation are detailed in the subsequent sections.

Unlike $CD4^+$ T cells, $CD8^+$ T cells do not adopt such distinct phenotypes to the same extent, but they nonetheless also play critical roles in immune responses via their cytolytic function. During viral infections, their main functions are to secrete

effector cytokines, primarily IFN-γ and TNF-α, and to eliminate infected cells directly via the delivery of perforin and granzymes to the infected cell [6].

1.3 The T cell – APC interaction

$CD4^+$ T cells are activated by T cell receptor (TCR) recognition of antigenic protein-derived peptides bound to major histocompatibility complex II (MHCII) proteins on the surface of APCs. The activation of naïve T cells, or “priming”, occurs in secondary lymphoid organs, such as lymph nodes, and is mediated by a professional APC, usually a DC. Aside from recognition of a particular peptide/MHCII complex, activation of a naïve T cell is also thought to require a second costimulatory signal. This “signal 2” is typically provided by APC-derived CD80 or CD86 binding to CD28 on the T cell surface, and its absence results in T cell anergy rather than activation [1, 7-9]. The functional outcome of $CD4^+$ T cell activation is further influenced by specific cytokine signals provided by the APC at the time of activation [2]. Altogether, the cytokine milieu present, in combination with costimulatory signals as well as the strength and duration of the peptide/MHCII interaction [10, 11], dictates the activation and Th phenotype that will be adopted by the $CD4^+$ T cell. $CD8^+$ T cell activation occurs in a similar manner, although the $CD8^+$ T cell TCR recognizes specific peptide/MHCI complexes (not MHCII).

After T cell activation occurs, effector T cells proliferate, then exit the lymph nodes and traffic to the site of injury or infection. Effector T cell activation is further modulated in the periphery by interaction with cognate peptide/MHC expressing cells that express a diverse array of additional costimulatory molecules, inhibitory receptor

ligands, and adhesion molecules, which may serve to re-expand or suppress T cells [7, 8, 12-14]. The phenotypic function of $CD4^+$ T cells may also be altered in tissues by peripheral MHCII-expressing cells and changes in the cytokine environment, although the true plasticity of Th phenotypes is not fully understood [15, 16].

As recognition of specific peptide in the context of MHCII is a critical requirement for both $CD4^+$ T cell priming and downstream regulation in the periphery, a major emphasis of this work is to understand how the formation of these peptide/MHCII complexes is regulated. This includes understanding how antigenic peptides are generated from source proteins and delivered to MHCII molecules, as well as how MHCII protein expression is restricted in a cell-type specific manner.

1.4 Pathways of MHCII antigen processing and presentation

There are a variety of pathways by which peptides may be generated and loaded onto MHCII. These pathways can be broadly classified based on whether they use extracellular or intracellular proteins as initial substrates.

MHCII presentation of peptides derived from extracellular proteins has historically been the most well studied and characterized by far. In the “classical” pathway of exogenous MHCII presentation, extracellular protein is first taken up by an APC into an endocytic compartment [17]. Protein degradation then occurs in the endosomal network, with the final peptides being generated in the late endosome [18]. Nascent MHCII molecules are synthesized in the endoplasmic reticulum (ER) and are composed of one α and one β chain [18]. In the ER, these MHCII heterodimers associate with the chaperone protein invariant chain, which stabilizes

MHCII and helps it traffic to the late endosomal compartment [19-21]. In the late endosome, invariant chain is degraded by cathepsin proteases into the class II-associated invariant chain peptide (CLIP), which remains in the MHCII peptide binding groove [22-26]. Another chaperone protein, H2M, then facilitates the removal of CLIP, which then allows the binding of antigenic peptides [27-30]. Peptide/MHCII complexes then traffic to the cell surface [17, 18].

Deviations from the classical pathway of MHCII presentation that still rely on the uptake of extracellular antigen include different locations of peptide generation and loading. One alteration involves the generation of peptides that bind to MHCII molecules in the early endosome rather than the late endosome; this scenario also differs in that the source of MHCII is primarily recycling MHCII from the cell surface, rather than *de novo* synthesized MHCII, and that peptide loading can be either H2M dependent or independent [31-34]. This is most likely predominant for epitopes that would be otherwise fully degraded by the harsher pH and proteolytic environments of the late endosome or for scenarios in which MHCII biosynthesis is halted. Another alternative to the classical pathway is the loading of pre-formed extracellular peptides. While the loading of synthetic peptides is commonly used as an *in vitro* laboratory experimental tool, there is also evidence that extracellular processing and loading occurs *in vivo* [35-38]. Whether these peptides directly displace other MHCII-bound peptides on the cell surface or require internalization for loading is still unclear [39, 40].

Apart from the MHCII presentation of extracellularly acquired antigen, MHCII molecules also efficiently present peptides derived from intracellularly produced proteins. Although this property was demonstrated more than 30 years ago [41-45],

and has been demonstrated to be the predominant mechanism of epitope generation in certain settings, such as influenza virus infections [46], comparatively little attention has been paid to understanding the mechanisms by which endogenous MHCII processing and presentation occur. Studies that have explored these mechanisms demonstrate that a highly complex system of intracellular machinery is involved, which spans multiple subcellular compartments and can include factors such as cytosolic proteases, lysosomal enzymes, and the macroautophagy pathway [46-51]; however, the precise processing mediators required differ depending on the particular epitope produced. Because of this complexity, and the relative lack of mechanistic work in this area, the exact cellular factors required for the MHCII presentation of intracellular antigens are far less well characterized compared to classical MHCII presentation of exogenous antigen and seem to represent more of a "network" rather than one linear pathway. Nonetheless, one prerequisite for all endogenous processing and presentation is that, by definition, proteins must be synthesized *de novo* inside an APC. Thus, these protein substrates include host proteins as well as intracellularly produced pathogen-derived proteins, such as viral proteins synthesized within directly infected cells.

The wide variety of methods by which peptides may be generated and loaded onto MHCII diversifies the potential repertoire of MHCII-restricted peptides that can be presented by APCs. Furthermore, as there is no one strict set of machinery required for the generation of all epitopes, this suggests that MHCII antigen processing can be performed by a variety of different MHCII-expressing cell types, with each APC type using its own unique cohort of cellular mediators. This maximizes the likelihood that an MHCII-expressing cell type will be capable of

presenting antigen, but also suggests that there is substantial variability in antigen presentation capacity among candidate APCs both in aggregate and on an epitope-specific basis. Such complexity also suggests that there are numerous points where epitope generation and presentation may be regulated.

1.5 The regulation of MHCII expression

Transcription of MHCII is driven by the class II transactivator (CIITA), a non-DNA-binding co-activator. CIITA initiates transcription by binding to a ubiquitously expressed protein complex (composed of RFX, CREB/ATF, and NF-Y), which then binds to a conserved promoter-proximal enhancer SXY element upstream of the MHCII α and β chain gene loci [52]. CIITA then recruits chromatin remodeling complexes and the transcriptional machinery to facilitate gene expression, and may facilitate long-range promoter interactions to enhance expression as well [52, 53].

As the SXY module is also present upstream of the MHCII associated genes encoding the invariant chain, H2M, and the H2M-antagonist H2O, expression of these genes is coregulated along with MHCII by CIITA [54]. Although CHIP-seq, ATAC-seq, and DNAse hypersensitivity studies have demonstrated that CIITA is also present at hundreds of other locations within the genome that are not typically associated with MHCII, it is unclear to what extent this translates into true transcriptional regulation and whether these targets require CIITA binding for transcription [55-57].

Unlike most other genes, which rely on combinatorial transcription factor binding to modulate transcription, the transcription of MHCII is essentially exclusively

controlled by CIITA. Thus, MHCII expression is regulated by the mechanisms that regulate the transcription and expression of CIITA.

Transcription of CIITA begins at three distinct promoter sites within the CIITA locus: pI, pIII, and pIV. Transcriptional initiation occurs at each promoter in response to different cell-type and context-specific stimuli. By convention, homeostatic recruitment of pI occurs in conventional DCs and macrophages, and pIII in B cells and plasmacytoid DCs, while CIITA pIV is recruited in nonhematopoietic cell types in response to the inflammatory cytokine IFNγ [58]. Thus, it is thought that DCs, macrophages, and B cells express MHCII constitutively, while nonhematopoietic cells only do so in the setting of inflammation. However, there are an increasing number of notable exceptions to this paradigm, as discussed in **1.7**. The three transcripts produced from pI, pIII, and pIV each differ in their first exon, and the resulting proteins at their N termini, but all are thought to function similarly in inducing expression of MHCII and associated genes [58].

Apart from the CIITA-induced transcription and expression of MHCII, cells may also acquire MHCII protein from extrinsic sources. There are three main mechanisms by which has been described to occur [59]. The first is by trogocytosis, a process in which direct cell-to-cell contact facilities the transfer of membranes rapidly between two cells [60, 61]; in this case the transferred membrane would contain MHCII proteins. The second is by exosome-mediated transfer, whereby an $MHCII^+$ cell releases small membrane vesicles [62] carrying MHCII molecules, that are then taken up by a recipient cell [63]. The third is via tunneling nanotubes, or long membrane protrusions that enable the transfer of cytoplasmic material as well as cell surface molecules between cells [64, 65].

1.6 The professional APCs and the requirements of an APC

Historically, MHCII antigen presentation has been studied as a property restricted to the group of cells termed “professional APCs”: B cells, macrophages, and DCs. A defining feature of this group is that, as discussed above, these cell types express MHCII at homeostasis by virtue of constitutive CIITA expression. Another key hallmark is that they are each highly specialized for the processing and presentation of antigen via MHCII, with particularly well-developed mechanisms of antigen uptake, degradation, and MHCII loading [17]. For example, circulating DCs exhibit robust macropinocytosis, which allows them to continuously sample and take up a wide variety of potential antigens that could be presented via MHCII [17, 66]. DCs are also highly phagocytic, as are macrophages [17, 67]. Furthermore, B cells exhibit extremely efficient endocytic uptake of proteins for which their B cell receptors (BCR) are specific [68-70]. The subcellular compartments of all three cell types are also uniquely tailored to MHCII antigen presentation; they contain an assortment of critical antigen processing and presentation enzymes and chaperones, and they are dynamically regulated in response to environmental cues to either promote or inhibit the presentation of antigens via MHCII [17, 69, 71-74].

However, as discussed above, besides the professional APCs, a variety of other cell types express MHCII in response to IFNγ induction of CIITA pIV (and in other scenarios [to be discussed in **1.7**]). Therefore, a better understanding of whether these “non-professional” MHCII-expressing cells can also act as APCs, and the possible contributions they might make as a result, is warranted. To this end, I begin by summarizing the key “required” features of an APC that would endow a non-professional MHCII$^+$ cell with MHCII antigen presentation capacity.

(1) The first requirement is antigen uptake. As discussed in **1.4**, MHCII molecules can present antigen from either intracellular or extracellular protein sources. Thus, all cell types should be capable of this “antigen uptake” step in general to some degree, as all cells express their own intracellular proteins. For the presentation of a peptide from a specific protein, this would necessitate that the cell could take up the protein of interest into the endocytic pathway from the extracellular space, or that the cell produce the specific protein *de novo*, either a self-protein or a pathogen protein when directly infected.

(2) After antigen uptake, appropriate proteolysis and peptide transport would be required. Thus, the cell must express enzymes capable of protein degradation, but also possess a proteolytic environment that is not so harsh that all epitopes are destroyed before the possibility of loading onto MHCII [75-77]. Most cells possess this capability to some degree, although the precise proteases and protein processing enzymes expressed varies considerably between cell types. As discussed in **1.4**, the specific degradative enzymes required are epitope dependent; thus, for the MHCII presentation of a specific epitope of interest, a cell would have to express the suite of enzymes required for generation of that particular peptide. Apart from the capacity to generate peptide fragments, a cell would also need to have appropriate transporters or vesicular trafficking and maturation to allow the peptides to reach the MHCII loading compartments, depending on where the peptide is initially generated and where it is loaded onto MHCII.

(3) A third critical property is the appropriate stabilization and trafficking of MHCII to the peptide loading compartment. By convention, this is accomplished by the

chaperone protein invariant chain [19-21]. However, cells from invariant chain deficient mice still express appreciable levels of surface MHCII, although they are reduced relative to their wild-type counterparts (**Fig 1.1**). Thus, while expression of invariant chain likely enhances presentation by a cell, it is not absolutely required for MHCII stabilization or trafficking, or for presentation [78, 79].

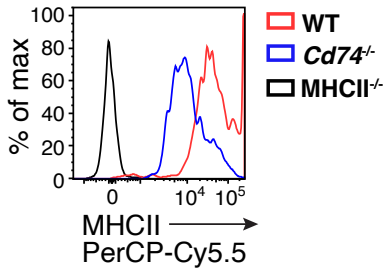

Figure 1.1: Invariant chain deficient mouse DCs express MHCII. MHCII protein expression by CD103$^+$ DCs from naïve C57Bl/6 (B6) wild-type (WT), invariant chain deficient (*Cd74*$^{-/-}$), and MHCII$^{-/-}$ mouse lungs measured by flow cytometry; represents n=3 mice per strain.

(4) The next step required for antigen presentation is peptide binding to MHCII. In the classical model of MHCII presentation, this requires the peptide-loading chaperone H2M, which unloads CLIP from the MHCII peptide-binding groove in the late endosome, allowing for the loading of other peptides. However, H2M is more accurately described as a peptide “editor” that exchanges lower affinity peptides for higher affinity ones. Thus, only some peptides are favored by and/or require the presence of H2M, such as those with (i) high affinity for MHCII, (ii) those restricted by MHCII molecules with high affinity for CLIP, or (iii) those loaded in the late endosome, where H2M is more abundant. Peptides that have low affinity for MHCII, are loaded in other compartments (such as the early endosome), or bind to MHCII molecules that have a low affinity for CLIP,

do not require H2M for loading onto MHCII and can actually be “edited out” by H2M when it is present. Thus, H2M is not required for the loading of all MHCII-restricted epitopes, and the presence of H2M actually hinders the presentation of some peptides [30, 46, 80-85].

In summary, the defining characteristics of a putative MHCII$^+$ APC – antigen uptake, measured proteolysis, appropriate peptide and MHCII trafficking, and peptide loading – are quite flexible in how they can be accomplished, and thus could be theoretically fulfilled by most MHCII$^+$ cell types in a general sense. However, MHCII presentation capacity likely does not operate on this yes-or-no basis but instead represents a spectrum from inefficient (less active antigen uptake, fewer proteolytic enzymes, no chaperone expression) to highly efficient like that of professional APCs (robust endocytosis, full suite of processing enzymes, both H2M and invariant chain are expressed). Furthermore, inefficient versus efficient MHCII presentation capacity can be interpreted on a global level (few versus many epitopes presented) or in relation to one epitope in particular (low versus high levels of specific peptide/MHCII complex formation).

Furthermore, although not required for MHCII presentation capacity, another important APC feature that would fine-tune the function of a putative APC is the expression of costimulatory molecules [7]. For example, expression of the conventional costimulatory molecules CD80 or CD86 alongside peptide/MHCII complexes would render a cell capable of priming a cognate naïve CD4$^+$ T cell; the absence of CD80/CD86 would instead suggest a role for the APC inducing naïve CD4$^+$ T cell tolerance [8, 9]. Expression of other non-canonical costimulatory molecules, such as ICAM-1, would allow the APC to promote the activation of

effector $CD4^+$ T cells, whereas expression of inhibitory receptors, such as PD-L1, would enable the suppression of $CD4^+$ T cell effector functions by the APC [12-14, 86]. The regulated expression of a broad array of these costimulatory molecules would endow an APC with the capacity to interact with $CD4^+$ T cells in a fine-tuned manner, providing activating or inhibitory cues depending upon the immunologic context.

Overall, it is likely that most non-professional MHCII-expressing cells exhibit MHCII antigen presentation capacity to some degree, their efficiency depending on how well they execute the required steps of MHCII processing and presentation outlined above; the manner in which these APCs influence $CD4^+$ T cell function is further influenced by the cohort of costimulatory molecules they express. Indeed, atypical $MHCII^+$ cells have been shown to make substantial contributions to $CD4^+$ T cell responses in a variety of immune settings, as detailed in the next section.

1.7 Non-professional MHCII-expressing APCs

Both at homeostasis and during disease states, there are various $MHCII^+$ cells aside from DCs, macrophages, and B cells. Here I provide a few examples of such cell types, and I briefly discuss the mechanisms regulating their MHCII expression as well as their reported antigen presentation functions.

The most extensively characterized $MHCII^+$ non-professional cell is the thymic epithelial cell (TEC). TECs express MHCII at homeostasis. As expected, since they are nonhematopoietic cells, their transcription of MHCII is driven by the pIV isoform of CIITA [87]. However, departing from the paradigm discussed in **1.5**,

their recruitment of CIITA pIV is IFNγ-independent. The main function of TECs is to mediate selection of T cells in the thymus, and they directly contribute to $CD4^+$ T cell development by presenting antigen via MHCII [88].

Another cell type more recently described to express MHCII are intestinal type 3 innate lymphoid cells (ILC3). ILC3s also express MHCII at homeostasis, but despite being HSC-derived immune cells, their expression of MHCII is driven by CIITA pIV. Similarly to TECs, they also do not require for IFNγ for pIV induction [89]. MHCII antigen presentation by ILC3s to $CD4^+$ T cells is critical for maintaining tolerance to the gut microbiota [89, 90].

Lymph node stromal cells (LNSC) also express MHCII at homeostasis. The expression of LNSC MHCII results from a combination of endogenous MHCII expression as well as the exogenous acquisition of MHCII proteins from hematopoietic cells [91-93]. In line with convention, LNSC intracellular production of MHCII is driven by CIITA pIV and requires IFNγ [91]. MHCII antigen presentation by LNSCs to $CD4^+$ T cells in secondary lymphoid organs contributes to the maintenance of peripheral tolerance and Treg induction [91-94].

Although they are not professional APCs, TECs, ILC3s, and LNSCs are all cells with primary functions in the immune system. However, several other ostensibly “non-immune” cell types also express MHCII at homeostasis. Although the precise CIITA regulatory mechanisms have not been explored for most of these cells, at the time of writing, all of the cell types whose regulation has been studied have been found to require IFNγ; thus, their homeostastic MHCII expression is driven by the low levels of IFNγ present at steady-state. For example, intestinal epithelial cells (IEC) [95], which have been demonstrated to contribute to graft-versus-host disease and

to protect against colitis via MHCII antigen presentation to $CD4^+$ T cells [96]. Endothelial cells (EC) are another such cell type (**Figs 2.2, 2.4, 2.5**), which have been demonstrated to present antigen via MHCII and to contribute to $CD4^+$ T cell trafficking, effector $CD4^+$ activation, as well as Treg induction [97-100].

The cell types discussed above are examples of some of the most well studied non-professional MHCII-expressing cells. However, other cell types have also been reported to express low levels of MHCII at homeostasis, and furthermore, in the setting of inflammation, essentially all nucleated cell types (except placental trophoblasts [101]) can be induced to produce MHCII in response to IFNγ. An exhaustive summary of the antigen presenting functions of these cell types is beyond the scope of this dissertation, and has been reviewed thoroughly by Kambayashi and Laufer [102] and Duraes *et al* [103].

Previous studies of bulk lung nonhematopoietic cells in particular have demonstrated that they also have the capacity to act as $MHCII^+$ APCs. For example, in a lung transplant model, nonhematopoietic lung cells induce the formation of Tregs *in vivo* [97], and flu-infected nonhematopoietic lung cells can stimulate flu-specific $CD4^+$ T cells to produce IFNγ *in vitro* [104]. Included in this nonhematopoietic $MHCII^+$ cell population are lung type II alveolar cells (AT2s). The major focus of this dissertation is on the MHCII expression regulation and MHCII antigen processing and presentation capacity of AT2s. AT2s have been described to express MHCII at homeostasis in both mice [105-108] and humans [109, 110]. In the following sections, I discuss the role of AT2s in basic respiratory homeostasis, as well as their known functions in immune responses, in particular their interactions with $CD4^+$ T cells via MHCII.

1.8 Functions of type II alveolar cells in lung physiology

The respiratory system can be functionally divided into two parts: (1) the proximal portion responsible for conducting air, and (2) the distal portion responsible for gas exchange. The distal lung gas exchange parenchyma is composed of alveoli, blind-ended sacs separated by extremely thin interstitium containing pulmonary capillaries. The alveolar structures are composed of two epithelial cell types: AT2s and type I alveolar cells (AT1), as well as some stromal cells. AT1s are the very thin, flat cells that facilitate gas exchange across the blood/air interface and make up most of the surface area of the alveoli. AT2s on the other hand are much smaller, but are more numerous, cuboidal polarized cells that also play critical roles in basic respiratory homeostasis [111, 112].

One major function of AT2s is to produce surfactant. Surfactant is a phospholipid-protein mixture that is secreted into the alveolar spaces, where it reduces surface tension to prevent alveolar collapse. Defects in surfactant production are either incompatible with life or result in severe respiratory disease. Surfactant is composed of approximately 10% protein (including specific surfactant proteins SP-A, SP-B, SP-C, and SP-D), and ~90% lipids/phospholipids . While some other cell types can produce select surfactant proteins, AT2s are the only cells capable of producing all of the lipid and protein components of surfactant, and the only cell type that synthesizes mature SP-C protein [111-113].

AT2s possess a highly specialized network of subcellular compartments that are tailored to the synthesis, secretion, and recycling of surfactant. The surfactant proteins and lipids are produced in the ER, with SP-C and SP-B first synthesized as pro-proteins. SP-A and SP-D exit the ER via the Golgi and then are released via the

constitutive secretory pathway. In contrast, pro-SP-C and pro-SP-B, along with lipids, traffic from the Golgi to multi-vesicular bodies (MVB), then to a specialized lysosome-like compartment called the lamellar body (LB). Throughout this trafficking process, pro-SP-B and pro-SP-C are subject to a number of controlled proteolytic cleavage events carried out by processing enzymes that include cathepsins and other proteases. The LB contents are then released into the alveolar spaces via regulated exocytosis. Surfactant components can also be taken up from the alveolar spaces by AT2s via endocytosis, first into early endosomes. Components can either traffic to the lysosome for degradation, or back to the MVB where they may be either recycled to the LB, or at that point targeted to the lysosome [111, 114].

Another major function of AT2s is to serve as stem cell-like progenitor cells in the distal lung. AT2s are capable of proliferation, self-renewal, and terminal differentiation, giving rise to both AT2 and AT1 daughter cells. This process operates at homeostasis, where cell turnover is relatively slow (on the order of weeks) [111]. Additionally, after lung injury, AT2s also contribute to the repopulation of the damaged alveolar epithelium [112, 115], in concert with other epithelial cell types [116].

Aside from these functions in respiratory biology and lung homeostasis, AT2s have also been described to have a number of immune functions. I will first introduce the immunologic environment of the lower respiratory tract in **1.9** and then discuss the known contributions of AT2s in **1.10**.

1.9 The lower respiratory tract immune system

The proximal conducting airways are lined by mucosal tissue and thus maintain a rich mucosal immune system that is populated by numerous immune cell types and tertiary lymphoid structures. In contrast, the gas exchange alveolated lung parenchyma is comprised of non-mucosal thin epithelium that represents a distinct immunologic context [117]. As this latter portion is where AT2s reside, I limit my discussion here to the immune environment of the alveolar portion of the lower respiratory tract.

The alveolar spaces contain a number of immune cells at homeostasis. The most abundant are alveolar macrophages, which reside inside the alveolar spaces [117]. There are also two main types of conventional DCs: $CD103^+$ DCs, which lie closer to the epithelial layer and extend processes into the alveolar spaces, and $CD11b^+$ DCs that reside more squarely in the interstitium [6]. The interstitium between alveolar spaces also contains various other myeloid cells, including interstitial macrophages, monocyte-derived DCs, and plasmacytoid DCs, as well as T and B cells, and mast cells, NK and innate lymphoid cells, and others [6, 117]. The extensive pulmonary vasculature embedded in the lung parenchyma also contains a variety of immune cells, including large numbers of T cells [117]. During inflammation there is an additional influx of cell types, depending on the type of immune response, including neutrophils, eosinophils, additional T cells, and inflammatory monocytes, among others [6, 117].

As one area of emphasis of this dissertation is the primary T cell response to respiratory viral pathogens, I will also outline briefly the current understanding of the key steps in the antiviral adaptive immune response in the lung, using the response

to influenza virus in mice as an example. The first cells to respond to influenza virus are epithelial cells, which are the major target of infection, as well as the highly phagocytic alveolar macrophages surveying the alveolar spaces [6]. Activation of innate sensors within these cells leads to the production of type I/III interferons and other inflammatory cytokines and chemokines that have direct antiviral effects and also serve to recruit and activate other immune cells [118]. This process, along with direct pathogen sensing, triggers antigen uptake and maturation of DCs, which then exit the lung to enter the draining lymph nodes where they interact with naïve T cells by presenting viral antigens via MHCI and MHCII. Although both lung DC types can prime naïve $CD4^+$ and $CD8^+$ T cells, $CD103^+$ DCs are thought to be the main contributors to $CD8^+$ T cell priming, arriving in large numbers to the draining lymph node earlier during the course of infection (days 2-4). $CD11b^+$ DCs are thought to be more important for cytokine and chemokine production in the lung and for the expansion of the effector T cell pool, and they peak in the lymph nodes later during infection (days 5-7) [6]. A subset of activated $CD4^+$ T cells remains in the lymph node as Tfh cells that interact with B cells in germinal centers, leading to the differentiation of flu-specific memory B cells as well as plasma cells that produce high affinity neutralizing antibodies [6]. Antigen-specific effector Th1 $CD4^+$ T cells and $CD8^+$ T cells traffic back to the lung, where they interact with both directly infected and antigen-bearing APCs via recognition of cognate peptide/MHC complexes. These antigen-specific T cell/APC interactions *in situ* are critical for direct effector T cell functions that facilitate viral elimination, such as direct cytolysis of infected cells by CD8s, and by CD4s to a small extent [119], as well as for Th1 $CD4^+$ and $CD8^+$ production of antiviral cytokines such as TNFα and IFNγ. In general, these direct

TCR-peptide/MHC interactions in the lung tissue, along with concomitant costimulatory or inhibitory signals and particular cytokines, serve to support and regulate the viability, proliferation, and function of effector T cells locally [6, 120-125]. Once the virus is cleared, the responding effector T cell populations contract, and a memory T cell pool persists both centrally and in the lung tissue. A failure to properly regulate these T cell responses, in terms of magnitude, duration, or phenotype, can result in lung immunopathology [126].

1.10 Type II alveolar cells in lung innate and adaptive immune responses

Aside from their roles in respiratory function and lung regeneration, AT2s have also been described to play a number of key immune functions at homeostasis and during infection.

AT2s contribute to constitutive immune defenses in the lung. Surfactant proteins SP-A and SP-D produced by AT2s can act as opsonins, binding to the surface of various pathogens and accelerating their uptake by alveolar macrophages [127]. AT2s also secrete complement components as well as lysozyme, which help facilitate microbial clearance [128, 129]. AT2s also contribute to immune tolerance in the lung at homeostasis by providing negative regulatory signals to alveolar macrophages via the CD200/CD200R and TGFβ axes [6, 117, 118].

During infection, AT2s express a number of pattern recognition receptors, such as TLRs as well as the nucleic acid sensors MDA-5 and RIG-I, which allow them to detect pathogens and initiate further immune responses [130, 131]. AT2s can also secrete a number of different cytokines and chemokines, such as IL-6, IL-8,

IL-1β, GM-CSF, IL-4, IFN-γ, type I/III IFNs, and others, which can serve to recruit and promote the survival and function of inflammatory cells [111, 130, 132-136].

More than 30 years ago, it was first described that AT2s express MHCII at homeostasis in rodents and humans [137, 138], and a number of subsequent studies have confirmed these expression findings [105-110, 139-141]. However, there have been relatively few studies directly addressing the contribution of AT2s to adaptive immune responses via MHCII, and those that have been performed report somewhat conflicting functions. Cunningham and colleagues first explored the antigen presenting capabilities of AT2s. They found that primary human AT2s were unable to stimulate allogeneic $CD4^+$ T cells to proliferate in a 5 day *in vitro* co-culture; however, proliferation could be induced by adding high concentrations of anti-CD28 antibody (≥10μg/mL) to the culture [110]. Debbabi *et al.* subsequently demonstrated that primary murine AT2s pre-incubated with *M. tuberculosis* (Mtb) sonicate could stimulate polyclonal Mtb-experienced $CD4^+$ T cells to produce IFNγ in a 48 hour *in vitro* co-culture, without the need for exogenous co-stimulation. They also demonstrated that in the presence of Mtb protein antigen, AT2s could stimulate the Mtb-specific $CD4^+$ T cell hybridomas to produce IL-2 [106]. Conversely, Lo and colleagues demonstrated that ovalbumin protein (Ova) treated AT2s failed to stimulate Ova-specific $CD4^+$ T cell hybridomas as well as primary Ova-specific $CD4^+$ T cells (OT-II) to produce IL-2 or proliferate, even in the presence of synthetic Ova peptides or when the AT2s had been pre-treated *in vivo* with IFNγ. They further demonstrated that OT-II cells pre-incubated with AT2s *in vitro* become tolerized, or are suppressed in an antigen specific manner from subsequent DC-mediated activation [108]. In contrast, using the same Ova system, Gereke *et al.* demonstrated

that primary mouse AT2s treated with Ova protein *in vitro* or *in vivo* were capable of stimulating proliferation of naïve OT-IIs in *in vitro* co-culture. They also showed that primary AT2s expressing HA protein endogenously under the SP-C promoter (derived from SPC-HA mice) could stimulate naïve HA-specific $CD4^+$ T cells (derived from TCR-HA mice) to proliferate *in vitro*. They further proposed that the effect of AT2s on $CD4^+$ T cells is context dependent, as AT2s derived from TCR-HA x SPC-HA mice, which experience severe autoimmune lung disease, instead induced TCR-HA T cells to become Tregs *in vitro* rather than to proliferate. They also suggest that AT2s mediate these dynamic interactions with naïve $CD4^+$ T cells *in vivo* as well, by demonstrating TCR-HA proliferation in the lungs of SPC-HA CD11c-DTR mice and of SPC-HA mice treated with the lymph node egress inhibitor, FTY720; however, whether their experimental interventions reflect endogenous MHCII antigen presentation by AT2s or MHCII presentation by residual $CD11c^+$ or other non-$CD11c^+$ hematopoietic lung-resident APCs that acquire exogenous HA from the AT2s is unclear [107].

In summary, these prior studies exhibit substantial variation in their findings of AT2 MHCII antigen presentation capacity and its functional influence on the $CD4^+$ T cell response. Furthermore, only Gereke and colleagues [107] attempted to explore the *in vivo* impact of AT2 MHCII presentation, and they did so in the context of a model system that forces high and artificial protein expression in the AT2s, and where it is unclear whether the *in vivo* MHCII presentation measured was mediated by AT2s or by other lung APCs. Importantly, no prior studies have investigated the contribution of AT2 MHCII to host defense *in vivo*, nor have any explored mechanisms regulating homeostatic AT2 MHCII expression. In this dissertation, I

aim to shed light on these previously unexplored areas and to clarify the discrepancies previously reported in AT2 MHCII function.

1.11 Goals for the thesis

The overarching goal of this dissertation is to better understand the function of MHCII on AT2s. Specifically, I aim to elucidate (1) how MHCII expression by AT2s is regulated, (2) the contribution of AT2 MHCII to lung antiviral host responses, and (3) the MHCII antigen presentation capabilities of AT2s. A driving purpose for this work is the need to better understand how immune responses are carefully orchestrated in the lung parenchyma to facilitate rapid pathogen clearance while preventing collateral immunopathology that would damage the vital gas-exchange surface; I seek to understand if and how AT2s contribute to this regulation.

In **chapter 2**, I investigate the MHCII^{+} APC characteristics of AT2s. First, I explore the mechanisms by which AT2s express MHCII protein as well as the transcriptional mediators and cytokine signals required for AT2 MHCII expression. I also assess the capacity of AT2s to mediate antigen uptake and proteolysis, as well as their expression of conventional MHCII trafficking and peptide loading chaperones.

In **chapter 3**, I investigate the function of AT2 MHCII *in vivo*. Using a conditional mouse model, I selectively eliminate MHCII just on AT2s. I assess the impact of the loss of AT2 MHCII on disease and immune dysfunction at homeostasis as well as during lower respiratory tract viral infection.

In **chapter 4,** I explore the MHCII antigen presentation capabilities of AT2s. I assess the capacity of AT2s to process and present antigens via MHCII both *in vitro* and *in vivo*, using viral and model protein systems to look on an aggregate and epitope-specific basis.

In **chapter 5**, I discuss the implications of our findings and consider future avenues of investigation.

In **chapter 6**, I detail the materials and methods used for all studies in the preceding chapters.

CHAPTER 2:

TYPE II ALVEOLAR CELLS CONSTITUTIVELY EXPRESS MAJOR HISTOCOMPATIBILITY COMPLEX II INDEPENDENT OF CONVENTIONAL INFLAMMATORY MEDIATORS

Adapted from the following manuscript:

Sushila A. Toulmin, Chaitali Bhadiadra, Andrew J. Paris, Jeremy Katzen, Maria C. Basil, Edward E. Morrisey, G. Scott Worthen, and Laurence C. Eisenlohr. (*Manuscript submitted*)

2.1 Introduction

$CD4^+$ T cell responses are initiated by T cell receptor (TCR) recognition of cognate major histocompatibility complex II (MHCII)/peptide complexes on the surface of antigen presenting cells (APCs). By convention, constitutive MHCII expression is restricted to a few specialized types of cells, including the "professional APCs" B cells, dendritic cells (DCs), and macrophages, as well as thymic epithelial cells (TECs) [52]. In contrast, all other cell types are thought to produce MHCII only in the setting of inflammation, specifically in response to the cytokine interferon-γ (IFNγ) [58]. However, more recently, an increasing number of other cell types have been shown to express MHCII at homeostasis, violating this expression paradigm, as discussed in **1.7**. These include intestinal ILC3s [89, 90], which express MHCII independent of IFNγ, as well as several nonhematopoietic cell types, such as lymph node stromal cells [91-94], vascular endothelial cells [98-100], and intestinal epithelial cells [95, 96, 142], whose MHCII production is driven by the basal IFNγ present at steady state.

Type II alveolar cells (AT2s) are an additional nonhematopoietic cell type that have been reported to express MHCII at homeostasis in both mice [105-108] and humans [109, 110]. As described in **1.8**, AT2s are epithelial cells present in the lung parenchyma, and their main physiologic functions are to produce surfactant and to serve as stem-like cells in the distal lung [112, 115, 143, 144]. Their constitutive MHCII expression suggests that they may participate in lung adaptive immune responses as well. Previous studies of AT2 MHCII function have varied widely in their findings [106-108, 110], and as such, the capacity of AT2s to act as $MHCII^+$ APCs remains unclear. Furthermore, no prior studies have attempted to understand the mechanisms driving this unusual homeostatic MHCII expression by AT2s. Thus, here I report on the

mechanisms regulating AT2 MHCII expression at homeostasis, and I begin to assess their MHCII antigen presentation capacity by evaluating the basic APC characteristics of AT2s.

2.2 Results

AT2s express MHCII protein at homeostasis to uniformly high levels

To verify prior reports of homeostatic AT2 MHCII expression, we assessed MHCII on both mouse and human AT2s by flow cytometry. Mouse AT2s were identified as $CD45^{-}CD31^{-}EpCAM^{int}$ cells (**Fig 6.1**) [105], while human AT2s were identified by expression of the cell surface marker HT2-280 (**Fig 6.2**) [145]. Consistent with prior studies, we found that naïve wild-type C57Bl/6 (B6) AT2s uniformly express MHCII (**Fig 2.1a**). Similarly, healthy human AT2s express the human MHCII protein HLA-DR (**Fig 2.1b**).

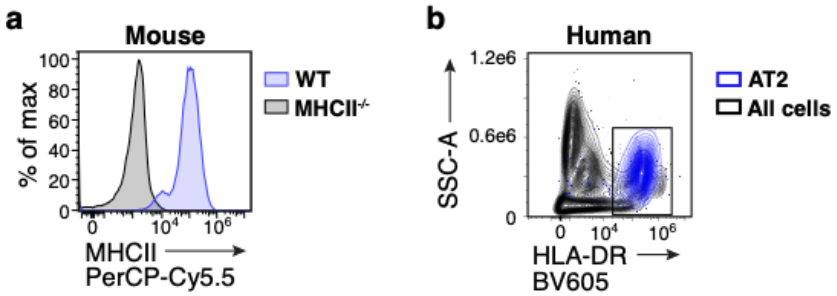

Figure 2.1: Mouse and human AT2s express MHCII at homeostasis. a, MHCII protein expression by AT2s from naïve C57Bl/6 (B6) wild-type (WT) and $MHCII^{-/-}$ mice measured by flow cytometry; represents n>10 mice per strain total from >5 independent experiments. **b,** MHCII (HLA-DR) protein expression by AT2s and distal lung cells from a healthy human donor measured by flow cytometry; represents n=1 donor, and gate was drawn based on fluorescence minus one (FMO) controls.

We next compared MHCII levels on AT2s to other well studied MHCII-expressing lung cells in naïve mice. AT2s express MHCII at a magnitude similar to that of lung professional APCs, dendritic cells (DCs) and B cells, and higher than alveolar macrophages (**Fig 2.2a**). Besides AT2s, vascular endothelial cells (ECs) are another nonhematopoietic cell type in the lung that express MHCII at homeostasis [97]. Compared to ECs, AT2 MHCII expression is higher and more homogeneous (**Fig 2.2b**).

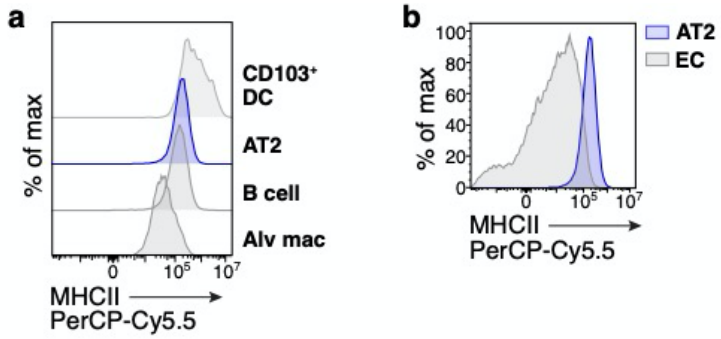

Figure 2.2: AT2s express high levels of MHCII similar to professional APCs. a,b, MHCII protein expression by AT2s, CD103$^+$ dendritic cells (CD103$^+$ DC), B cells, alveolar macrophages (Alv mac), and endothelial cells (EC), from naïve B6 WT mouse lungs measured by flow cytometry; represents n>10 mice per strain total from >5 independent experiments.

MHCII protein may be synthesized intracellularly or extrinsically acquired [59] from conventional APCs. We examined the source of AT2 MHCII by qPCR and by creating CD45.1 MHCII$^{+/+}$ (B6$^{CD45.1}$) and CD45.2 MHCII$^{-/-}$ B6 (MHCII$^{-/-}$) bone marrow chimeric mice. AT2s express transcript for both the α and β chains of the MHCII allele in B6 mice, I-A^b (**Fig 2.3a**), and AT2s retained MHCII protein expression to high levels in MHCII$^{-/-}$ → B6$^{CD45.1}$ mice (**Fig 2.3b**). Thus, AT2s synthesize their own MHCII and do not depend on acquisition of MHCII protein from hematopoietic APCs.

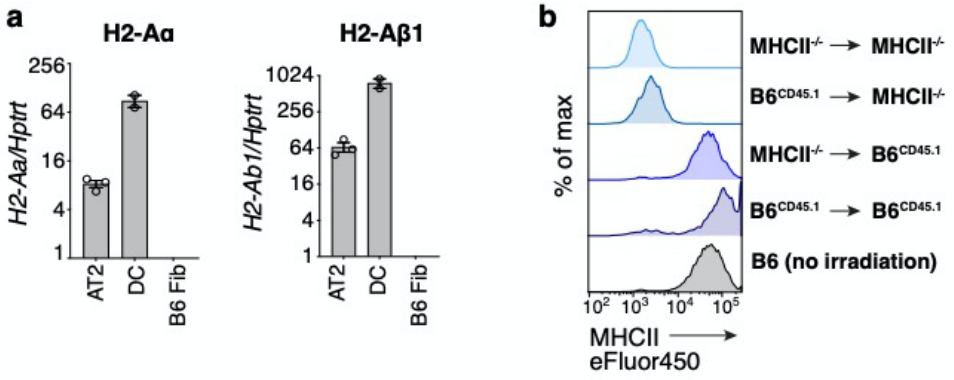

Figure 2.3: AT2s synthesize their own MHCII transcript and protein. a, I-A^b α (H2-Aα) and β (H2-Aβ1) chain transcript abundance relative to housekeeping gene Hprt1, in AT2s and lung dendritic cells (DC) sorted from naïve B6 WT mice, and a B6 fibroblast cell line (B6 Fib), measured by quantitative RT-PCR; n=3 mice for AT2s, n=2 mice for DCs, bars represent mean plus standard error of the mean (SEM), 1 representative experiment shown of 2 similar independent experiments. **b,** MHCII protein expression by AT2s in MHCII$^{-/-}$ and CD45.1 B6 (B6$^{CD45.1}$) bone marrow chimeric mice, measured 8 weeks post-transplantation with transfers as indicated; histograms represent n=2-4 mice per group in 1 experiment.

In sum, AT2s represent a unique population of nonhematopoietic lung cells that produce MHCII protein at homeostasis uniformly to high levels, similar to that of professional APCs.

AT2 MHCII expression is regulated in an unconventional, IFNγ-independent manner

The class II transactivator (CIITA) is the master transcription factor that drives MHCII expression [58]. To determine whether AT2 MHCII expression is dependent on CIITA, we assessed MHCII in the lungs of *Ciita*$^{-/-}$ mice. Lack of CIITA results in the complete loss of MHCII expression on AT2s, as well as lung DCs and ECs (**Fig 2.4**). As discussed in **1.5,** transcription of CIITA begins at three different promoter sites (pI, pIII, and pIV) depending on cell and context specific stimuli. Recruitment of pI occurs in DCs and macrophages, pIII in B cells and plasmacytoid DCs, and pIV in ILC3s and nonhematopoietic cells [58, 89]. To assess whether AT2 MHCII is dependent on pIV, we evaluated mice lacking just the pIV region within the CIITA locus [146]. AT2s from *Ciita pIV*$^{-/-}$ mice fail to express MHCII, as do ECs, while DCs retain MHCII expression as expected (**Fig 2.4**).

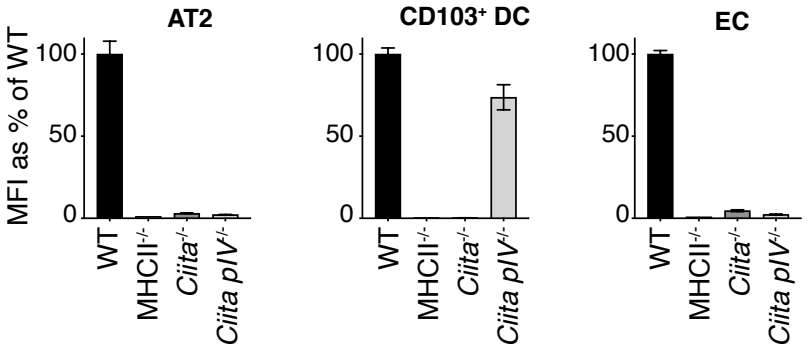

Figure 2.4: AT2 MHCII expression is driven by CIITA pIV. MHCII protein expression by AT2s, CD103^{+} DCs, ECs from naïve B6 WT, MHCII$^{-/-}$, *Ciita*$^{-/-}$, and *Ciita pIV*$^{-/-}$ mouse lungs, measured by flow cytometry. For each strain, MHCII expression is displayed as a percentage reflecting the average median fluorescence intensity (MFI) of MHCII on each cell type relative to the average MHCII MFI on the same cell type in WT mice; n=2-4 mice per strain total from 1-2 independent experiments pooled. Data are shown as mean plus SEM.

The recruitment of pIV in all nonhematopoietic cells (except for thymic epithelial cells (TECs)) is thought to require induction by the cytokine IFNγ [58]. We evaluated MHCII in mice deficient in IFNγ, IFNγR, and the associated downstream pIV-binding transcription factor, STAT1. AT2s retain MHCII expression in *Ifng*$^{-/-}$, *Ifngr1*$^{-/-}$, and *Stat1*$^{-/-}$ mice in a manner similar to DCs and in contrast to ECs, whose MHCII expression is abrogated in the absence of IFNγ signaling (**Fig 2.5**). AT2s, like DCs, exhibit a small reduction in MHCII expression in *Stat1*$^{-/-}$ mice, indicating that IFNγ signaling may upregulate MHCII expression in AT2s, but it is not required for steady state expression.

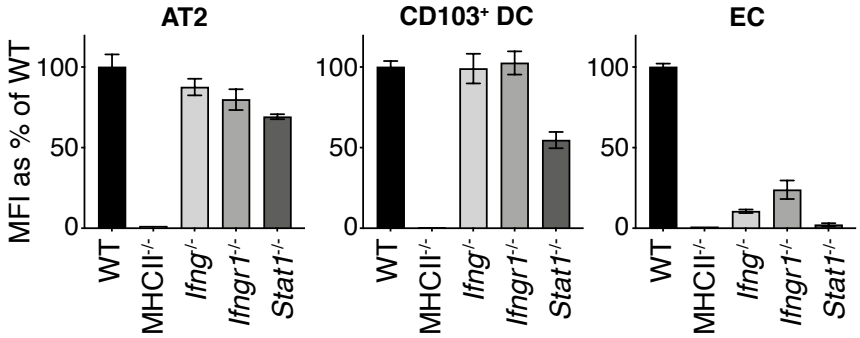

Figure 2.5: AT2 MHCII expression does not require canonical IFNγ inflammation. MHCII protein expression by AT2s, CD103^{+} DCs, ECs from naïve B6 WT, MHCII$^{-/-}$, *Ifng*$^{-/-}$, *Ifngr1*$^{-/-}$, *and Stat1*$^{-/-}$ mouse lungs, measured by flow cytometry. For each strain, MHCII expression is displayed as a percentage reflecting the average median fluorescence intensity (MFI) of MHCII on each cell type relative to the average MHCII MFI on the same cell type in WT mice; n=2-4 mice per strain total from 1-2 independent experiments pooled. Data are shown as mean plus SEM.

Besides IFNγ, no other cytokine has been shown to be sufficient to induce MHCII expression in nonhematopoietic cells. However, given the IFNγ-independent expression of MHCII by AT2s, we also examined the requirement of a broad array of conventional innate and adaptive immune mediators, by assessing *Ifnar1*$^{-/-}$, *Ifnar1*$^{-/-}$ *x Ifngr1*$^{-/-}$, *Myd88*$^{-/-}$, *Stat6*$^{-/-}$, and germ-free mice. AT2s express MHCII at wild-type levels

in all cases (**Fig 2.6**), indicating that they also do not require a wide spectrum of other, non-IFNγ inflammatory signals for MHCII expression, including type I IFNs, TLR ligands, IL-1, IL-18, IL-33, Th2 cytokines, and the microbiota.

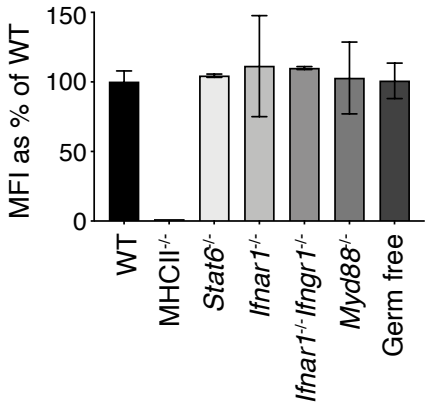

Figure 2.6: AT2s express MHCII independent of a variety of broad innate and adaptive inflammatory mediators. MHCII protein expression by AT2s, from naïve B6 WT, MHCII$^{-/-}$ *Stat6*$^{-/-}$, *Ifnar1*$^{-/-}$, *Ifnar1*$^{-/-}$*Ifngr1*$^{-/-}$, *Myd88*$^{-/-}$, and germ-free mice, measured by *ex vivo* flow cytometry analysis and displayed as MFI of AT2s from each strain relative to WT AT2s; n=2-3 mice per strain total from 1-2 independent experiments pooled. Data are shown as mean plus SEM.

Altogether, these data demonstrate that AT2 homeostatic MHCII expression is CIITA pIV-dependent, but IFNγ-independent. This same transcriptional configuration has been reported for only two other cell types: TECs[87], which are present in a primary immune organ, and ILC3s [89], which are immune cells. To our knowledge it has never been described for a cell outside of the immune system.

<u>AT2s possess classical APC characteristics and MHCII antigen processing and presentation machinery</u>

Although the spectrum of “required” machinery for MHCII antigen processing and presentation can vary widely depending on the particular epitope generated and

APC involved, as discussed in **chapter 1**, we nonetheless sought to understand to what extent AT2s possess general characteristics that would contribute to their capacity to act as MHCII$^+$ APCs.

We first examined whether AT2s possess mediators of classical MHCII presentation. By convention, this pathway begins with extracellular antigen acquisition followed by proteolysis in the endocytic compartment [17, 18, 147]. To assess these steps, we evaluated the capacity of AT2s to catabolize DQ-Ova, a self-quenched conjugate of ovalbumin protein that fluoresces after receptor-mediated endocytosis and proteolytic digestion. AT2s exhibited a temperature-dependent increase in fluorescence when incubated with DQ-Ova, less so than DCs but similarly to B cells, indicating that they are capable of active antigen uptake and degradation (**Fig 2.7**).

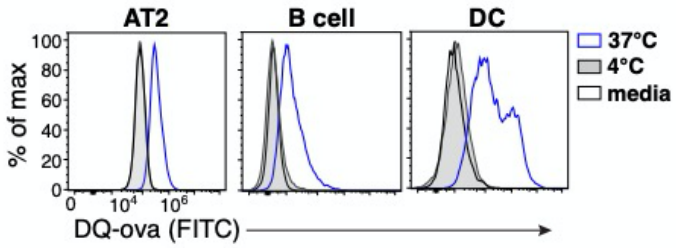

Figure 2.7: AT2s are capable of extracellular antigen uptake and degradation. Fluorescence of AT2s, B cells, and DCs sorted from naïve B6 WT lungs then incubated with DQ-ovalbumin (DQ-ova) or media at the temperatures indicated, measured by flow cytometry; histograms represent n=2 mice total from 2 independent experiments.

Optimal MHCII presentation also requires appropriate stabilization and trafficking of MHCII. Classically, this is facilitated by the chaperone protein invariant chain [17, 18, 147]. We evaluated invariant chain expression by flow cytometry and, consistent with prior reports [105, 148], found that AT2s express intracellular invariant chain in both mice (**Fig 2.8a**) and humans (**Fig 2.8b**).

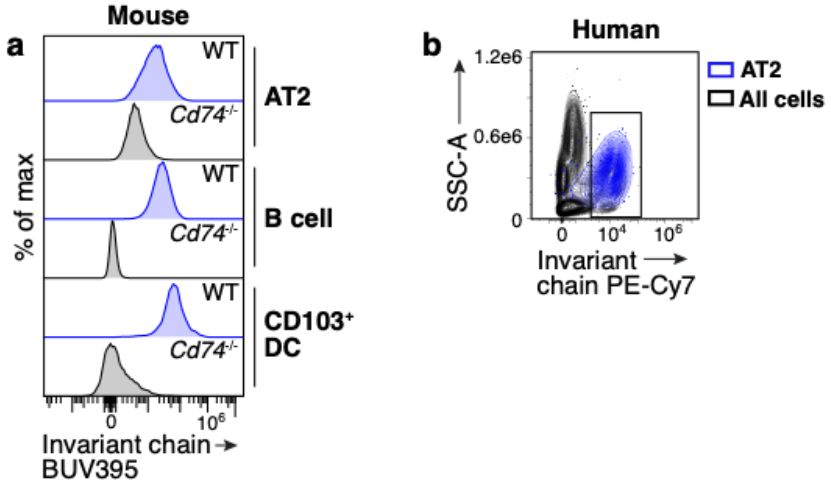

Figure 2.8: AT2s express invariant chain protein. a, Intracellular invariant chain protein expression by AT2s, lung CD103$^+$ DCs, and splenic B cells from B6 WT or invariant chain deficient (*Cd74*$^{-/-}$) mice measured *ex vivo* by flow cytometry; histograms represent n=3-9 mice per strain from 3 independent experiments. **b,** Intracellular invariant protein expression by AT2s and distal lung cells from a healthy human donor measured by flow cytometry; represents n=1 donor, and gate was drawn based on fluorescence minus one (FMO) controls.

Classical MHCII processing also depends on the protein H2M, which facilitates removal of the invariant chain peptide remnant CLIP from the MHCII peptide-binding groove in the late endosome [17, 18, 147]. We evaluated H2M expression by qPCR and flow cytometry. In mice, H2M is a heterodimeric protein composed of one α chain pairing with one of two β chains, β1 or β2 [30]; H2M$\alpha\beta$1 and H2M$\alpha\beta$2 are thought to function similarly [149, 150]. AT2s expressed detectable levels of transcripts encoding the α and β chains of H2M (**Fig 2.9a**), using β primers that capture both β1 and β2. However, by flow cytometry AT2s did not express H2M$\alpha\beta$2 protein (**Fig 2.9b**). Thus, the predominant form of H2M in naïve mouse AT2s is H2M$\alpha\beta$1, consistent with publicly availably RNA-seq data (**Fig 2.10)** deposited on the LungMAP Consortium (U01HL122642). We also evaluated H2M function by flow cytometric detection of the CLIP/MHCII complex CLIP/I-A^b in B6 mice. If H2M is functionally present, then the

number of CLIP/I-A^b complexes will be low, as CLIP peptide will be edited out. AT2s from wild-type mice have low expression of CLIP/I-A^b complexes, similar to hematopoietic MHCII$^+$ lung cells, and in contrast to both cell types from H2M-deficient mice that have high levels of CLIP/I-A^b (**Fig 2.9c**). We also assessed the expression of the human H2M-equivalent, HLA-DM, in human AT2s, by flow cytometry. As in mice, healthy human AT2s expressed HLA-DM (**Fig 2.9d**).

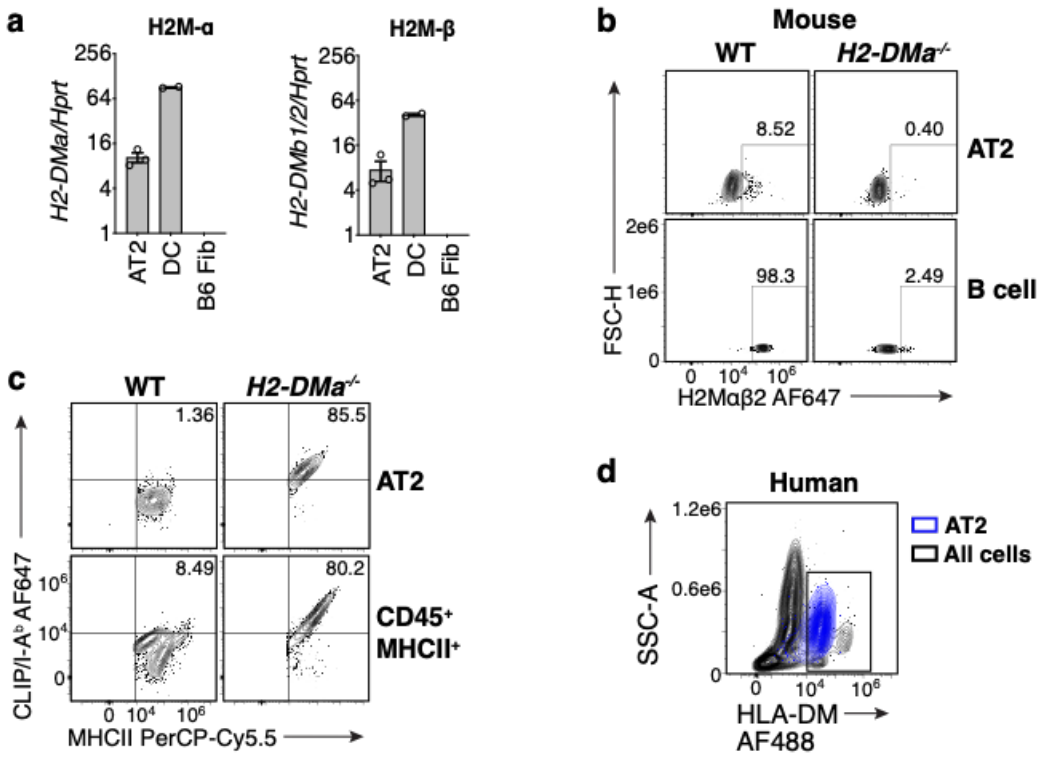

Figure 2.9: AT2s express functional H2M protein. a, H2Mα and H2M-β chain transcript abundance relative to housekeeping gene Hprt1, in AT2s and DCs sorted from naïve B6 WT mouse lungs, and a B6 fibroblast cell line (B6 Fib), measured by quantitative RT-PCR; n=3 mice for AT2s, n=2 mice for DCs, data shown are mean plus SEM, 1 representative experiment shown of 2 similar independent experiments. **b,** Intracellular H2Mαβ2 protein expression by AT2s and lung B cells from B6 WT or H2Mα deficient (*H2-DMa*$^{-/-}$) mice measured *ex vivo* by flow cytometry with frequency of H2Mαβ2$^+$ cells shown; plots represent n>10 mice per strain total from >5 independent experiments. Gates were drawn separately for AT2s and B cells based on their H2Mα deficient cell counterparts. **c,** Surface MHCII and CLIP/I-A^b H2Mαβ2 protein expression by AT2s and bulk CD45$^+$MHCII$^+$ cells from B6 WT or H2Mα deficient mice measured *ex vivo* by flow cytometry with frequency of MHCII$^+$CLIP/I-A^{b+} cells shown; plots represent n>6 mice per strain total from >3 independent experiments. **d,** Intracellular HLA-DM protein expression by AT2s and distal lung cells from a healthy human donor measured by flow cytometry; represents n=1 donor, and gate was drawn based on fluorescence minus one (FMO) controls.

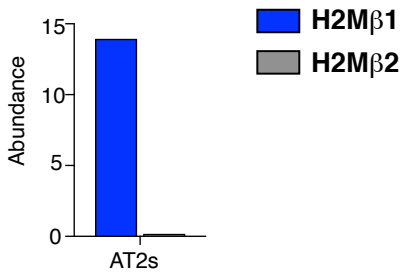

Figure 2.10: AT2s express exclusively H2Mβ1 transcripts, not H2Mβ2, at homeostasis. H2Mβ1 and H2Mβ2 chain transcript abundance measured by bulk RNA-seq, normalized by RPKM, in AT2s from naïve 4 week old B6 mice. The results shown here are in whole based upon data deposited on the LungMAP Consortium by J. Whitsett and Y. Xu. They were downloaded from (www.lungmap.net), on Nov 18, 2018. The LungMAP consortium and the LungMAP Data Coordinating Center (1U01HL122638) are funded by the National Heart, Lung, and Blood Institute (NHLBI).

Besides extracellular antigens, MHCII also presents peptides derived from intracellular proteins [35, 47, 49]. For example, in influenza (flu) virus infections in B6 mice, endogenous MHCII presentation of peptides from viral proteins synthesized within infected cells, instead of engulfed extracellular viral material, drives the majority of the antiviral $CD4^+$ T cell response [46]. Endogenous MHCII presentation involves a heterogenous network of machinery that are less well characterized compared to the classical pathway, precluding an exhaustive study of specific mediators here. However, one prerequisite for endogenous processing is expression of intracellular antigen by the APC. We assessed whether AT2s produce viral proteins intracellularly after exposure to live influenza virus and found that AT2s expressed both hemagglutinin (HA) as well as nucleoprotein (NP) to high levels (**Figs 4.2, 4.4**). This suggests that AT2s possess abundant substrate material for endogenous processing during flu infections, and this presumably extends to other respiratory viral infections for which they are also main targets.

Beyond peptide/MHCII complex formation, another component of APC function is the provision of costimulation. In general, priming of naïve T cells requires APC expression of the proteins CD80 or CD86, while the reactivation of effector T cells is less costimulation-dependent and may be influenced by a wider spectrum of costimulatory molecules [7, 151]. Prior studies indicate that naïve AT2s do not express CD80 or CD86, but that they express the noncanonical costimulatory molecule ICAM-1 [106-108]. We also assessed AT2s for CD80, CD86, and ICAM-1 expression and found that AT2s expressed ICAM-1, but not CD80 or CD86, both at homeostasis and after influenza infection (**Fig 2.11**).

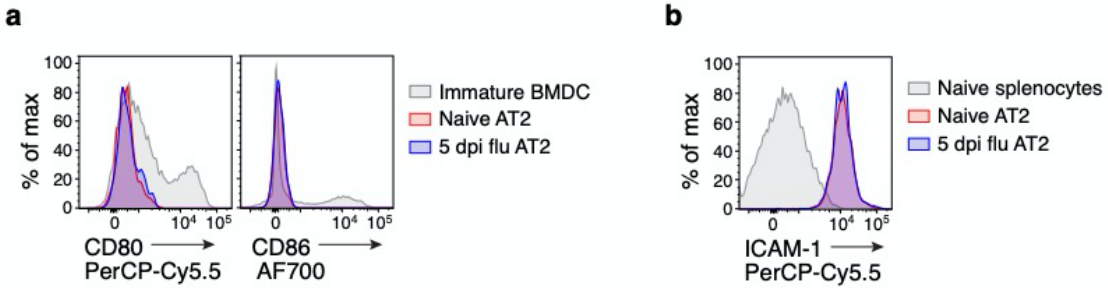

Figure 2.11: AT2s express noncanonical costimulatory molecule ICAM-1, but not CD80 or CD86. a, Surface expression of CD80 (left) and CD86 (right) by AT2s from naïve mice or mice 5 days post influenza virus infection, and B6 WT BMDCs cultured *in vitro*. **b,** Surface expression of ICAM-1 by AT2s from naïve mice or mice 5 days post influenza virus infection, and B6 WT splenocytes from naïve mice. Histograms represent n=2 mice (naïve) or n=6 mice (flu infected) in total across 2 experiments.

Taken together, these data indicate that AT2s possess the requisite characteristics and intracellular machinery to endow them with MHCII antigen presentation capacity; in combination with the expression of ICAM-1 but not CD80/CD86, this would predict that AT2s have the ability to act as APCs, activating effector, but not naïve, $CD4^+$ T cells that enter the lung.

2.3 Discussion

Here we establish that AT2 cells stand alone in a new category of MHCII-expressing cells, as non-immune cells that nonetheless constitutively express MHCII in an IFNγ-independent manner. We also demonstrate that AT2s express conventional MHCII-associated antigen processing machinery and APC qualities that should equip them with the capacity to present antigen to $CD4^+$ T cells.

We confirm prior reports of homeostatic MHCII expression by AT2s but also provide new insight into the magnitude of AT2 MHCII expression. We demonstrate that AT2s uniformly express high levels of MHCII, making them unusual in comparison to other nonhematopoietic cell types that express MHCII at homeostasis, which typically do so to lower levels; for example, lung endothelial cells (**Fig 2.2b**) and lymph node stromal cells [93] exhibit low to intermediate levels and much less homogeneous expression of MHCII. As AT2s comprise about 15% of lung parenchymal cells [111], this makes them one of the most abundant high-MHCII-expressing cells in the lung, even including the professional APCs.

Prior to our work, no previous studies of AT2s had investigated the mechanisms driving their homeostatic MHCII expression. Based on the accepted paradigm for MHCII expression in nonhematopoietic cells, we hypothesized that AT2 MHCII would be driven by CIITA pIV in response to IFNγ. Intestinal epithelial cells, which, like AT2s, are epithelial cells at a barrier site continuously exposed to antigen, express MHCII at homeostasis driven by the low levels of basal IFNγ that are present at steady state [95]; we presumed that AT2s would follow this same pattern. However, we demonstrated that AT2 MHCII, while dependent on CIITA pIV, is independent of IFNγ and a number of other mediators that span multiple broad arms

of the immune system. This indicates that CIITA pIV recruitment in AT2s follows a novel transcriptional induction mechanism that departs from the conventional model of CIITA regulation for non-immune cells. Furthermore, it suggests that AT2 MHCII is not driven by an inflammatory stimulus, but rather depends on other environmental cues or is an intrinsic part of the AT2 identity. Future work will aim to identify the general upstream signals and transcription factors that induce CIITA pIV and subsequent MHCII in AT2s, as detailed in **chapter 5**. Regardless of the specific mechanisms driving AT2 MHCII, constitutive expression to such high levels suggests that AT2 MHCII plays an important functional role in the lung.

We demonstrated that AT2s are capable of acquiring exogenous and endogenous antigens and that they express conventional MHCII processing and presentation chaperones. Although there is no one set of intracellular mediators that is required for all MHCII presentation, the fact that AT2s possess these characteristics suggests that they have the capacity to be potent MHCII$^+$ APCs. As AT2s lack CD80/CD86 expression, this suggests that AT2s play a role in modulating the function of lung-infiltrating effector CD4$^+$ T cells and/or in tolerizing naïve CD4$^+$ T cells that migrate through the lungs [152], rather than mediating priming of naïve CD4$^+$ T cells.

We observed that AT2s express only the H2M$\alpha\beta$1 isoform of H2M. We were intrigued by this differential expression of H2M$\alpha\beta$1 and H2M$\alpha\beta$2, since by convention they should be co-regulated under the control of CIITA. Per publicly available RNA-seq data deposited in the Immunological Genome Project [153], conventional APC populations also exhibit differential expression of H2M$\alpha\beta$1 and H2M$\alpha\beta$2, and the preferred isoform differs depending on cell type (**Fig 2.12**). B cells

appear to favor H2Mαβ2, DCs express both H2Mαβ1 and H2Mαβ2 to approximately equal levels, while macrophages are more variable depending on the tissue of origin but seem to favor H2Mαβ1 like AT2s. Given that both of these genes should theoretically be driven by the same transcription factor, this discordant expression suggests that there are cell-type specific mechanisms that further control transcription of each H2Mβ gene. The functional significance of this regulation is unclear, as H2Mαβ1 and H2Mαβ2 have been shown to function similarly [149, 150], although admittedly no prior studies have addressed this very extensively. Furthermore, as the duplication of H2Mβ seems to be unique to mice, it is unclear what relevance this differential expression has to humans; humans have only one gene for H2Mβ, although it is polymorphic within the population as a whole [154, 155].

Overall, AT2s constitutively express high levels of MHCII and possess promising MHCII$^+$ APC characteristics. In the next chapter, we will directly examine how this translates into the function of AT2 MHCII at homeostasis and during lung infection.

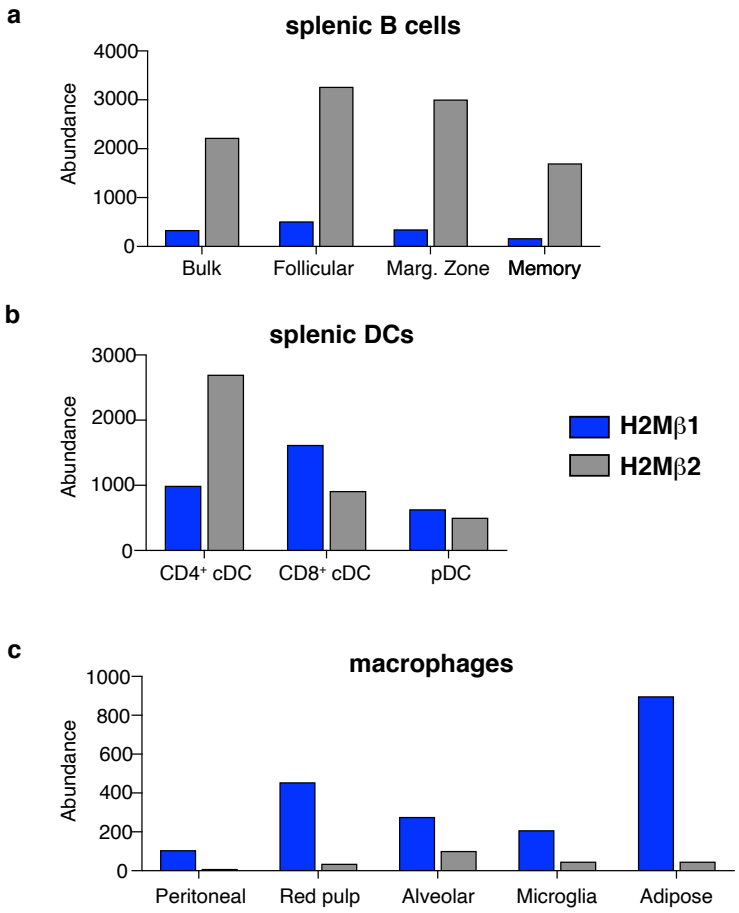

Figure 2.12: APCs differentially express H2Mβ1 and H2Mβ2. a-c, H2Mβ1 and H2Mβ2 chain transcript abundance detected by bulk RNA-seq, normalized by DESeq2, of the splenic B cell subsets (**a**), splenic DC subsets (**b**), and macrophage populations (**c**) indicated, in naïve 6 week old B6 mice. Data were obtained from the Immunological Genome Project (ImmGen).

CHAPTER 3:

TYPE II ALVEOLAR CELL MAJOR HISTOCOMPATIBILITY COMPLEX II CONTRIBUTES MODESTLY TO LUNG T CELL HOMEOSTASIS AND PROTECTION DURING RESPIRATORY VIRAL INFECTION

Adapted from the following manuscript:

Sushila A. Toulmin, Chaitali Bhadiadra, Andrew J. Paris, Jeremy Katzen, Maria C. Basil, Edward E. Morrisey, G. Scott Worthen, and Laurence C. Eisenlohr.

(*Manuscript submitted*)

3.1 Introduction

In **chapter 2** we demonstrated that AT2s possess robust APC characteristics, including constitutive and high MHCII expression. In this chapter, we examine how these features may translate into their *in vivo* function.

In general, T cell responses are initiated and largely shaped by the priming of naïve T cells and their subsequent proliferation in a draining lymph node. However, effector T cells that then circulate back to the site of infection can also be further regulated by cognate peptide/MHC-expressing cells in the tissue. For example, in the lung during viral infections in particular, this has been demonstrated for both $CD8^+$ and $CD4^+$ T cell function and proliferation [120, 122-125]. Furthermore, fine tuning of $CD4^+$ T cell responses, during either the priming or effector phase, also occurs in a number of other tissues and can be mediated by a variety of unconventional $MHCII^+$ cells [102, 103]. For example, ILC3s have been demonstrated to induce deletion of commensal-specific $CD4^+$ T cells via MHCII presentation in the intestine, which is critical to prevent gut immunopathology [89, 90]. Intestinal epithelial cells have also been shown to regulate gut $CD4^+$ T cells differentially depending on the disease setting; they contribute to worst graft-versus-host disease pathogenesis by priming $CD4^+$ T cells, but also regulate the Th1/Treg balance in the gut to prevent colitis [95, 96]. Furthermore, MHCII presentation by vascular endothelial cells has been demonstrated to modulate effector $CD4^+$ T cell functions and trafficking [98, 99], while lymph node stromal cell MHCII presentation is important for the maintenance of peripheral $CD4^+$ T cell tolerance [92, 94].

Regulation of $CD4^+$ T cell function in the periphery by these $MHCII^+$ APCs primarily occurs via TCR binding to cognate peptide/MHCII complexes along with

accompanying activating or inhibitory receptor/ligand interactions, which serves to either amplify T cell activation or suppress T cell function. However, aside from antigen presentation, MHCII can also serve another role in regulating effector T cell function. MHCII is one of the major ligands for the inhibitory receptor LAG3, which is expressed on activated T cells. LAG3 binds directly to surface MHCII and this ligation results in suppression of T cell proliferation and effector function. MHCII binding to LAG3 restrains both $CD4^+$ and $CD8^+$ T cell responses in a number of disease settings, including viral infection, autoimmunity, and cancer [156].

Only one prior study has assessed the *in vivo* function of MHCII on AT2s and how this might regulate T cell responses in the lung [107]. In this study, AT2s were reported to be capable of activating naïve $CD4^+$ T cells in the healthy mouse lung and of inducing $CD4^+$ Treg formation in the setting of lung inflammation. However, how well this experimental system, which relied on forced expression of a model protein to very high levels in AT2s and used responding TCR transgenic $CD4^+$ T cells, represents a physiologic setting is unclear. Furthermore, while AT2s expressed the protein from which the MHCII-restricted epitope of interest was derived, it is unclear whether they were interacting directly with $CD4^+$ T cells via MHCII or were simply releasing antigen that was then acquired and presented by professional APCs. Thus, the *in vivo* contribution of AT2 MHCII is still largely unknown, and in particular, its contribution to lung homeostasis and to lung host responses has never been explored to our knowledge. Thus, here we examine the function of AT2 MHCII *in vivo* both at homeostasis and in the setting of respiratory virus infection.

3.2 Results

A mouse model allows inducible and selective loss of MHCII on AT2 cells

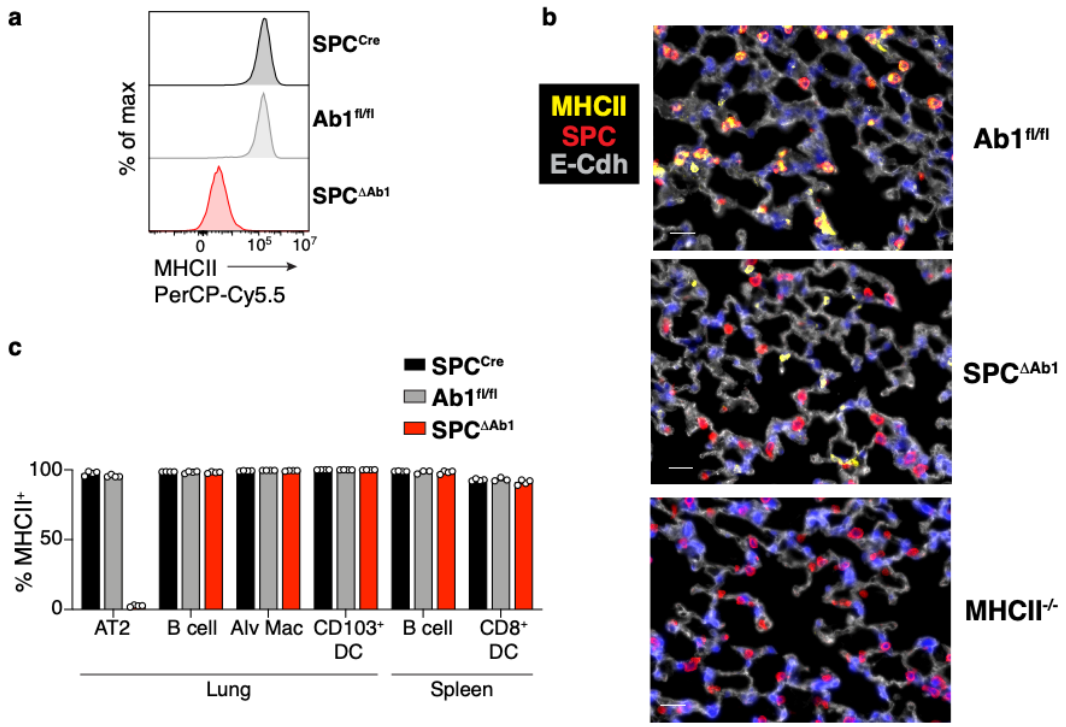

Figure 3.1: SPC$^{\Delta Ab1}$ mice demonstrate specific deletion of MHCII on AT2s. a, MHCII expression by AT2s from naïve SPC-Cre-ERT2$^{+/-}$ (SPC^{Cre}), H2-Ab1$^{fl/fl}$ (Ab1$^{fl/fl}$), and SPC-Cre-ERT2$^{+/-}$ × H2-Ab1$^{fl/fl}$ (SPC$^{\Delta Ab1}$), lungs measured by flow cytometry; histograms represent n>50 mice per strain total from >10 independent experiments. **b**, Immunofluorescence detection of MHCII, SPC, and E-Cadherin in Ab1$^{fl/fl}$, SPC$^{\Delta Ab1}$, and MHCII$^{-/-}$ lungs; scale bar depicts 20 μm and images represent n=1-2 mice per strain. **c,** Percent of each cell type expressing MHCII protein for lung AT2s, B cells, alveolar macrophages, CD103^{+} DCs, and spleen B cells and CD8^{+} DCs, from naïve SPC^{Cre}, Ab1$^{fl/fl}$, and SPC$^{\Delta Ab1}$ mice, measured by *ex vivo* flow cytometry analysis; bars show n=4 mice per strain from 1 experiment, representative of 2 similar independent experiments for the Ab1$^{fl/fl}$ and SPC$^{\Delta Ab1}$ strains (n=8 mice total per strain).

As AT2s express both MHCII and the conventional MHCII-associated APC machinery, we predicted that AT2 MHCII presentation would contribute to immune responses *in vivo*. To test this, we generated mice with an AT2-specific deletion of MHCII by breeding mice to have both (1) a tamoxifen-inducible Cre enzyme controlled by the AT2-specific surfactant protein C (SPC) promoter [157] and (2) LoxP sites flanking exon 1 of the I-A^{b} β chain on both alleles [158] (SPC-Cre-ERT2$^{+/-}$ × H2-Ab1$^{fl/fl}$; aka "SPC$^{\Delta Ab1}$"). Upon tamoxifen administration, SPC$^{\Delta Ab1}$ mice exhibit uniform deletion

of MHCII from AT2s (**Fig 3.1**), in contrast to the parental strains whose AT2s retain MHCII: those expressing the Cre enzyme with a wild-type I-A^b locus (SPC-Cre-$ERT2^{+/-}$ only; aka "SPC^{Cre}"), as well as those with homozygous floxed I-A^b alleles but no Cre (H2-$Ab1^{fl/fl}$ only; aka "$Ab1^{fl/fl}$").

To ensure that the deletion of MHCII in $SPC^{\Delta Ab1}$ mice was restricted to AT2s, we compared MHCII on various other APCs in the lungs and spleens of all three strains. Similar frequencies of lung B cells, alveolar macrophages, lung $CD103^+$ DCs, splenic B cells, and splenic $CD8\alpha^+$ DCs, expressed MHCII in all three strains, suggesting that the Cre-mediated deletion of MHCII was AT2-specific (**Fig 3.1c**). However, the overall magnitude of MHCII on certain APCs, such as B cells and $CD103^+$ DCs, was lower in both the $SPC^{\Delta Ab1}$ and $Ab1^{fl/fl}$ mice compared to the SPC^{Cre} strain (**Fig 3.2**); this suggests that in mice of the H2-$Ab1^{fl/fl}$ genetic background, the I-A^b targeting construct diminishes MHCII expression in some cell types, independent of Cre expression. Based on these data, we considered the $Ab1^{fl/fl}$ mice the most appropriate comparators for the $SPC^{\Delta Ab1}$ mice, so these two strains were paired for our *in vivo* studies.

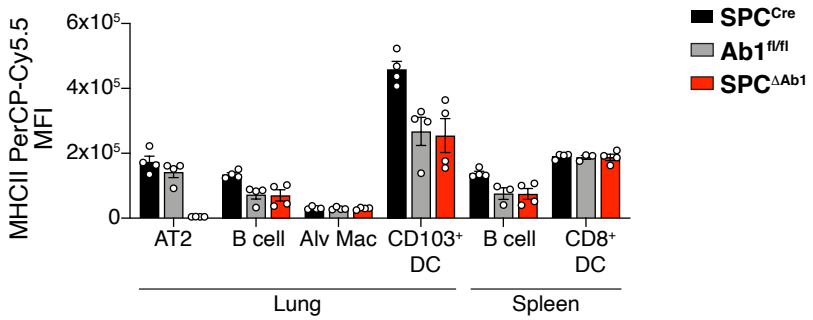

Figure 3.2: Mice of the $Ab1^{fl/fl}$ background demonstrate lower expression of MHCII in some professional APCs, independent of Cre. MFI of each cell type expressing MHCII protein for lung AT2s, B cells, alveolar macrophages, $CD103^+$ DCs, and spleen B cells and $CD8^+$ DCs, from naïve SPC^{Cre}, $Ab1^{fl/fl}$, and $SPC^{\Delta Ab1}$ mice, measured by *ex vivo* flow cytometry analysis; bars show n=4 mice per strain from 1 experiment, representative of 2 similar independent experiments for the $Ab1^{fl/fl}$ and $SPC^{\Delta Ab1}$ strains (n=8 mice total per strain).

AT2 MHCII contributes to lung T cell homeostasis in aged mice

We first assessed whether loss of MHCII on AT2s resulted in immune dysfunction at homeostasis. To this end, we examined lung immune cells and splenic T cells by flow cytometry in naïve 7-month-old and 14-month-old $SPC^{\Delta Ab1}$ and $Ab1^{fl/fl}$ mice.

At 14 months of age, the $SPC^{\Delta Ab1}$ mice exhibited a number of differences from $Ab1^{fl/fl}$ mice in the lung T cell compartment. While the overall numbers of lung $CD4^+$ and $CD8^+$ T cells were similar between the strains, significantly lower proportions of $CD4^+$ and $CD8^+$ T cells were effector memory phenotype ($CD44^+$ $CD62L^-$), and higher proportions were naïve ($CD44^-$ $CD62L^+$), in $SPC^{\Delta Ab1}$ mice compared to $Ab1^{fl/fl}$ mice (**Fig 3.3**). Furthermore, significantly lower proportions of lung $CD4^+$ and $CD8^+$ T cells in $SPC^{\Delta Ab1}$ mice expressed the inhibitory receptor PD1, which is a marker of T cell activation and/or exhaustion, and the proliferation marker Ki67 (**Fig 3.3**). As surface MHCII is the main ligand for the T cell inhibitory receptor LAG3, which is also an activation/exhaustion marker, we also evaluated LAG3-expressing T cells in the lungs of both strains; we found that $SPC^{\Delta Ab1}$ mice had reduced frequencies of $LAG3^+$ $CD4^+$, but not $CD8^+$, T cells (**Fig 3.3**). We also examined lung Tregs and found that the frequency was significantly reduced in $SPC^{\Delta Ab1}$mice compared to $Ab1^{fl/fl}$ mice (**Fig 3.3**). Frequencies of $CD69^+CD11a^+$ $CD4^+$ and $CD69^+$ $CD8^+$ T cells in the lungs were also lower in $SPC^{\Delta Ab1}$mice, although did not meet statistical significance for $CD4^+$s, reflecting lower proportions of tissue resident-memory (Trm) [159] and/or recently activated T cells in $SPC^{\Delta Ab1}$mice (**Fig 3.3**).

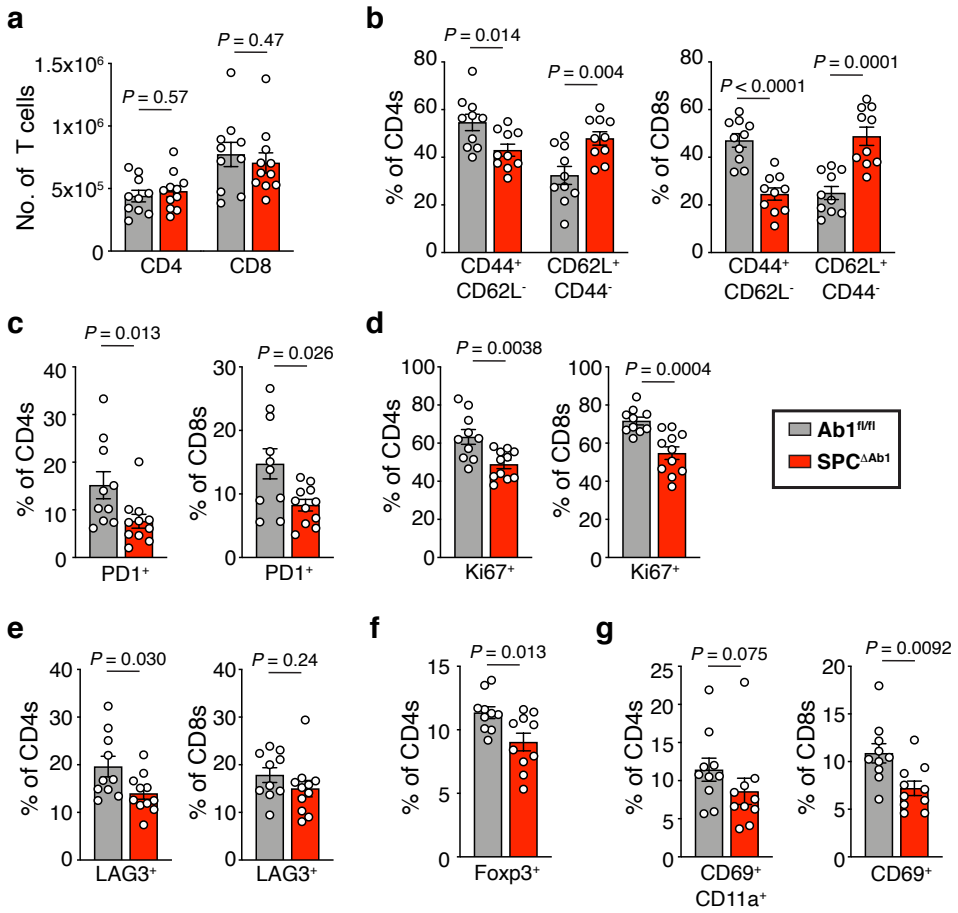

Figure 3.3: 14-month-old SPC$^{\Delta Ab1}$ mice demonstrate disrupted lung T cell homeostasis. a-g, *Ex vivo* flow cytometry analysis of naïve 14 month old Ab1$^{fl/fl}$ and SPC$^{\Delta Ab1}$ mice lung T cells. Absolute number of lung CD4$^+$ and CD8$^+$ T cells (**a**), and frequency of lung CD4$^+$ and CD8$^+$ T cells expressing CD44, CD62L (**b**), PD1 (**c**), Ki67 (**d**), LAG3 (**e**), Foxp3 (**f**), and CD69, CD11a (**g**), as indicated; n=10-11 mice per strain from 1 experiment. Data shown are mean plus SEM, analyzed by unpaired two-tailed Student's *t*-test, Welch's *t*-test, or Mann-Whitney test depending on the distribution of the data.

In contrast to the lungs, the spleen T cell compartments were more comparable between 14-month-old SPC$^{\Delta Ab1}$ and Ab1$^{fl/fl}$ mice, although they did demonstrate some of the same, but less pronounced, trends in T cell activation and memory marker expression (**Fig 3.4**).

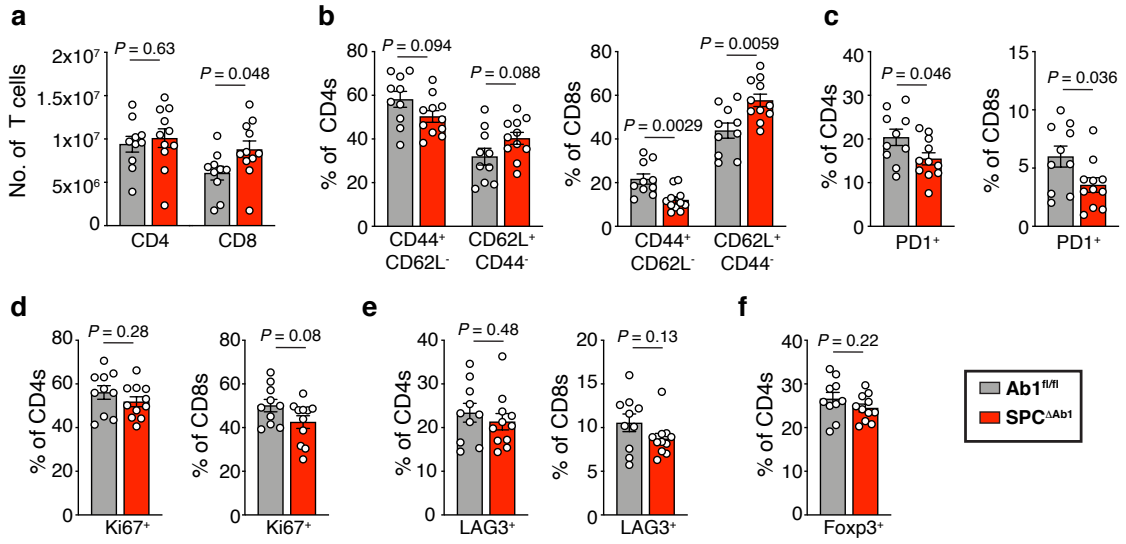

Figure 3.4: 14-month-old SPC$^{\Delta Ab1}$ mice demonstrate relatively normal T cell homeostasis in the spleen. a-f, *Ex vivo* flow cytometry analysis of naïve 14 month old Ab1$^{fl/fl}$ and SPC$^{\Delta Ab1}$ mice spleens. Absolute number of splenic CD4$^+$ and CD8$^+$ T cells (**a**), and frequency of CD4$^+$ and CD8$^+$ T cells expressing CD44, CD62L (**b**), PD1 (**c**), Ki67 (**d**), LAG3 (**e**), and Foxp3 (**f**), as indicated; n=10-11 mice per strain from 1 experiment. Data shown are mean plus SEM, analyzed by unpaired two-tailed Student's *t*-test or Mann-Whitney test depending on the distribution of the data.

Furthermore, there were no differences in the frequencies and numbers of other lung immune cells, including alveolar macrophages, neutrophils, NK cells, γδT cells, and B cells between 14-month-old SPC$^{\Delta Ab1}$ and Ab1$^{fl/fl}$ mice (**Fig 3.5**).

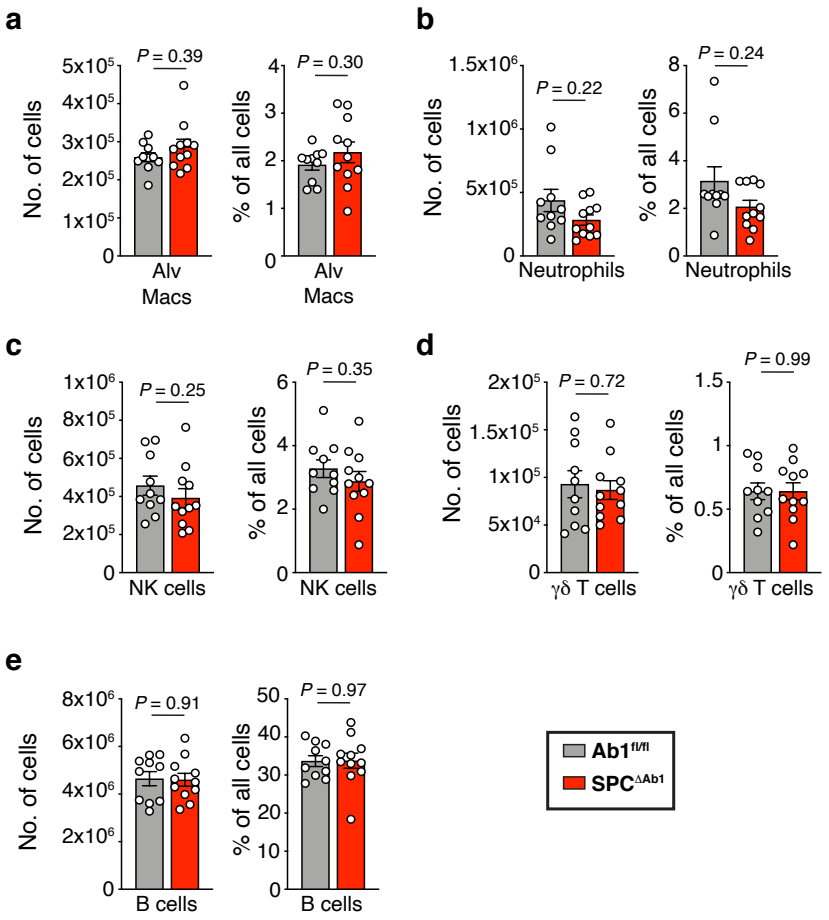

Figure 3.5: 14-month-old SPC$^{\Delta Ab1}$ mice exhibit normal numbers and frequencies of immune cells in the lung. a-e, *Ex vivo* flow cytometry analysis of naïve 14 month old Ab1$^{fl/fl}$ and SPC$^{\Delta Ab1}$ mice lungs. Frequency and numbers of alveolar macrophages (**a**), neutrophils (**b**), NK cells (**c**), γδ T cells (**d**), and B cells (**e**), as indicated; n=10-11 mice per strain from 1 experiment. Data shown are mean plus SEM, analyzed by unpaired two-tailed Student's *t*-test or Mann-Whitney test depending on the distribution of the data.

In contrast to the 14-month-old mice, naïve 7-month-old SPC$^{\Delta Ab1}$ and Ab1$^{fl/fl}$ mice demonstrated no differences in numbers or frequencies of the same lung or spleen T cell subsets or other immune cell populations (**Figs 3.6-3.8**).

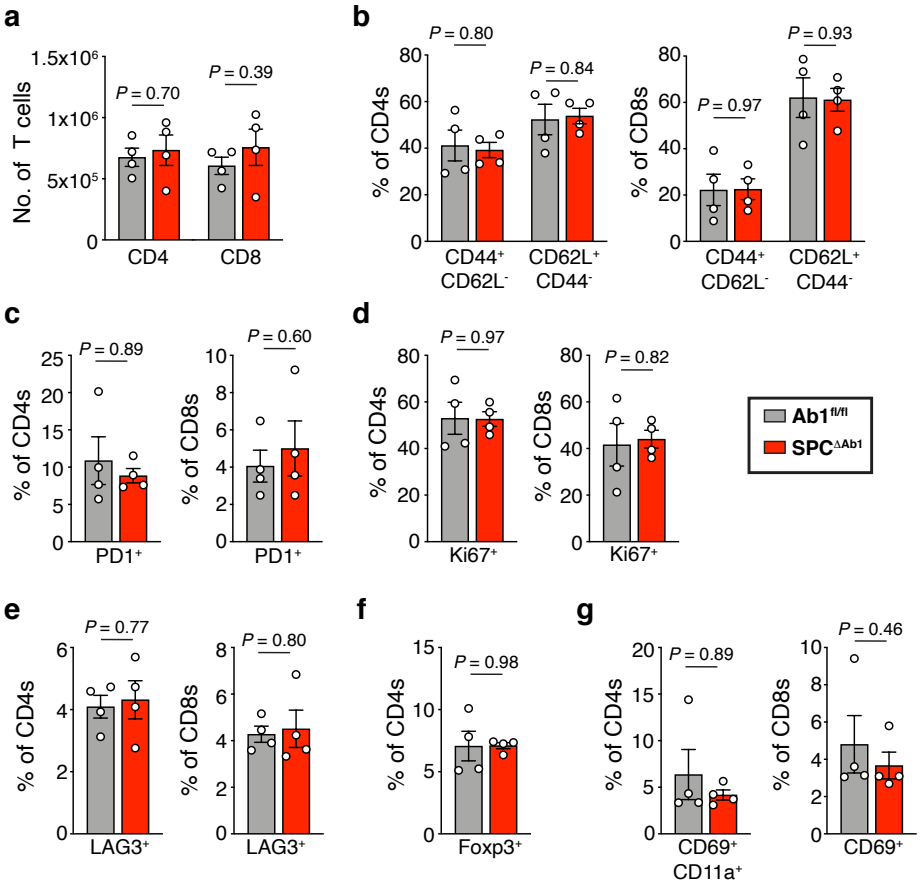

Figure 3.6: 7-month-old SPC$^{\Delta Ab1}$ mice demonstrate normal T cell homeostasis in the lung. a-g, *Ex vivo* flow cytometry analysis of naïve 7-month-old Ab1$^{fl/fl}$ and SPC$^{\Delta Ab1}$ mice lung T cells. Absolute number of lung CD4$^+$ and CD8$^+$ T cells (**a**), and frequency of lung CD4$^+$ and CD8$^+$ T cells expressing CD44, CD62L (**b**), PD1 (**c**), Ki67 (**d**), LAG3 (**e**), Foxp3 (**f**), and CD69, CD11a (**g**), as indicated; n=4 mice per strain from 1 experiment. Data shown are mean plus SEM, analyzed by unpaired two-tailed Student's *t*-test, Welch's *t*-test, or Mann-Whitney test depending on the distribution of the data.

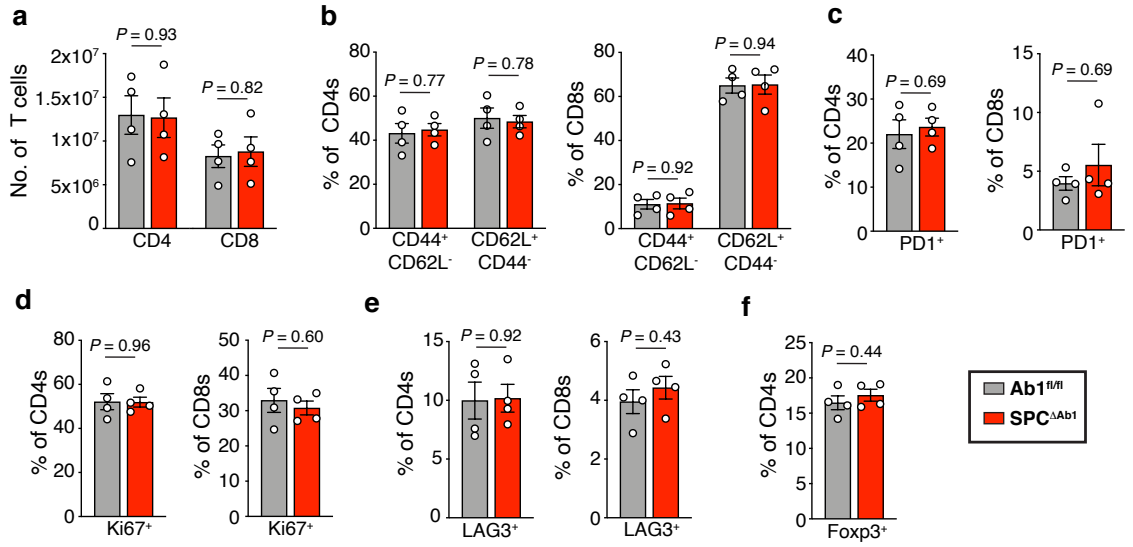

Figure 3.7: 7-month-old SPC$^{\Delta Ab1}$ mice demonstrate normal T cell homeostasis in the spleen. **a-f,** *Ex vivo* flow cytometry analysis of naïve 7-month-old Ab1$^{fl/fl}$ and SPC$^{\Delta Ab1}$ mice spleens. Absolute number of splenic CD4^{+} and CD8^{+} T cells (**a**), and frequency of CD4^{+} and CD8^{+} T cells expressing CD44, CD62L (**b**), PD1 (**c**), Ki67 (**d**), LAG3 (**e**), and Foxp3 (**f**), as indicated; n=4 mice per strain from 1 experiment. Data shown are mean plus SEM, analyzed by unpaired two-tailed Student's *t*-test or Mann-Whitney test depending on the distribution of the data.

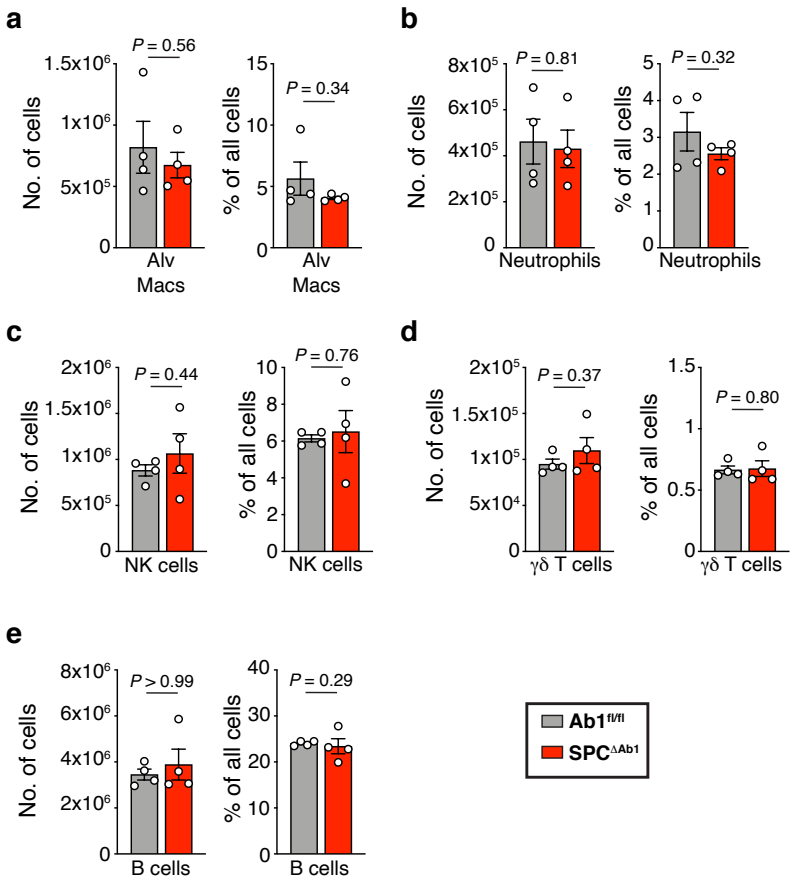

Figure 3.8: 7-month-old SPC$^{\Delta Ab1}$ mice exhibit normal numbers and frequencies of immune cells in the lung. a-e, *Ex vivo* flow cytometry analysis of naïve 7-month-old Ab1$^{fl/fl}$ and SPC$^{\Delta Ab1}$ mice lungs. Frequency and numbers of alveolar macrophages (**a**), neutrophils (**b**), NK cells (**c**), γδ T cells (**d**), and B cells (**e**), as indicated; n=4 mice per strain from 1 experiment. Data shown are mean plus SEM, analyzed by unpaired two-tailed Student's *t*-test or Mann-Whitney test depending on the distribution of the data.

Overall, these data suggest that at homeostasis, AT2 MHCII facilitates the development of various antigen-experienced lung CD4$^+$ and CD8$^+$ T cell populations, including regulatory T cells, as well as memory T cells and those expressing markers of activation and proliferation. The impact of AT2 MHCII on the T cell compartment is less pronounced in the spleen, it does not appear to impact non-T cell lung immune populations, and its contribution only becomes apparent with advanced mouse age.

We next explored whether the loss of AT2 MHCII and its impact on lung T cells might result in lung disease at homeostasis. To do this, we compared hematoxylin and eosin (H&E) staining of naïve 9-month-old SPC$^{\Delta Ab1}$ and Ab1$^{fl/fl}$ lungs. Both strains demonstrated normal, healthy lung architecture with minimal infiltrates (**Fig 3.9**), suggesting that loss of AT2 MHCII does not result in overt lung disease in these mice.

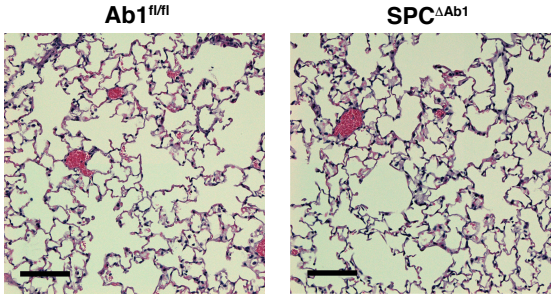

Figure 3.9: 9-month-old SPC$^{\Delta Ab1}$ mice demonstrate healthy lung histology with no inflammatory infiltrates. H&E staining of naïve 9-month-old Ab1$^{fl/fl}$ and SPC$^{\Delta Ab1}$ lungs, representative of n=3 mice per strain. Scale bar depicts 100 μm.

Finally, we also investigated whether AT2 MHCII might play a non-immunologic role at homeostasis. Specifically, we asked whether AT2 MHCII is required for the two main physiologic functions of AT2s: lung regeneration and surfactant production. AT2s sorted from SPC$^{\Delta Ab1}$ and Ab1$^{fl/fl}$ mice formed similar numbers of lung organoids *in vitro* (**Fig 3.10**). Furthermore, the SPC$^{\Delta Ab1}$ mice did not experience any respiratory disease at homeostasis, clinically or histologically (**Fig 3.9**); significant lung disease would be expected if surfactant biosynthesis were disrupted. Together, this suggests that AT2 MHCII is not required for either of these critical functions.

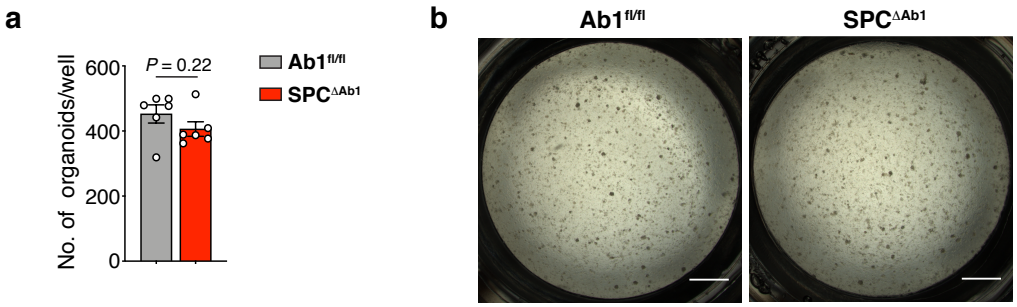

Figure 3.10: Loss of AT2 MHCII does not affect regenerative capacity. a, b, Numbers (**a**) and representative images (**b**) of lung organoid cultures formed by AT2s sorted from either or Ab1$^{fl/fl}$ and SPC$^{\Delta Ab1}$ mice. Data represent n=6 organoid cultures per strain, grown from AT2s originally sorted from n=1 mouse per strain. **a,** Bars represent mean plus SEM, and the data were analyzed by unpaired two-tailed Student's *t*-test. **b,** Scale bar depicts 1000 μm.

In summary, at homeostasis AT2 MHCII contributes to the regulation of the lung T cell compartment, promoting the development of various antigen-experienced T cell subsets. However, its impact is relatively modest in magnitude, only becoming apparent in older mice (14 m.o.), and it does not appear to result in overt lung disease.

<u>AT2 MHCII contributes to protection from respiratory viral disease</u>

We next assessed whether AT2 MHCII contributes to the outcome of lung infection. To do this, we used two respiratory virus infection models: mouse lung-adapted PR8 influenza A virus (IAV) as well as Sendai virus (SeV), a natural mouse pathogen similar to human parainfluenza virus. To assess the impact of AT2 MHCII on viral disease, we measured weight loss of SPC$^{\Delta Ab1}$ and Ab1$^{fl/fl}$ mice after infection with either IAV or SeV. SPC$^{\Delta Ab1}$ and Ab1$^{fl/fl}$ mice demonstrated similar weight loss IAV infection (**Fig 3.11a, Table 3.1**). However, after SeV infection, SPC$^{\Delta Ab1}$ mice on average experienced substantially more weight loss and delayed recovery compared

to the Ab1$^{fl/fl}$ group (**Fig 3.11b, Table 3.2**). We also assessed the impact of AT2 MHCII on mortality after infection with both viruses. SPC$^{\Delta Ab1}$ mice experienced reduced survival after IAV infection compared to Ab1$^{fl/fl}$ controls, 24% vs 50% respectively (**Fig 3.11c**). Similarly, after SeV infection, SPC$^{\Delta Ab1}$ mice had worse survival with approximately 2-fold higher mortality (28%) compared to the Ab1$^{fl/fl}$ controls (12%) (**Fig 3.11d**). Of note, here we display the aggregate analyses of multiple independent experiments, between which we did observe some variability in disease outcome; in some experiments the disease severity differences between the SPC$^{\Delta Ab1}$ and Ab1$^{fl/fl}$ mice were more pronounced, and in others less so (**Fig 3.12**).

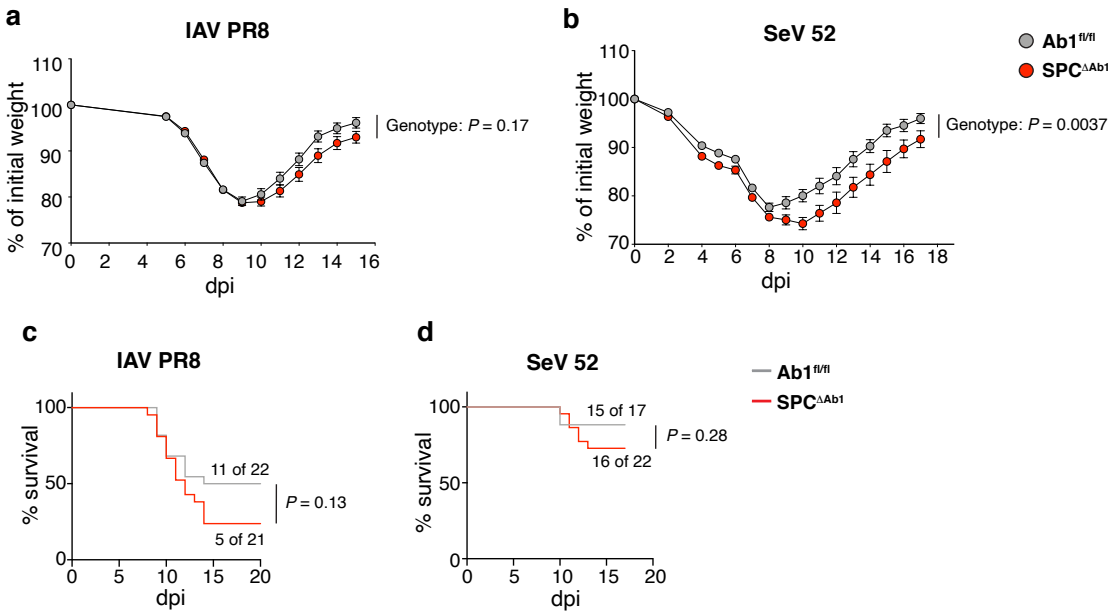

Figure 3.11: Loss of AT2 MHCII results in greater weight loss and reduced survival after respiratory viral infection. a-d, Comparison of Ab1$^{fl/fl}$ and SPC$^{\Delta Ab1}$ mice after infection with influenza strain PR8 (IAV PR8) (**a,c**) and Sendai virus strain 52 (SeV 52) (**b,d**). **a**,**b,** Weight loss with weights displayed relative to day of infection; n=43-53 mice per strain pooled from 6 independent experiments (**a**), and n=17-22 mice per strain pooled from 2 independent experiments (**b**). **c,d**, Mortality, with curves representing proportion surviving; n=21-22 mice per strain pooled from 2 independent experiments (**c**), and n=17-22 mice per strain pooled from 2 independent experiments (**d**). **a,b**, Data are mean plus SEM, analyzed by mixed-effects model with post-hoc multiple comparisons with Sidak's correction at each dpi. *P* values displayed represent overall model effects. Full statistical test results are in Tables 3.1 and 3.2. **c,d**, Survival curves were compared via Log-rank test.

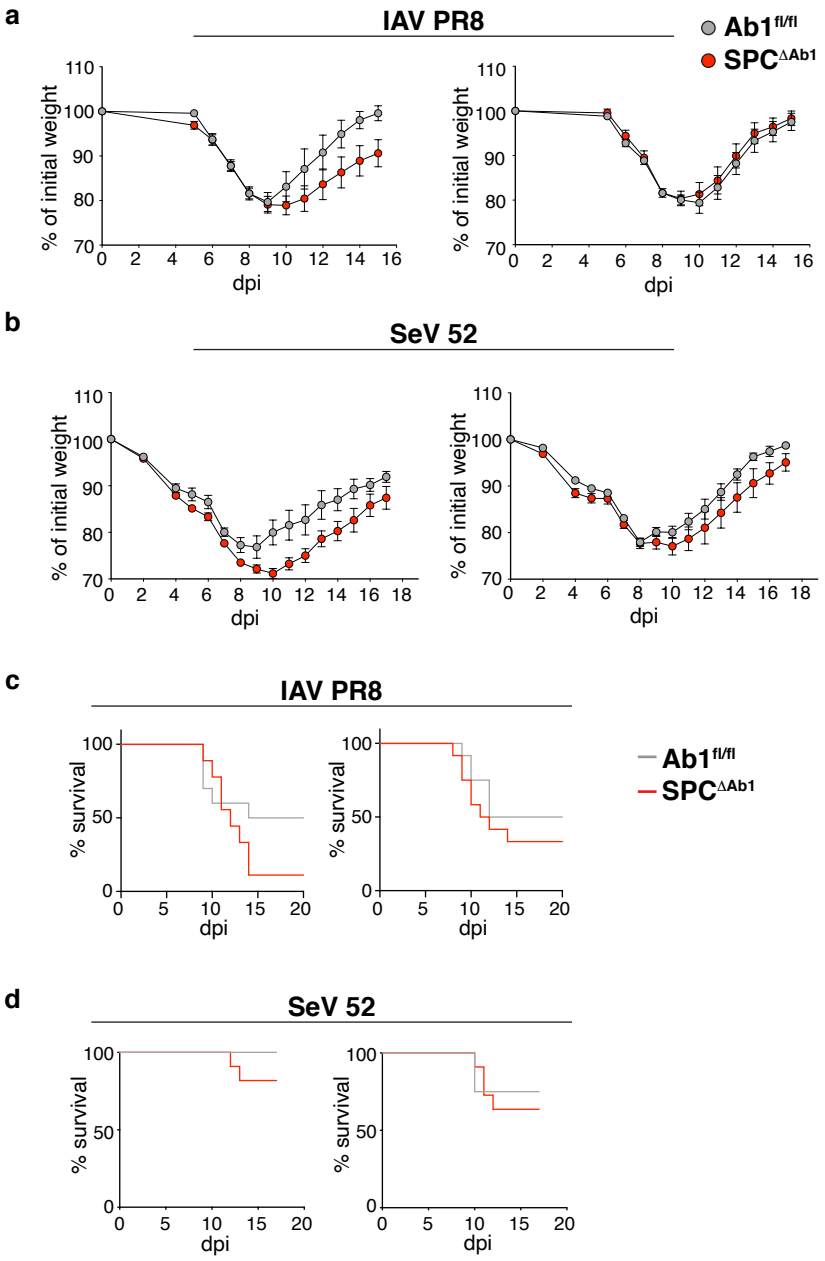

Figure 3.12: Differences in weight loss and survival between Ab1$^{fl/fl}$ and SPC$^{\Delta Ab1}$ mice were subject to experiment to experiment variation. **a-d**, Representative independent experiments of Ab1$^{fl/fl}$ and SPC$^{\Delta Ab1}$ mice after infection with influenza strain PR8 (IAV PR8) (**a,c**) and Sendai virus strain 52 (SeV 52) (**b,d**). **a**,**b,** Weight loss with weights displayed relative to day of infection; n=6-12 mice per strain (**a, left**), n=7-12 mice per strain (**a, right**), n=8-11 mice per strain (**b, left**), and n=9-11 mice per strain (**b, right**). **c,d**, Mortality, with curves representing proportion surviving; n=9-10 mice per strain (**c, left**), n=12 mice per strain (**c, right**), n=9-11 mice per strain (**d, left**), and n=8-11 mice per strain (**d, right**). **a-d,** Data are mean plus SEM of mice within one experiment only per graph.

We next asked whether AT2 MHCII antigen presentation might contribute to the control of viral replication, by measuring lung virus titers after infection with either IAV or SeV. There were no significant differences in IAV titers 7 days after infection between SPC$^{\Delta Ab1}$ and Ab1$^{fl/fl}$ mice (**Fig 3.13a**). Similarly, SeV titers 4, 7, and 9 days after infection were similar between the two strains (**Fig 3.13b**). As LAG3 has been shown to restrict lung CD4^{+} and CD8^{+} T cell responses during respiratory viral infections [160, 161], we also considered whether AT2 MHCII is required for LAG3-mediated T cell suppression during infection. However, we found similar frequencies and numbers of LAG3^{+} CD4^{+} and CD8^{+} T cells in the lungs of SPC$^{\Delta Ab1}$ and Ab1$^{fl/fl}$ mice 9 days after IAV infection (**Fig 3.14**). Thus, MHCII on AT2s serves to reduce morbidity and mortality in the setting of respiratory viral illness, without impacting LAG3^{+} T cell expansion or lung viral burden.

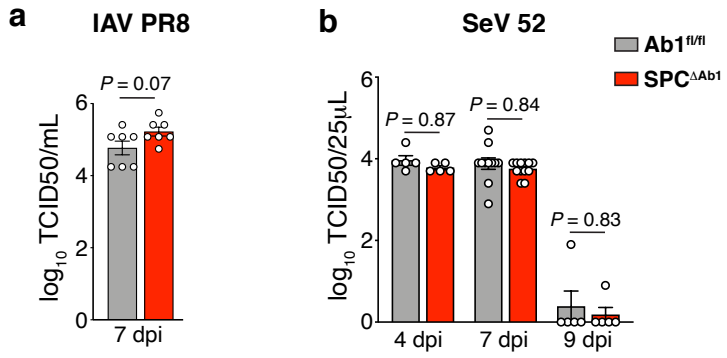

Figure 3.13: Loss of AT2 MHCII does not affect lung virus titers after respiratory viral infection. Comparison of Ab1$^{fl/fl}$ and SPC$^{\Delta Ab1}$ mice after infection with influenza strain PR8 (IAV PR8) (**a**) and Sendai virus strain 52 (SeV 52) (**b**). Lung virus titers on the days post-infection (dpi) indicated; n=7 mice per strain from 1 experiment (**a**), and n=5 mice per strain for days 4 and 9, n=11-12 per strain for day 7, pooled from 2 independent experiments (**b**). Bars are mean plus SEM of $\log_{10}$ transformed values, analyzed by unpaired two-tailed Student's *t*-test (**a**), and two-way ANOVA (genotype effect: *P*=0.2197) with post-hoc multiple comparisons with Sidak's correction. *P* values displayed represent post-hoc comparisons (**b**).

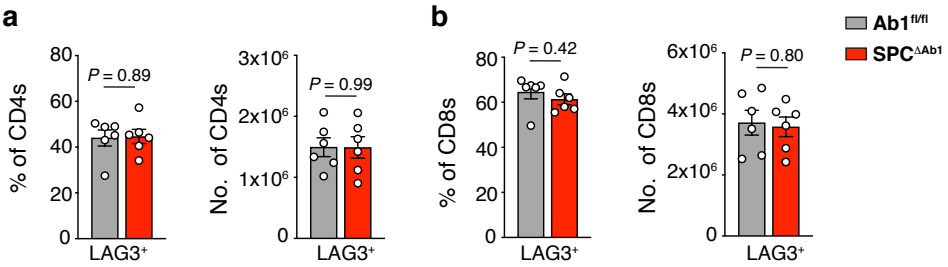

Figure 3.14: Loss of AT2 MHCII does not alter frequencies of LAG3⁺ T cells after influenza virus infection. a,**b** *Ex vivo* flow cytometry analysis of LAG3 expression by CD4⁺ and CD8⁺ T cells in Ab1$^{fl/fl}$ and SPC$^{\Delta Ab1}$ mice. Frequency and number of lung LAG3⁺ CD4⁺ (**a**) and CD8⁺ (**b**) T cells 9 days post IAV infection; n=6 mice per strain from 1 experiment. Data shown are mean plus SEM, and were analyzed by unpaired two-tailed Student's *t*-test.

In summary, these studies suggest that *in vivo* AT2 MHCII expression confers an appreciable advantage in respiratory viral disease outcome.

Overall model effects	
Factor	***P*-value**
Time	<0.0001
Genotype	0.1696
Genotype x Time	0.0002

Post-hoc comparison results by day	
Day post-infection	***P*-value**
5	>0.9999
6	>0.9999
7	0.9995
8	>0.9999
9	>0.9999
10	0.987
11	0.8544
12	0.738
13	0.3238
14	0.6217
15	0.5448

Table 3.1: Mixed-effects model analysis results for weight loss after IAV infection. Results of repeated measures mixed-effects model (REML) analysis with Geisser-Greenhouse correction factoring in both genotype and day post IAV infection as variables, with post-hoc multiple comparisons with Sidak's correction between the strains at each time point post infection. *P* values for the overall effects as well as for each post-hoc comparison are reported, calculated based on weights expressed as a percentage of initial weight. Data depicted in this table are in Figure 3.11a.

Overall model effects	
Factor	***P*-value**
Time	<0.0001
Genotype	0.0037
Genotype x Time	<0.0001

Post-hoc comparison results by day	
Day post-infection	***P*-value**
2	0.5271
4	0.095
5	0.1109
6	0.5318
7	0.4242
8	0.741
9	0.4465
10	0.0429
11	0.2627
12	0.6094
13	0.4114
14	0.352
15	0.2886
16	0.4587
17	0.5085

Table 3.2: Mixed-effects model analysis results for weight loss after SeV infection. Results of repeated measures mixed-effects model (REML) analysis with Geisser-Greenhouse correction factoring in both genotype and day post SeV infection as variables, with post-hoc multiple comparisons with Sidak's correction between the strains at each time point post infection. *P* values for the overall effects as well as for each post-hoc comparison are reported, calculated based on weights expressed as a percentage of initial weight. Data depicted in this table are in Figure 3.11b.

3.3 Discussion

Here we demonstrate that AT2 MHCII modestly improves the outcome of respiratory virus disease *in vivo,* and that it also contributes to an increase in antigen-experienced T cells at homeostasis.

Given that AT2s constitutively express MHCII, we were surprised to find that mice lacking AT2 MHCII did not exhibit overt clinical disease at homeostasis in our studies. However, we did observe that the loss of AT2 MHCII resulted in alterations in lung T cell phenotypes in aged mice. We found that 14-month-old mice lacking AT2 MHCII had lower frequencies of lung memory $CD4^+$ and $CD8^+$ T cells and higher frequencies of naïve T cells. Furthermore, in $SPC^{\Delta Ab1}$ mice, fewer lung T cells expressed markers of activation or proliferation, and fewer $CD4^+$ T cells had developed into Tregs, compared to $Ab1^{fl/fl}$ mice. All these observations are consistent with either less T cell activation/antigen-encounter overall, or less proliferation or survival of antigen-experienced T cells, in the lungs of $SPC^{\Delta Ab1}$ mice. We did not observe the same impact on T cell phenotypes in the spleen – differences were smaller, if not absent – suggesting that the impact on T cells in $SPC^{\Delta Ab1}$ mice is primarily in the lung. The most likely mechanistic explanation is that, at homeostasis, AT2 MHCII antigen presentation to $CD4^+$ T cells enhances the local expansion and/or survival of antigen-specific $CD4^+$ T cells in the lungs. As $CD4^+$ T cell help is critical for the development of memory $CD8^+$ T cells [162-164], this AT2 MHCII-dependent $CD4^+$ T cell expansion would also promote lung $CD8^+$ T cell memory formation; this is consistent with our observations that $Ab1^{fl/fl}$ control mice demonstrate higher levels of activated and memory $CD8^+$ T cells, in addition to $CD4^+$s, compared to $SPC^{\Delta Ab1}$ mice. Overall, our data suggest that, at homeostasis, local AT2 MHCII antigen presentation

promotes an increase in both antigen-experienced $CD4^+$ and $CD8^+$ T cells in the lungs.

We did not observe the same alterations to lung T cells in 7-month-old $SPC^{\Delta Ab1}$ mice, nor did we observe any histological evidence of lung disease in 9-month-old $SPC^{\Delta Ab1}$ mice. One potential reason for this is that the specific pathogen free (SPF) homeostasis environment of our mouse colony is characterized by artificially low levels of antigen. Thus, the putative antigens presented by AT2 MHCII at homeostasis to lung $CD4^+$ T cells are limited to the narrow range of inhaled environmental antigens present under SPF conditions. The restricted nature of these homeostatic exposures may explain why we only observed significant impacts on the lung T cell compartment in 14-month-old, but not 7-month-old adult mice; it is likely that a longer duration of this low level antigen exposure is needed for the differences in T cell activation to become amplified. Along these lines, as our lung histological analyses demonstrating the absence of lung disease in $SPC^{\Delta Ab1}$ mice were performed in 9-month-old mice, it is possible that these studies were undertaken at too young an age; if lung pathology were assessed at an older age, for example when T cell alterations are readily apparent, it is possible that histological disease would be present. However, it is also possible that under SPF conditions of such restricted antigen encounter, the modest lessening in T cell activation and memory formation we observed would not lead to lung disease even at an advanced age. Alternatively, it is also possible that even in more physiologic situations of abundant environmental antigen encounter, the contribution of AT2 MHCII may still be accessory, impacting lung T cell phenotypes, but in a manner too small to result in true lung disease at homeostasis.

Overall, our data suggest that AT2 MHCII contributes to the development of antigen-experienced memory, activated, and regulatory T cells in the lung at

homeostasis. While the impact we observed was statistically significant, it represented an overall modest change in T cell subset frequencies, and it did not result in lung disease. We further expand on the potential reasons for this and the potential role for AT2 MHCII at homeostasis in more detail in **chapter 5**.

Although the effect was not dramatic and not observed in all experiments, we nonetheless found that, on average, AT2 MHCII also confers some degree of protection in the setting of primary respiratory virus infection, particularly for survival. Although the mechanism underlying this effect is still under active investigation, the most likely explanation is that it is $CD4^+$ T cell mediated. $CD4^+$ T cells play a number of important roles during the primary response to respiratory virus infections that could be affected by the loss of MHCII AT2.

$CD4^+$ T cells have been demonstrated to be cytolytic during influenza virus infections [119] and can facilitate complete flu and Sendai viral clearance in $CD8^+$ T cell-deficient mice [165, 166]. Thus, one possibility is that AT2 MHCII facilitates $CD4^+$ T cell recognition and killing of AT2s, which are major targets of infection *in vivo*, thereby leading to faster viral clearance and improved diseased outcomes. While this potential cytolysis may indeed be lost in $SPC^{\Delta Ab1}$ mice, it does not appear to be necessary for viral clearance or to substantially change virus loads in our studies (**Fig 3.13**), corroborating prior work demonstrating that nonhematopoietic cell MHCII expression is not required for clearance of influenza virus infection [167]. Thus, loss of $CD4^+$ T cell cytolysis of infected AT2s is an unlikely explanation for the worse disease we observed in $SPC^{\Delta Ab1}$ mice.

Another function of $CD4^+$ T cells during primary infection is to provide help to $CD8^+$ T cells, which are the major drivers of viral clearance during infection. The

similarity in virus loads between mice with and without AT2 MHCII in both infection models (**Fig 3.13**) suggests that $CD8^+$ T cell cytolytic function is not substantially altered. Whether or not this means that $CD4^+$ T cell help to $CD8^+$ T cells is also unaffected by loss of AT2 MHCII is unclear. Mice deficient in $CD4^+$ T cells exhibit essentially normal viral clearance in both primary influenza and Sendai virus infections; although $CD8^+$ T cells may exhibit poorer per-cell cytotoxicity [168], virus clearance in only slightly delayed [166, 168-171]. Thus, it is possible that $CD4^+$ T cell help is suboptimal in the absence of AT2 MHCII but this may not be manifest in bulk virus titers at the time points studied. Even if $CD4^+$ T cell help is impaired in $SPC^{\Delta Ab1}$ mice, given that $CD8^+$ viral clearance seems to remain intact, poor $CD4^+$ T cell help to $CD8^+$s is unlikely to account for the increased mortality observed in our studies.

As virus titers were not affected by the loss of AT2 MHCII, it is possible that, instead of an inadequate antiviral response, the lack of AT2 MHCII results in increased immunopathology, which is what then leads to worse survival. Indeed, key future histological studies will assess whether the increased mortality that results from loss of AT2 MHCII is associated with more severe lung damage and inflammation. One mechanism by which a loss of MHCII could exacerbate inflammatory damage would be via a LAG3-dependent mechanism. The T cell inhibitory receptor LAG3 contributes to the restriction of T cell responses during Sendai and influenza virus infections [160, 161], and MHCII is its major ligand; if MHCII specifically on AT2s is a primary ligand for these antiviral T cells in the lung, then the loss of this inhibitory checkpoint would result in excessive T cell expansion and inflammation. However, we demonstrated similar numbers and frequencies of $LAG3^+$ $CD4^+$ and $CD8^+$ T cells in mice with and without MHCII on AT2s during infection, suggesting that AT2 MHCII is not required to

regulate this population. Thus, loss of LAG3-mediated T cell suppression is unlikely to account for the worse disease in SPC$^{\Delta Ab1}$ mice.

Another mechanism by which loss of AT2 MHCII could result in immunopathology is by altering the cytokine production characteristics of lung infiltrating CD4$^+$ T cells. Although CD4$^+$ T cells are primed in the lymph nodes to develop into a particular Th phenotype, Th1 in the case of Sendai and influenza viral infections, their functional properties retain some degree of plasticity and can be further modified at the site of infection in the effector phase [6, 15, 16, 120, 121]. Thus, it is possible that AT2s help to reinforce Th1 CD4$^+$ phenotype and facilitate the development of a protective CD4$^+$ T cell cytokine milieu. Future studies will assess whether loss of AT2 MHCII results in changes to the quality of CD4$^+$ cytokine production, for example skewing towards the production of Th2 or Th17 cytokines that are associated with immunopathology [4, 5, 172].

A final possibility is that AT2 MHCII helps to facilitate proper CD4$^+$ T cell localization during infection to specific regions within the lung experiencing high virus loads. Thus, AT2 MHCII may not directly lead to changes in CD4$^+$ T cell number or function, but instead may help to distribute them to sites experiencing particularly severe alveolar damage. Previous studies demonstrate that during lung injury, CD4$^+$ Tregs help to facilitate lung repair by enhancing AT2 proliferation [173, 174]. Thus, it is possible that AT2 MHCII helps to facilitate disease recovery and prevent mortality by targeting CD4$^+$ T cells to the areas most in need of healing. Future imaging studies will address this localization question.

Overall, although we did observe that loss of AT2 MHCII results in worse survival during flu and Sendai virus infections, which may occur via the potential

mechanisms just described, the effects were modest and not always consistent. One possible explanation for this small effect is that in situations of inadequate $CD4^+$ T cell function – failure to develop cytotoxic capacity, failure to provide $CD8^+$ T cell help, low Th1 cytokine production – other immune mechanisms can compensate to fill the void and facilitate recovery, masking the defect. Indeed, during primary flu or Sendai virus infections, even mice totally deficient in $CD4^+$ T cells experience similar disease and mortality to wild-type mice, with almost normal virus clearance kinetics [166, 168-171] (although, importantly, these studies were done with less pathogenic strains of influenza and Sendai virus). Thus, it is possible that looking at clinical outcomes such as mortality and weight loss during primary respiratory virus infection will not capture even large differences in $CD4^+$ T cell function that result from the loss of AT2 MHCII. Another explanation for the small benefit afforded by AT2 MHCII is that the contribution is truly small, that AT2 MHCII does not alter the $CD4^+$ T cell response to a significant degree. To understand which of these explanations is more likely, a more extensive characterization of the antiviral $CD4^+$ T cell response and $CD4^+$ T cell functionality and localization in mice with and without AT2 MHCII is needed and will be a major focus of future study. Additionally, as discussed in **chapter 5**, we will explore other disease models in which $CD4^+$ T cell dysfunction may be more impactful and phenotypically apparent.

We observed experiment-to-experiment variability in viral infection disease outcome, particularly weight loss; in some experiments, $SPC^{\Delta Ab1}$ mice exhibited substantially worse weight loss compared to controls, but in other experiments they were similar (**Fig 3.12**). In this dissertation we have displayed the averages and aggregated data across all of these experiments to best summarize the consequences

of loss of AT2 MHCII that we observed, but we still do not fully understand the reason for such variability between experiments. The most likely explanation is that there is an additional modifying or contributing factor that exacerbates the impact of AT2 MHCII loss; when this factor is present, the additional loss of AT2 MHCII causes $SPC^{\Delta Ab1}$ mice to have more severe disease, but when it is not, absent AT2 MHCII expression is not sufficient to induce a worse phenotype. We explored various explanations as to what this stochastic variable could be including mouse age, sex, starting weight, age of tamoxifen administration, time between tamoxifen administration and infection, and time of day at which the mice were infected. None of these parameters appeared to explain the instances in which $SPC^{\Delta Ab1}$ mice experience more or less severe disease compared to controls. One additional possibility we considered was the effect of humidity, as this has been shown to alter influenza disease severity [175]; however, the humidity in the animal facilities is carefully controlled, and we observed variability in disease outcome in some experiments that were performed only days apart. Another potential modifier that we considered but have not yet explored is temporal changes in the microbiome, which is heterogeneous in the lung across time and between mice [176], and can alter their susceptibility to respiratory viral infections [177].

Another possible reason for the experiment to experiment variability we observed could stem from caveats in the mouse model we used for these experiments. As shown in **Fig 3.2**, mice of the floxed $I\text{-}A^b$ background, regardless of Cre expression, demonstrate heterogeneous and, on average, lower MHCII expression by a variety of MHCII-expressing cell types compared to mice without floxed MHCII alleles. This floxed $I\text{-}A^b$ background alone increases disease severity in the mice; compared to

SPC^{Cre} mice, the Ab1$^{fl/fl}$ controls look overtly more hunched, ruffled, and inactive, and also exhibit more severe weight loss and mortality, as well as somewhat slower viral clearance, after infection (**Fig 3.15**), even though both have intact AT2 MHCII expression. Based on this observation, we used Ab1$^{fl/fl}$ mice as controls for the SPC$^{\Delta Ab1}$ mice in our experiments since both are subject to this floxing effect; however, this heterogeneity in APC MHCII expression afforded by the floxed I-A^{b} background could have contributed the differences in disease severity we observed. A major reason for the inter-experiment variability we experienced was that the Ab1$^{fl/fl}$ control mice exhibited different disease severity from experiment to experiment, which made the differences relative to SPC$^{\Delta Ab1}$ mice bigger or smaller; it is possible that variable MHCII expression on key APCs from the floxed I-A^{b} background between experiments contributed to different disease outcomes in the Ab1$^{fl/fl}$ strain. It is also possible that there are additive effects with these alterations and loss of AT2 MHCII in the SPC$^{\Delta Ab1}$ mice; for example, perhaps loss of AT2 MHCII is particularly impactful on disease outcome in the mice with especially low DC or B cell MHCII expression from the floxed I-A^{b} background. Given these considerations, an important avenue of future work in our laboratory will be to generate a new strain of floxed I-A^{b} mice that do not exhibit the same global disruptions to MHCII expression, which will ideally serve as a “cleaner” system to isolate just the impact of AT2 MHCII.

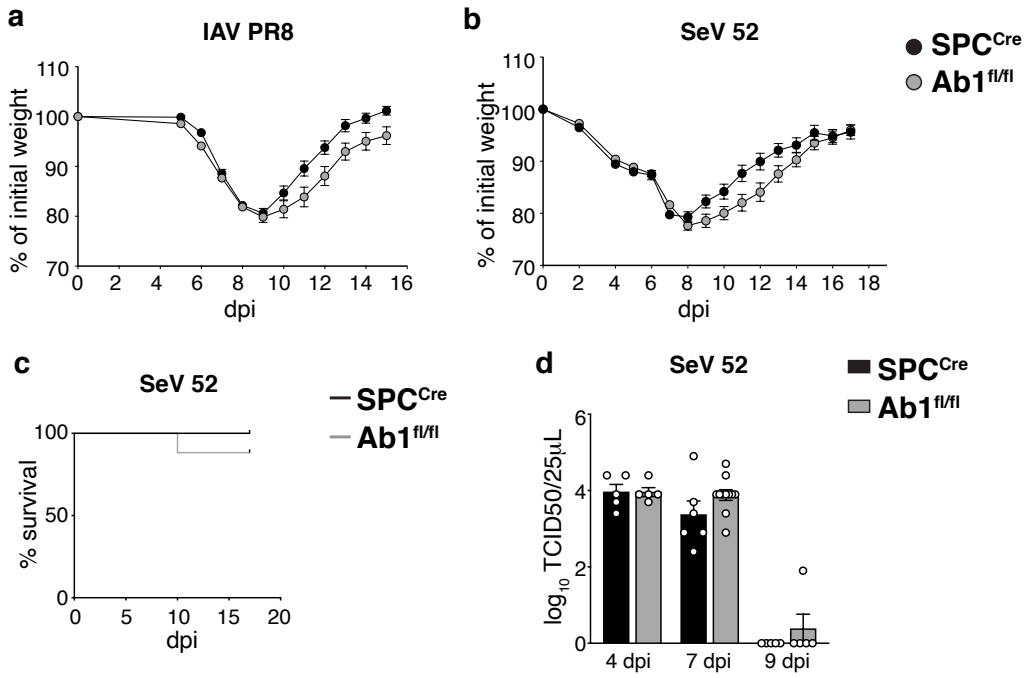

Figure 3.15: Ab1$^{fl/fl}$ control mice exhibit worse weight loss and disease and delayed viral clearance compared to SPC^{Cre} control mice after virus infection. a-d, Comparison of Ab1$^{fl/fl}$ and SPC^{Cre} mice after infection with influenza strain PR8 (IAV PR8) (**a**) and Sendai virus strain 52 (SeV 52) (**b-d**). **a**,**b,** Weight loss with weights displayed relative to day of infection; n=21-27 mice per strain pooled from 3 independent experiments (**a**), and n=17-20 mice per strain pooled from 2 independent experiments (**b**). **c,** Mortality, with curves representing proportion surviving; n=17-20 mice per strain pooled from 2 independent experiments. **d,** Lung virus titers on the days post-infection (dpi) indicated; n=5 mice per strain for days 4 and 9, n=5-11 per strain for day 7, pooled from 2 independent experiments. Bars are mean plus SEM of log_{10} transformed values. **a,b**, Data are mean plus SEM. Mortality and viral titers of SPC^{Cre} mice after IAV PR8 infection were not studied and therefore no graphs are shown.

In summary, we observed that loss of AT2 MHCII resulted in lower proportions of memory, activated, and regulatory phenotype lung T cells at homeostasis, although this effect was only apparent in in aged mice and did not result in overt lung disease. In the setting of respiratory virus infection, we found that, on average, the loss of AT2 MHCII results in modestly increased weight loss and mortality. As previously discussed, there are a variety of potential mechanisms underlying the effects of AT2

MHCII we observed *in vivo*, both in terms of how its effects could be mediated and why its impact is relatively small. In the next chapter, I more closely examine the latter, by more rigorously and directly assessing the capacity of AT2s to present antigen via MHCII to $CD4^+$ T cells.

CHAPTER 4:

TYPE II ALVEOLAR CELLS EXHIBIT RESTRAINED MAJOR HISTOCOMPATIBILITY COMPLEX II ANTIGEN PRESENTATION

Adapted from the following manuscript:

Sushila A. Toulmin, Chaitali Bhadiadra, Andrew J. Paris, Jeremy Katzen, Maria C. Basil, Edward E. Morrisey, G. Scott Worthen, and Laurence C. Eisenlohr. (*Manuscript submitted*)

4.1 Introduction

In the previous chapter, we demonstrated that loss of AT2 MHCII results in more severe disease in the setting of respiratory virus infection. Furthermore, we observed that in the absence of AT2 MHCII at homeostasis in aged mice, higher proportions of lung $CD4^+$ and $CD8^+$ T cells remain naïve to antigen encounter. However, the impact of AT2 MHCII was relatively modest in both cases. In **3.3** and **5.6**, we discuss potential explanations for these small effects, relating to caveats of the particular homeostasis and disease models we used. However, in this chapter, we also explore the possibility that the more restrained impact of AT2 MHCII *in vivo* results from limited AT2 MHCII presentation to $CD4^+$ T cells.

Other groups have explored AT2 MHCII antigen presentation previously, but their reports have been conflicting [106-108, 110]. Furthermore, in these prior studies it is difficult to discern the true MHCII antigen presentation capacity of AT2s for several reasons, discussed at length in **4.3** with key limitations mentioned here briefly. One major consideration is that in all previous studies, $CD4^+$ T cell activation is used as the main read out of AT2 MHCII presentation; however, $CD4^+$ T cell activation can also be influenced by factors other than MHCII presentation, primarily by costimulation, and this was only controlled for directly in one prior study [110]. Furthermore, in no prior studies was AT2 MHCII presentation compared directly to that of professional APCs, and in no case was the amount of available source antigen quantified. Therefore, the relative efficiency and magnitude of AT2 MHCII presentation is still largely unknown. Thus, here we more rigorously examine the capacity of AT2s to present antigen via MHCII, comparing to professional APCs, both *in vitro* and *in vivo* in multiple antigen systems.

4.2 Results

AT2s exhibit restrained antigen presentation capacity via MHCII

Although loss of AT2 MHCII worsened respiratory virus disease, the effect was smaller than anticipated based on the abundance of AT2s in the lung [111] and the magnitude of AT2 MHCII expression. A potential explanation is limited MHCII antigen processing and presentation by AT2s, which would be advantageous in constraining the amplification of inflammatory T cell responses that could disrupt the lung gas-exchange parenchyma.

To investigate the antigen presentation function of AT2s, we first evaluated the ability of AT2s to stimulate flu peptide/MHCII complex-specific costimulation-independent T cell hybridomas (**Fig 4.1a**). AT2 presentation of five different epitopes from live virus was undetectable (**Fig 4.1b,c**), in contrast to professional APCs that presented all five. Poor presentation by AT2s was not due to a failure of *in vitro* infection, as AT2s were infected to levels higher than comparator professional APCs (**Fig 4.2**). Limited presentation was observed across multiple MHCII alleles, B6 I-A^b (**Fig 4.1b**) and BALB/c I-E^d (**Fig 4.1c**), was not the result of protein source, as both HA and NA-derived epitopes were similarly affected (**Fig 4.1b, c**), and was similar for epitopes generated by both exogenous ($HA^{107-119}$) and endogenous (NA^{79-93}) processing pathways [178] (**Fig 4.1c**). Even when pulsed with synthetic peptides, AT2s were able to present only three out of five epitopes (HA^{91-107}, $HA^{302-313}$, NA^{79-93}) (**Fig 4.1b,c**). Thus, AT2s exhibited a global impairment in the capacity to present MHCII-restricted epitopes *in vitro*.

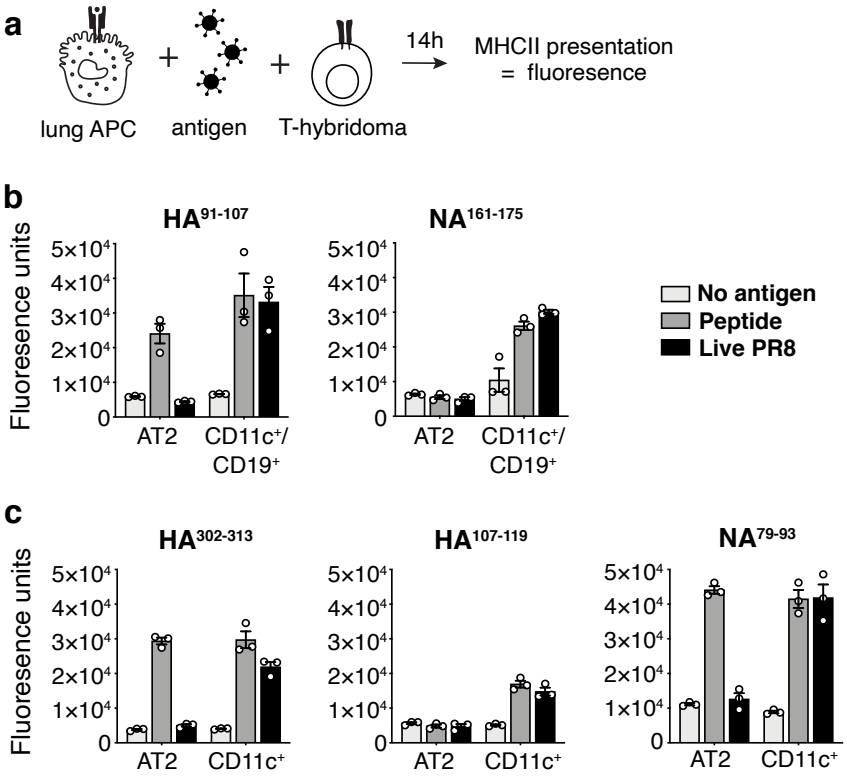

Figure 4.1: AT2s exhibit a globally restricted capacity to present individual influenza virus epitopes via MHCII *in vitro*. a, Schematic of hybridoma presentation assay. **b**,**c**, Presentation of MHCII-restricted flu peptides by B6 AT2s and a mixed population of CD11c$^+$ and CD19$^+$ lung cells (**b**) or BALB/c AT2s and CD11c$^+$ lung cells (**c**) sorted from naïve mice then incubated with synthetic peptide or live virus, reflected by NFAT-*LacZ*-inducible T cell hybridoma activation and cleavage of a fluorogenic β-galactosidase substrate; bars shown represent 3 technical replicates plus SEM from 1 experiment, representative of 3 similar independent experiments for (**b**).

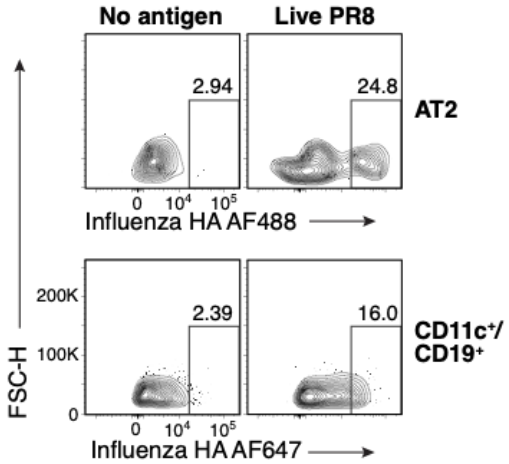

Figure 4.2: AT2s are robustly infected with influenza virus *in vitro*. Surface influenza hemagglutinin (HA) expression by B6 AT2s (top) and a mixed population of CD11c$^+$ and CD19$^+$ lung cells (bottom) sorted from naïve mice then incubated with no antigen (left) or live virus (right) in vitro for 14h. These plots reflect the APCs used in the hybridoma assay in Figure 4.1b. The frequency of HA$^+$ cells is shown above the gates, which were drawn based on the no antigen conditions. Two different fluorophore conjugated versions of the same anti-HA antibody were used because the AT2 and CD11c$^+$/CD19$^+$ populations were already labeled with different fluorophores (APC and FITC, respectively) from the cell sorting process.

Assays of AT2 function *in vitro* may be suboptimal due to reduced viability after cell sorting and the gradual de-differentiation of AT2s in standard tissue culture [179, 180]. Additionally, measuring presentation on an individual epitope basis may underestimate the presentation of all possible MHCII-restricted flu peptides. Thus, we next examined AT2 *in vivo* flu peptide/MHCII complex formation, by co-culturing *in vivo*-infected AT2s from wild-type or MHCII$^{-/-}$ B6 mice taken 4 days post influenza infection with polyclonal splenic CD4$^+$ or CD8$^+$ T cells taken 9 days post-infection, in the presence of soluble anti-CD28 (**Fig 4.3a**). MHCII presentation was detected via T cell IFNγ production captured by ELISpot. AT2s from flu-infected mice were capable of stimulating both CD4$^+$ and CD8$^+$ T cells to produce IFNγ (**Fig 4.3b**). Stimulation of CD4$^+$ T cells, but not CD8$^+$ T cells, was abrogated when MHCII$^{-/-}$ flu-infected AT2s were used as APCs, confirming that stimulation of CD4$^+$ T cells by AT2s was MHCII-dependent. However, consistent with our *in vitro* studies, AT2 presentation to CD4$^+$ T

cells was markedly less efficient than professional APCs, in this case CD103$^+$ CD11c$^+$ cells taken from the same lungs; despite being 9 times more infected, AT2s (99% infected, **Fig 4.4**) stimulated less than half the IFNγ production than the comparator APCs (11% infected, **Fig 4.4**).

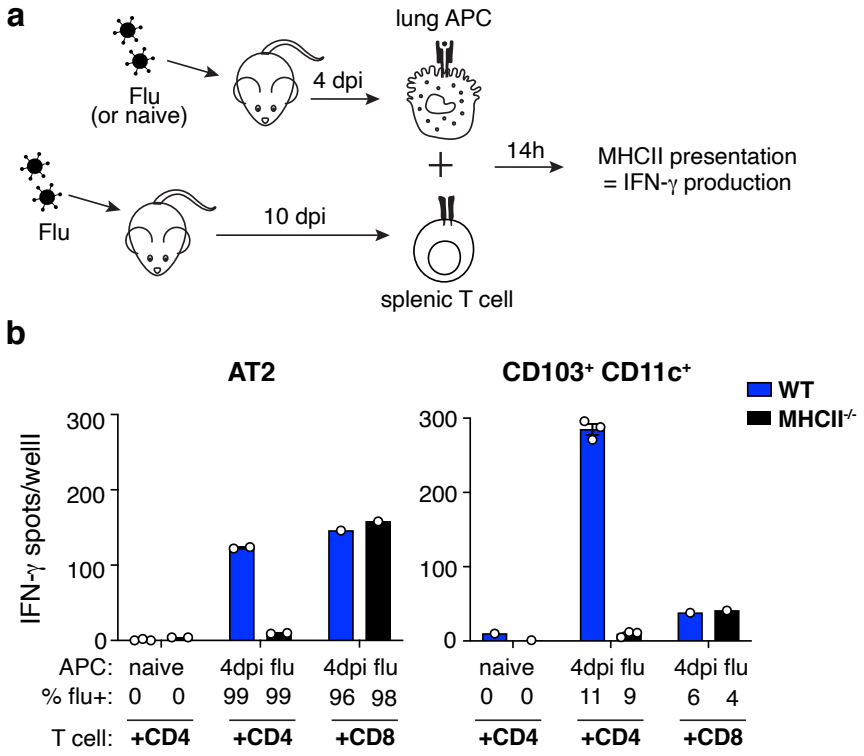

Figure 4.3: *In vivo*-infected AT2s exhibit poor presentation of influenza virus epitopes to polyclonal CD4$^+$ T cells via MHCII. a, Schematic of primary T cell ELISpot presentation assay. **b,** Presentation of MHCII-restricted flu peptides by lung AT2s and CD103$^+$ CD11c$^+$ APCs sorted from naïve or flu-infected WT or MHCII$^{-/-}$ B6 mouse lungs 4 dpi, measured as the production of IFN-γ by responding flu-experienced splenic CD4$^+$ and CD8$^+$ T cells (as indicated); "APC %flu+" numbers describe the proportion of each APC type that was flu-infected (shown in Fig 4.4), and bars shown represent 1-3 technical replicates plus SEM from 1 experiment, representative of 2-3 similar independent experiments.

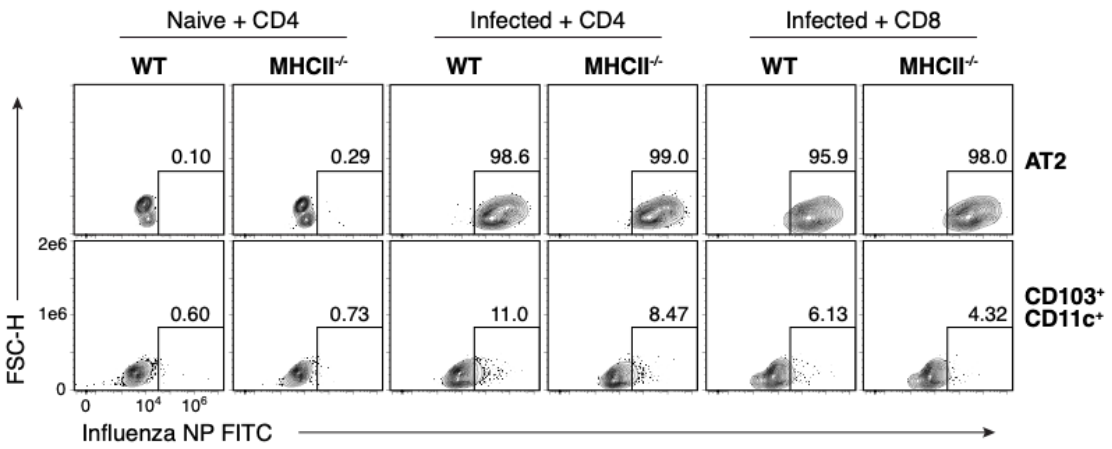

Figure 4.4: AT2s are robustly infected with influenza virus *in vivo*. Intracellular influenza nucleoprotein (NP) expression by B6 AT2s (top) and $CD103^+CD11c^+$ lung cells (bottom) sorted from naïve or flu-infected WT or $MHCII^{-/-}$ B6 mouse lungs 4 dpi and incubated with $CD4^+$ and $CD8^+$ T cells *in vitro* for 14h (as indicated). These plots reflect the antigen presenting cells used in the ELISpot presentation assay illustrated in Figure 4.3b. The frequency of NP^+ cells is shown above the gates, which were drawn based on the naïve conditions.

We considered that the high degree of AT2 infection in our assays might impair their capacity to process and present antigen. To address this, we measured MHCII antigen presentation using a non-infectious model system, by staining lungs directly *ex vivo* with the peptide/MHCII complex-specific "YAe" antibody [181] (**Fig 4.5a**). YAe detects $E\alpha^{52-68}$/I-A^b complexes, which form in [BALB/c x B6] F1 mice as they are composed of a peptide from I-E^d (BALB/c-derived) presented by I-A^b (B6-derived). In naïve F1 mice, AT2s had low yet detectable YAe staining above the background levels of B6 AT2s (**Fig 4.5b,c**). However, YAe staining of F1 AT2s was significantly lower than that of F1 lung B cells (**Fig 4.5b,c**). This could not be explained by differences in expression of the source proteins, I-A^b and I-E^d, which are similarly expressed by AT2s and B cells at homeostasis, if not slightly higher in AT2s (**Fig 4.6a,b**). These results indicate that AT2s are capable of forming $E\alpha^{52-68}$/I-A^b complexes at steady state, but they do so far less efficiently than do B cells.

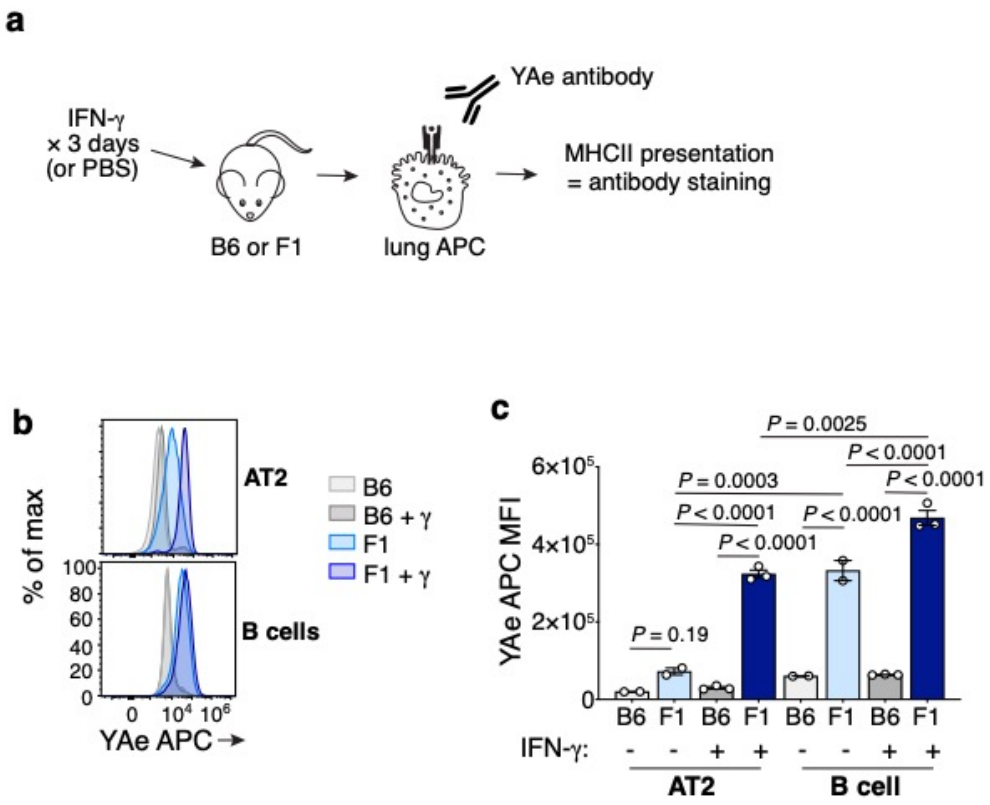

Figure 4.5: AT2 MHCII presentation capacity is enhanced in the setting of inflammation but remains limited. a, Schematic of YAe presentation assay. **b,c,** $E\alpha^{52-68}$/I-A^b complex formation by AT2s and B cells, detected by *ex vivo* YAe antibody staining of lungs from WT B6 or F1 [BALB/c x B6] mice treated with PBS or IFNγ. **b,** Plots represent n=4-6 mice per group total from 2 independent experiments. **c,** Bars represent mean plus SEM and depict n=2-3 mice per group from 1 experiment, representative of 2 similar independent experiments (total n=4-6). Data were analyzed by three-way ANOVA with multiple comparisons with Sidak's correction. *P* values displayed represent post-hoc comparisons of interest.

To better approximate the setting of viral infection, we also treated mice with IFNγ and then measured $E\alpha^{52-68}$/I-A^b complex formation. AT2 YAe staining was significantly increased in F1 mice after treatment with IFNγ, but was again lower than B cells in the same mice (**Fig 4.5b,c**). To assess the contributors to increased MHCII presentation in AT2s, we evaluated changes in expression of I-A^b, I-E^d, and H2M, all of which are required for $E\alpha^{52-68}$/I-A^b complex formation [80]. Both I-A^b and I-E^d increased in AT2s after IFNγ administration (**Fig 4.6a,b**). IFNγ also induced some AT2s to express

H2M$\alpha\beta$2, which is absent at baseline (**Fig 4.6c,d**). Although H2M$\alpha\beta2^+$ AT2s exhibited more YAe staining than H2M$\alpha\beta2^-$ AT2s, both populations stained highly (**Fig 4.6e**), suggesting that a higher magnitude of H2M contributes to enhanced Eα^{52-68}/I-A^b presentation, but the specific H2M$\alpha\beta$2 isoform is not required. Thus, AT2 MHCII presentation increases during IFNγ inflammation due to the upregulation of several MHCII presentation mediators, but it is still less efficient than that of professional APCs.

Taken together, these data demonstrate that AT2s are capable of presenting antigen via MHCII to CD4$^+$ T cells, and this is enhanced in the setting of inflammation; however, compared to professional APCs they exhibit limited antigen presentation of MHCII-restricted epitopes derived from both viral and endogenous proteins, as well as some extracellular peptides. This restrained presentation capacity may explain the variability seen in prior studies of AT2 function owing to differences in the model systems used, in particular the level of antigen provided to the AT2s, as well as the specific epitopes studied.

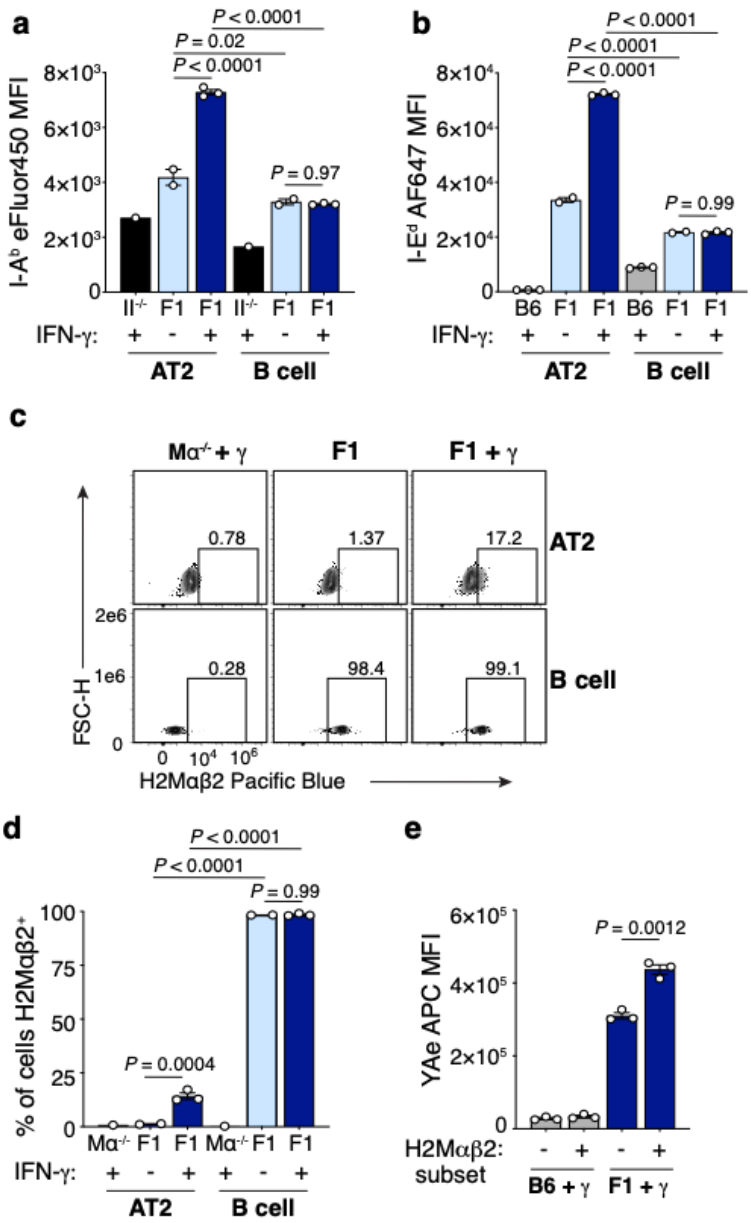

Figure 4.6: Expression of I-A^b, I-E^d, and H2M in AT2s increases after *in vivo* treatment with IFN-γ, but does not explain poor MHCII presentation. a,b, I-A^b (**a**) and I-E^d (**b**) expression by AT2s and B cells, detected by *ex vivo* flow cytometry staining of lungs from MHCII$^{-/-}$ (II$^{-/-}$) B6 (**a**), WT B6 (**b**), or F1 (**a,b**) mice treated with PBS or IFNγ (as indicated). **c,d,** Intracellular H2Mαβ2 expression by AT2s and lung B cells from F1 or *H2-DMα*$^{-/-}$ (Mα$^{-/-}$) B6 mice treated with PBS or IFNγ. Frequency of H2Mαβ2$^+$ cells is shown above gates (**c**), which were drawn separately for AT2s and B cells based on corresponding *H2-DMα*$^{-/-}$ cells. **e,** YAe staining of H2Mαβ2$^+$ and H2Mαβ2$^-$ subpopulations of AT2s from B6 and F1 mice treated with IFNγ. **c,** Plots represent n=4-6 mice per group total from 2 independent experiments. **a,b,d,e,** Bars represent mean plus SEM and depict n=2-3 mice per group from 1 experiment, representative of 2 similar independent experiments (total n=4-6) (**d,e**) or n=1-3 mice per group from 1 experiment (**a,b**). Data were analyzed by two-way ANOVA with multiple comparisons with Tukey's correction (**a,b,d**), and unpaired two-tailed Student's *t*-test (**e**). *P* values displayed represent post-hoc comparisons of interest (**a,b,d**).

4.3 Discussion

Here we demonstrate that, in contrast to professional APCs, AT2s exhibit a program of globally restrained MHCII antigen presentation. We believe that our findings represent the most accurate and definitive study of AT2 MHCII antigen presenting function to date, in comparison to conflicting prior reports on this subject, for the reasons outlined below.

In our assays, we used FACS to isolate AT2s, based on published cell surface markers [105] that we also validated in house (**Fig 6.1**). Using this method, we routinely obtained purities of >95%. Thus, our studies likely reflect the activities of AT2s rather than contaminating cells.

When cultured on plastic dishes *in vitro*, AT2s lose their defining characteristics and de-differentiate within a few days [144, 179, 180]. We took great care to avoid this issue, by assessing AT2 presentation capacity directly *ex vivo* with no *in vitro* maintenance required (YAe), or in *in vitro* co-cultures lasting no longer than approximately 14 hours (hybridomas, ELISpot). Furthermore, in two different approaches (YAe, ELISpot), we measured AT2 peptide/MHCII complexes that formed *in vivo*, to avoid artificial defects in AT2 MHCII presentation of *in vitro*-encountered antigens that might be an artifact of the instability of AT2 function *in vitro*.

In assays where MHCII antigen presentation is detected by $CD4^+$ T cell activation, the provision of costimulation is a critical modifier; failure to see $CD4^+$ T cell activation by an APC thus can result either from poor MHCII presentation or from a lack of costimulation. We avoided this confounding factor by using experimental approaches that were independent of AT2-derived costimulation; T cell hybridomas do not require costimulation, we provided exogenous anti-CD28 antibody to the

ELISpot assay, and the YAe antibody is a direct readout of $E\alpha^{52-68}$/I-A^b complexes. Thus, in our studies we feel confident that we were able to isolate the effects of just AT2 peptide/MHCII complex formation from the effect of costimulatory signals.

Another factor that directly impacts MHCII antigen presentation of a given epitope is the availability of the source antigen to the APC. For example, an APC may be highly capable of presenting a particular epitope, but if it expresses very low levels of the source protein, then peptide/MHCII presentation will be low. In our assays, we were able disentangle these influences by quantifying the antigen burden in our APCs of interest; we measured levels of influenza virus infection (hybridomas, ELISpot) and also quantified the levels of I-A^b and I-E^d (Yae) in AT2s and comparator APCs. Thus, we are able to interpret true efficiency of MHCII antigen presentation relative to the amount of available antigen.

Finally, MHCII antigen presentation capacity can be viewed on a global scale and also in relation to one particular epitope. For example, based on the expression of relevant processing mediators, an APC could exhibit poor ability to generate a wide diversity of MHCII-restricted epitopes (poor global MHCII presentation), but could still able to present a few specific peptide/MHCII complexes (efficient epitope-of-interest presentation). In our studies, we measured both bulk AT2 MHCII presentation to polyclonal $CD4^+$ T cells, as well as the presentation of specific I-E^d and influenza derived epitopes. Thus, we were able to capture MHCII presentation by AT2s at the individual epitope level and on a broader scale by assessing multiple antigen systems and polyclonal responses.

The variability in prior reports of AT2 MHCII antigen presentation capacity and its impact on $CD4^+$ T cell activation likely result from a combination of technical

limitations and differences in how the studies were performed, particularly in relation to the considerations discussed above. In previous studies of AT2 MHCII presentation, the methods used to isolate AT2s were variable, as were the purities obtained. Cunningham *et al*. used differential centrifugation combined with magnetic bead depletion to isolate human AT2s; while they do not report the exact AT2 purity, it is likely lower than that achieved by FACS [110]. Subsequent studies in mice also used either magnetic beads or FACS for isolation, with purities ranging widely from 70% to >95% [106-108]. Furthermore, most of these studies focused on *in vitro* AT2 processing and presentation, in which AT2s were placed in culture for extended periods of time, from 48 hours up to 5 days, and at the assay endpoints AT2 cells were not analyzed to assess the maintenance of AT2 phenotypic integrity. Additionally, different types of $CD4^+$ T cells used between these studies – T cell hybridomas, primary naïve T cells, and primary effector T cells – likely contributes to the variation, as these T cells differ in their requirement for costimulatory signals, and the role of costimulation was not directly isolated or examined, except for in one study [110]. Finally, different model systems employed by each study likely results in widely differing amounts of antigen available to the AT2s for processing and presentation, and also depends on the analysis of distinct epitopes of interest between studies. In none of these studies was antigen availability to AT2s directly quantified, and only one report assessed AT2 MHCII presentation in the context of more than one antigen system (two epitopes total, one from each system) [107]. In summary, the conflicting nature of prior reports of AT2 MHCII function likely results from heterogeneity in all of these respects.

In our work, we have attempted to rigorously address all of these potential experimental caveats and shortcomings, and using multiple orthogonal approaches, we have demonstrated that AT2s exhibit inefficient MHCII presentation. This limited MHCII presentation capacity by AT2s is consistent with the relatively modest impact that loss of AT2 MHCII has *in vivo* described in **chapter 3**. However, it is surprising given that AT2s seem to possess many promising MHCII$^+$ APC characteristics, as outlined in **chapter 2,** which should theoretically render them capable of robust MHCII antigen presentation. In the next chapter, I will discuss possible mechanisms restricting AT2 MHCII presentation and will offer our perspective on its why such limited presentation might be favorable in AT2s.

CHAPTER 5:

DISCUSSION AND FUTURE DIRECTIONS

AT2s were first described to express MHCII at homeostasis decades ago. Despite this expression being highly unusual behavior for non-professional APC, let alone a cell that ostensibly is not part of the formal immune system, very few reports over the last 30 years have sought to understand the biological function of MHCII on AT2s, and none has explored the mechanisms controlling AT2 MHCII expression. To expand our understanding of AT2 MHCII regulation and function, in this dissertation I have examined the factors driving steady-state AT2 MHCII expression, the role of AT2 MHCII *in vivo* at homeostasis and during respiratory viral infection, and the MHCII antigen presentation capacity of AT2s.

In **chapter 2**, I investigated the mechanisms driving AT2 MHCII expression and also assessed other APC characteristics of AT2s. I demonstrated that AT2s produce their own MHCII protein and that this expression is dependent on the CIITA pIV transcription factor. I further showed that, contrary to convention, AT2 MHCII expression does not require IFNγ, nor does it require a number of other broad inflammatory signals including the microbiota. I also found that AT2s possess ample APC characteristics aside from constitutive MHCII expression: they are capable of exogenous protein uptake and endogenous antigen expression, they possess functionally competent classical antigen processing mediators, and they express non-canonical costimulatory molecules. Altogether, I demonstrated that AT2s have the potential to be robust MHCII$^+$ APCs both at homeostasis and during infection.

Based on these promising MHCII$^+$ APC characteristics, in **chapter 3**, I sought to elucidate the *in vivo* function of AT2 MHCII. I found that loss of MHCII from AT2s did not result in clinical or histological lung disease at homeostasis. However, in aged mice, the absence of AT2 MHCII resulted in changes to the homeostatic lung T cell compartment; higher proportions of lung T cells were naïve, and lower frequencies were antigen-experienced, compared to controls. Furthermore, I demonstrated that in the setting of lower respiratory tract viral infection, mice lacking MHCII on AT2s exhibited greater mortality and weight loss compared to controls. However, the impacts at homeostasis and during infection were relatively modest, and less than expected based on the magnitude of AT2 MHCII expression and abundance of AT2s in the lung.

In **chapter 4**, I examined the MHCII antigen presentation capabilities of AT2s. I demonstrated that AT2s are capable of processing and presenting both viral and self protein antigens via MHCII, but their presentation capacity is substantially limited compared to that of professional APCs, even when they have access to significantly more epitope source protein and express similarly high levels of MHCII. Furthermore, I found that in some cases, AT2s even failed to present synthetic peptides. Thus, I found that AT2s exhibit globally restrained MHCII antigen presentation capacity, which is consistent with the more measured contribution they make via MHCII at homeostasis and to the outcome of lung viral infection as observed in **chapter 3**.

Below I discuss the implications of these findings and provide insight into key future areas of study.

5.1 Constitutive MHCII expression paired with restrained antigen presentation: a model for AT2 MHCII function tailored to the unique requirements of the lung

Despite constitutively expressing high levels of MHCII protein similar to professional APCs (**chapter 2**), the MHCII antigen presentation capacity of AT2s is substantially limited in comparison (**chapter 4**). At first glance, it seems that AT2s thus exhibit an opposing and counterproductive combination of features. However, I suggest that this particular configuration – of high MHCII expression and restricted antigen presentation – is advantageous and specifically tailored to the unique immune environment of the lung, where excessive T cell activation would be especially damaging in comparison to other organs.

In this model, high MHCII expression poises AT2s to amplify lung adaptive immune responses, but restricted MHCII presentation establishes a higher threshold that must be overcome in order to do so. Such a system would enable MHCII presentation by AT2s to trigger cognate T cell activation only in the setting of high antigen burden, such as a severe lung infection, but would prevent excessive AT2-induced amplification of T cells in response to continuous low levels of inhaled innocuous environmental antigens, avoiding what would otherwise be constant inflammatory lung damage. Furthermore, even in the setting of high antigen burden, restrained presentation would ensure that AT2s amplify T cell responses in a more tempered way to prevent excessive inflammation in the lung tissue. Although not explored here, this model would suggest that just as the loss of AT2 MHCII resulted in worse outcomes after viral infection, artificially increasing AT2 MHCII presentation to DC-like levels would presumably also have a detrimental effect. In summary, I propose that AT2s possess a unique combination of APC characteristics that are

optimized specifically for their organ of residence, to enhance lung immune responses but prevent immunopathologic destruction of the delicate gas exchange-surface that is necessary to sustain life. Overall, this results in a more measured contribution of AT2 MHCII to immune responses in the lung, as demonstrated in **chapter 3**.

5.2 Possible contributors to poor MHCII antigen presentation by AT2s

I demonstrated in **chapter 4** that AT2s exhibit globally impaired capacity to process and present antigen via MHCII. This suggests that AT2s possess impairments in one or more of the key APC requirements detailed in **1.6**: antigen uptake, proteolysis, appropriate peptide and MHCII trafficking, and peptide loading.

AT2s have intact mechanisms of antigen uptake. As demonstrated in **Fig 2.7**, AT2s are capable of endocytosing exogenous antigen, and overall they have robust endocytic mechanisms by virtue of their surfactant recycling function [111]. AT2s also expressed high levels of the endogenous self and viral proteins containing the epitopes whose presentation I measured specifically (**Figs 4.2, 4.4, 4.6**), and in general as the main targets of a variety of lung viral infections [182, 183], they likely produce abundant endogenous antigens in those cases as well.

AT2s also have robust enzymatic processing capacity. They express a number of enzymes in the endosomal network that are critical for the appropriate proteolytic processing of surfactant proteins, such as Cathepsin H [114, 184]. They also express conventional proteases that have been implicated in classical MHCII antigen presentation. For example, either Cathepsin S or L can mediate the final steps of

invariant chain processing into the CLIP peptide remnant and are important for antigen processing, and AT2s express Cathepsin L [24-26, 185]. They also express the asparagine endopeptidase (AEP), and the reducing enzyme gamma-interferon-inducible lysosomal thiol reductase (GILT), both of which play key roles in the generation of antigenic epitopes and in the maturation of other antigen processing proteases and components [46, 76, 186-189] (**Fig 5.1**).

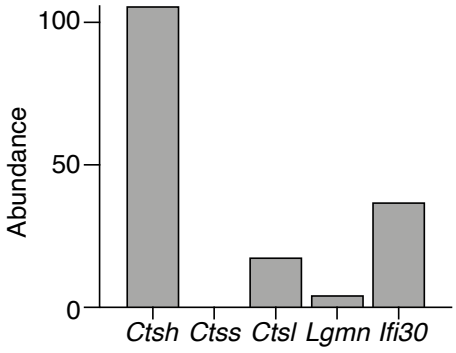

Figure 5.1: AT2s express proteases associated with antigen processing and presentation. Cathepsin H (*Ctsh*), Cathepsin S (*Ctss*), Cathepsin L (*Ctsl*), AEP (*Lgmn*), and GILT (*Ifi30*), transcript abundance measured by bulk RNA-seq, normalized by RPKM, in AT2s from naïve 4 week old B6 mice. The results shown here are in whole based upon data deposited on the LungMAP Consortium by J. Whitsett and Y. Xu. They were downloaded from (www.lungmap.net), on Nov 18, 2018. The LungMAP consortium and the LungMAP Data Coordinating Center (1U01HL122638) are funded by the National Heart, Lung, and Blood Institute (NHLBI).

I also showed that AT2s express the conventional MHCII-associated antigen presentation mediators H2M and invariant chain (**Figs 2.8, 2.9**). While these mediators are not required for the MHCII presentation of all epitopes, their presence strongly suggests that AT2s have intact MHCII trafficking and peptide loading mechanisms. I found that AT2s express only one heterodimeric isoform of H2M, H2M$\alpha\beta$1, in contrast to conventional potent APCs, such as B cells and DCs, which also express H2M$\alpha\beta$2 (**Figs 2.9**, **2.10**, **2.12**). This led us to speculate that limited antigen presentation by AT2s might result from functional inferiority of H2M$\alpha\beta$1 as compared to H2M$\alpha\beta$2.

However, consistent with prior reports [149, 150], I demonstrated that the H2M$\alpha\beta$1 was capable of enabling complete CLIP removal (**Fig 2.9**), and of facilitating Eα^{52-68}/I-A^{b} complex formation (**Fig 4.6**).

Thus, AT2s appear to possess all of the requisite MHCII^{+} APC capabilities and do so robustly. However, they nonetheless exhibit restricted presentation. This is highly unusual; in prior studies, the Eisenlohr laboratory has found that simply transducing skin fibroblasts with CIITA, which induces expression of MHCII, invariant chain, and H2M, is enough to render them highly presentation competent [46]. Overall, this suggests that there may be mechanisms operating in AT2s that actively oppose MHCII presentation.

The endosomal network of AT2s is highly specialized for the synthesis, secretion, and recycling of surfactant [114], as discussed in **1.8**. Thus, although AT2s have intact endocytic and proteolytic mechanisms that can facilitate MHCII antigen presentation, as well as appropriate MHCII trafficking and peptide loading mediators, it is possible that their endosomal compartments are so tailored toward surfactant production that they are dominantly incompatible with the trafficking, localization, and degradation requirements for optimal MHCII presentation. For example, it is possible that the proteolytic environments that enable proper surfactant pro-protein processing or degradation are too harsh for the preservation of antigenic epitopes, and thus the majority of candidate peptides are destroyed before loading. It is also conceivable that the endosomal maturation and trafficking pathways optimized for delivery of surfactant components to the lamellar body may prevent the efficient transport of antigenic peptides to MHCII-containing intracellular compartments.

It is also unusual that AT2s express such high levels of MHCII yet present only some synthetic peptides when provided exogenously (**Fig 4.1**). One possible explanation is that AT2 MHCII molecules are already bound to a high affinity peptide on the cell surface that can be displaced only by even higher affinity peptides. If such a peptide loads onto MHCII during the early stages of intracellular MHCII biosynthesis and trafficking, this would explain the poor presentation of protein-derived peptides by AT2s as well. One appealing candidate is a surfactant protein derived peptide, such as a pro-SP-C or pro-SP-B processing remnant, which would be abundant and present in the endosomal compartments where nascent MHCII molecules transit and peptide-loading generally occurs.

Understanding the factors limiting AT2 presentation will be an important area of future inquiry, and MHCII peptide elution studies are ongoing in order to investigate this latter hypothesis.

5.3 Drivers of constitutive MHCII expression by AT2s

I was unable to identify an immune signal required for AT2 MHCII expression despite investigating the conventional IFNγ axis as well as a variety of broad adaptive and innate mediators, including the microbiota. Although I did not examine every possibility, this strongly suggests that MHCII expression is not driven by inflammation. Publicly available single cell RNA-sequencing data suggest that AT2 MHCII expression is undetectable during embryogenesis and increases only after birth (**Fig 5.2**). Thus, it is possible that AT2 MHCII expression is induced and sustained by a non-immune environmental stimulus, for example, mechanical stretch

or a gaseous component of inhaled air, or is simply an intrinsic part of the AT2 cell developmental identity.

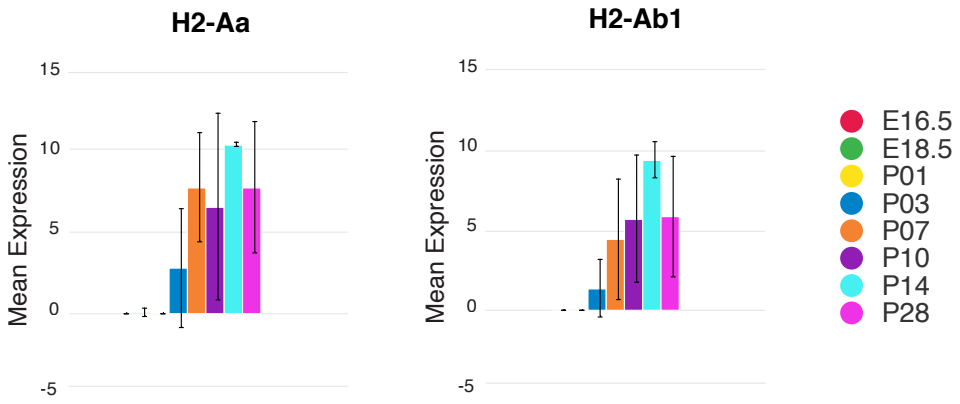

Figure 5.2: AT2s upregulate MHCII expression after birth. Expression of MHCII α and β chain (H2-Aa and H2-Ab1) transcripts measured by single cell RNA-seq in AT2s from mice on the embryonic or post-natal days indicated. The results shown here are in whole based upon data deposited on the LungMAP Consortium by J. Whitsett, B. Aronow, and S. Potter. They were downloaded from (www.lungmap.net), on June 26, 2020. The LungMAP consortium and the LungMAP Data Coordinating Center (1U01HL122638) are funded by the National Heart, Lung, and Blood Institute (NHLBI).

I identified the CIITA pIV isoform as the main transcriptional driver of AT2 MHCII expression; thus, in future work, I seek to determine the specific transcription factors that in turn initiate AT2 CIITA pIV recruitment in AT2s. The three transcription factors that have been described to bind to CIITA pIV are STAT1, IRF1, and USF1. USF1 is ubiquitously expressed; STAT1 is induced downstream of IFNγ and then in turn induces expression of IRF1 [58]. However, I demonstrated that AT2 MHCII expression is independent of IFNγ and STAT1 (**Figs 2.4, 2.5**). Since IRF1 is induced by STAT1, this suggests that AT2 pIV recruitment operates independently of both IRF1 and STAT1. Future studies will investigate the requirement of USF1, although it seems unlikely that USF1 alone would be sufficient to initiate transcription. Thus, future work will also seek to identify other transcription factors and their DNA binding

sites that mediate CIITA pIV transcription in AT2s. As AT2 MHCII is lost in mice lacking an 800bp segment encompassing the CIITA pIV promoter region (STAT1, IRF1, and USF1 binding sites), transcription start site (TSS), and first exon [58, 146], initial bioinformatics approaches will be used to identify candidate transcription factor motifs in this promoter region. However, since this 800 bp deletion does encompass the TSS, it is not possible to determine whether the relevant regulatory element is contained in this deletion as well. Thus, if initial studies of the DNA elements limited to this promoter region are not fruitful, I would expand my search to include the possibility of more distal regulatory DNA elements and candidate binding transcription factors.

Once the DNA regulatory elements and transcription factors are identified, it will also be of interest to determine whether AT2s share a similar transcriptional pathway with TECs and ILC3s, the other two cell types that exhibit IFNγ independent but CIITA pIV dependent expression of MHCII; the mechanistic drivers of CIITA pIV expression in ILC3s and TECs are still not understood.

5.4 Polarity of MHCII expression by AT2s

One aspect of AT2 MHCII expression that warrants further study is the surface localization of MHCII. As AT2s are polarized cells, they bear an apical membrane that is directed into the alveolar space, and a basolateral surface that borders the interstitium. Understanding the localization of MHCII on AT2s will provide valuable insight into its function. For example, if MHCII is pointed into the interstitium where it would be far more likely to encounter a $CD4^+$ T cell, especially at

homeostasis, this would support a stronger function for AT2 MHCII in regulating T cell function on a frequent basis. In contrast, if AT2 MHCII is pointed into the alveolar space, this would suggest MHCII presentation to $CD4^+$ T cells that is limited primarily to situations of substantial inflammation where more T cells infiltrate the alveolar spaces. Although I did examine AT2 MHCII expression *in situ* via immunofluorescence microscopy, the techniques I used were not sufficient to determine the polarity of AT2 MHCII. Higher resolution imaging studies will be necessary to resolve this, at a minimum confocal microscopy and possibly immuno-electron microscopy.

5.5 The possibility of novel functions of MHCII on AT2s

Publicly available bulk RNA-sequencing data of 4 week old mouse AT2s demonstrates that invariant chain and MHCII transcripts are some of the most highly expressed transcripts in AT2s; in terms of relative abundance, invariant chain (*Cd74*) is #16 and MHCII (*H2-Aa)* is #32 overall out of more than 20,000 transcripts measured (**Table 5.1**). This observation combined with such high levels of MHCII protein on AT2s that appear to be constitutive and inflammation-independent led me to wonder whether MHCII serves another key function in the basic biology of AT2s, besides interacting with $CD4^+$ T cells.

To this end, I asked whether MHCII was required for two critical functions of AT2s: regenerative capacity and surfactant production. I directly assessed their stem cell like function and found that loss of MHCII did not affect their capacity to generate organoids *in vitro* (**Fig 3.10**). Although surfactant production was not directly

assessed, if surfactant biosynthesis or secretion were substantially disrupted, then mice lacking MHCII on AT2s would experience severe respiratory failure and disease at homeostasis, which I did not observe either clinically or histologically (**Fig 3.9**). Thus, MHCII does not appear to be absolutely required for either of these two main AT2 functions, but further studies are necessary to determine whether MHCII makes a smaller contribution or serves another function in AT2s outside of these two.

Rank	Gene ID	RPKM
1	Sftpc	24084.6
2	Scgb1a1	18103.7
3	Rn45s	5978.34
4	Lyz2	5809.2
5	Sftpa1	1899.89
6	Cxcl15	1820.24
7	Malat1	1711.24
8	Sftpb	1325.51
9	Cbr2	1169.95
10	Slc34a2	1114.85
11	Lars2	981.425
12	Scd1	936.29
13	Lyz1	716.109
14	Rpl10	447.74
15	Tmsb4x	440.907
16	Cd74	438.262
17	Wfdc2	384.277
18	Sod1	382.71

Rank	Gene ID	RPKM
19	Rpl41	349.927
20	Cyp2f2	343.48
21	Lamp3	334.136
22	Chil1	313.113
23	Scgb3a2	302.334
24	Actb	294.986
25	Hc	275.855
26	Hspa8	275.259
27	Eef1a1	263.356
28	Ftl1	263.086
29	Sftpd	260.039
30	Tpt1	242.97
31	Atp1b1	236.5
32	H2-Aa	214.948
33	Rps23	210.497
34	S100a11	206.536
35	Scgb3a1	203.18
36	S100g	196.786

Table 5.1: MHCII and invariant chain transcripts are among the most highly abundant in AT2s. Abundance of the transcripts indicated, measured by bulk RNA-seq, normalized by RPKM, in AT2s from naïve 4 week old B6 mice. Highlighted are MHCII (H2-Aa) and invariant chain (Cd74) transcripts. The results shown here are in whole based upon data deposited on the LungMAP Consortium by J. Whitsett and Y. Xu. They were downloaded from (www.lungmap.net), on Nov 18, 2018. The LungMAP consortium and the LungMAP Data Coordinating Center (1U01HL122638) are funded by the National Heart, Lung, and Blood Institute (NHLBI).

Another possibility is that MHCII expression is simply a byproduct of its coordinated expression with the other CIITA-dependent genes, which instead might play the more important role in AT2s at homeostasis. One candidate is invariant chain, which has been reported to perform several functions outside of chaperoning MHCII [190]. Invariant chain is typically synthesized in molar excess of MHCII and thus can reach the cell surface without being associated with MHCII or degraded to CLIP peptide; indeed, it is detectable on the surface of AT2s [191]. Previous studies have demonstrated that surface invariant chain can serve as a receptor for the pleiotropic cytokine MIF-1 [192], and one group has demonstrated this specifically in AT2s, suggesting that it may contribute to lung epithelial repair [191]. Globally *Cd74*-deficient mice do not exhibit overt lung disease, suggesting that if invariant chain does play an alternative role in AT2s, it is not strictly required for their life-sustaining functions, similarly to MHCII.

In general, much more extensive characterization of AT2 function, proliferation, survival, gene and protein expression, and more, are needed to investigate whether there are other non-immunologic processes that are disrupted by the loss of MHCII and or associated genes in AT2s.

5.6 The potential role of AT2 MHCII in other immune settings

I found that the loss of AT2 MHCII resulted in subclinical changes to the proportions of naïve, activated, memory, and regulatory phenotype T cells in the lungs of aged mice. Specifically, in 14-month-old mice lacking AT2 MHCII, a higher proportion of lung $CD4^+$ and $CD8^+$ T cells remained naïve, compared to control mice

that had higher proportions of activated, effector memory, and regulatory T cells. As discussed in **chapter 3**, this suggests that AT2 MHCII presentation enhances the antigen encounter of lung $CD4^+$ T cells at homeostasis, supporting the formation of a variety of antigen-experienced $CD4^+$ and $CD8^+$ T cell subsets.

The majority of studies of other atypical $MHCII^+$ cells suggest that their MHCII expression plays a tolerogenic role at homeostasis. For example, mice lacking MHCII on all nonhematopoietic cells [92], or just on ILC3s [90], demonstrate increased frequencies of effector memory T cells at homeostasis. Thus, I was surprised to find that loss of AT2 MHCII resulted in a decrease in effector memory T cells, rather than an increase. As I observed decreases in both effector memory T cells and regulatory T cells in $SPC^{\Delta Ab1}$ mice, this suggests that the role of AT2 MHCII at homeostasis is more mixed and may promote both T cell activation as well as tolerance and Treg formation depending on the situation.

The ultimate importance of AT2 MHCII regulation of lung T cells at homeostasis is still unclear, given that its impact was small and only apparent in aged 14-month-old mice, but not 7-month-old adult mice. Furthermore, the mice did not exhibit any signs of lung disease upon loss of AT2 MHCII clinically or when measured histologically in 9-month-old mice. It is possible that the contribution of AT2 MHCII *in vivo* at homeostasis to lung T cells is indeed minor and is dispensable for a functionally intact lung immune environment. However, it is also possible that the homeostatic importance of AT2 MHCII may have been underestimated in our experiments, as discussed in **chapter 3** and below.

The fact that loss of AT2 MHCII did not result in overt lung disease at homeostasis was surprising for a few reasons. The first is that the constitutive and

high levels of MHCII expressed by AT2s, independent of inflammation, strongly suggests that AT2 MHCII serves an important function in preventing disease at steady state; if only important during inflammation, then presumably AT2s would instead behave like all other nonhematopoietic cells and only upregulate MHCII in response to IFNγ. The second is that homeostatic AT2 MHCII expression in naïve or healthy lungs seems to be evolutionarily conserved, at least between rodents and human, based on prior reports and our own findings, as demonstrated in **chapter 2**. I also found that MHCII expression by naïve AT2s is conserved across commonly used mouse strains C57Bl/6, BALB/c, and C3H (**Fig 5.3**). Consistent with a prior report [105], I did find that AT2s from one mouse strain, A/J, do not express MHCII; I will discuss the possible implications of this below. Thirdly, the two cell types that have IFNγ-independent, CIITA pIV-dependent MHCII induction mechanisms similar to AT2s – TECs and ILC3s – play critical roles at homeostasis in central T cell development and peripheral selection to prevent immunodeficiency, autoimmunity, and pathologic anti-commensal responses. Mice lacking MHCII on ILC3 develop spontaneous intestinal disease [90], and the absence of TEC MHCII results in the failure of $CD4^+$ T cell positive selection [87], resulting in severe immunodeficiency. Thus, I had hypothesized that AT2 MHCII might play an equally critical role at homeostasis. Although I did not observe such an overt disease-protecting function for AT2 MHCII at homeostasis in our mice housed under SPF conditions, a role may be more evident in humans or in wild mice that are exposed to a much larger repertoire of inhaled antigens and microbes and have a dramatically different, “less naïve” immune system [177, 193-195]; in this setting, the AT2 MHCII-induced increase in antigen-experienced lung T cells that I observed could have larger

clinical consequences. Furthermore, as discussed in **chapter 3**, it is also possible that in mice of more advanced age, beyond 9 months, histological lung disease may become more apparent, even under SPF conditions.

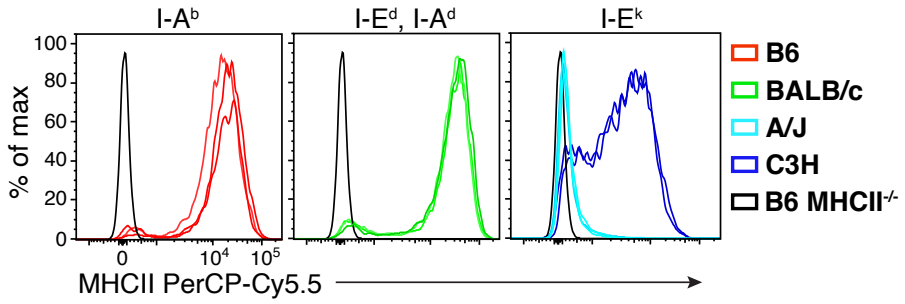

Figure 5.3: Homeostatic AT2 MHCII expression is conserved across multiple mouse strains but is absent in A/J mice. MHCII protein expression by AT2s from naïve C57Bl/6 (B6) wild-type (WT) and MHCII$^{-/-}$ mice, as well as WT BALB/c, A/J, and C3H mice, shown in the colors indicated. Expression was measured by flow cytometry using a pan I-A/I-E antibody; the allele that the antibody binds to in each strain is listed above each plot. Histograms depict n=2-3 mice per strain. Differences in overall MFI between strains are not necessarily reflective of differences in magnitude of expression, since the antibody may have different affinities for each MHCII allele.

I also explored the role of AT2 MHCII in the setting of a primary immune response to respiratory viral infection. While loss of MHCII on AT2s did result in an increase in disease severity, the impact was modest (**Fig 3.11**). While the factors responsible for this AT2 MHCII protective effective are not yet characterized, the most likely mechanism is CD4$^+$ T cell-mediated. Therefore, the moderate clinical effect of AT2 MHCII loss that I observed could reflect an equally modest impact on the CD4$^+$ T cell response; in prior sections I have suggested that this is due to inefficient MHCII antigen presentation by AT2s. However, it could also reflect the fact that CD4$^+$ T cells, while critical for optimizing the immune response, are also not absolutely required for successful viral clearance or eventual clinical recovery during

primary influenza or Sendai virus infections in mice [166, 168-171]. Thus, a primary influenza or Sendai virus infection model may not be the scenario in which the possible contributions of AT2 MHCII would be the most overtly clinically evident or immunologically impactful. Thus, in ongoing and future studies I aim to understand the contribution of AT2 MHCII in other disease settings.

The contribution of primary infection-induced $CD4^+$ T cells is far more evident clinically during a subsequent secondary infection. Mice lacking $CD4^+$ T cells during a primary infection demonstrate severely impaired B cell responses, limiting the development of neutralizing antibodies, and also exhibit poor formation of memory $CD8^+$ T cells [162, 163, 171, 196, 197]. Therefore, upon secondary challenge, these mice have impaired antibody-mediated protection and inferior capacity to clear the virus compared to wild type mice. Thus, a secondary infection challenge model would be a clearer way to study the clinical impacts of a potentially impaired CD4 response generated during primary flu or Sendai virus infection of $SPC^{\Delta Ab1}$ mice.

I am also interested in understanding whether AT2 MHCII affects the development of virus-specific $CD4^+$ memory T cells, as they correlate with heterosubtypic protection in humans [198]. Prior studies from the Swain laboratory suggest that robust influenza-specific memory $CD4^+$ T cell formation requires two cognate TCR-MHCII encounters: the first priming interaction in the lymph node, and a second around days 5-7 post-infection [124, 199]. The precise location of this second MHCII/antigen encounter is unknown, but as $MHCII^+$ AT2s are present at the site of infection where there would be available antigen and antigen-specific $CD4^+$ T cells, it is possible that AT2s deliver this second checkpoint and contribute to the optimal development of memory $CD4^+$ T cells. It is also possible that local MHCII

antigen presentation by AT2s helps to facilitate the development and retention specifically of the tissue-resident subset of memory $CD4^+$ T cells (Trm) [200-202]. The impact of AT2 MHCII on the development of antigen-specific $CD4^+$ Trm is of particular interest, as $CD4^+$ Trm can mediate protection upon viral challenge [203].

Other lung disease models in which AT2 MHCII may serve an important function are those in which $CD4^+$ T cells play a more direct protective or pathologic role. These include models of allergic asthma, in which Th2 phenotype $CD4^+$ T cells contribute to airway inflammation directly via the production of the inflammatory cytokines IL-4, IL-5, and IL-13 [204]. $CD4^+$ T cells also play a primary role in the pathogenesis of lung hypersensitivity pneumonitis, where repeated exposures to inhaled organic antigens leads to lymphocytic alveolitis, granulomatous inflammation, and progressive lung fibrosis [205-207]. AT2 MHCII could either help to protect against these diseases or worsen them. It is possible that AT2 MHCII helps to suppress these responses by inducing tolerance of naïve T cells to such allergens or environmental antigens; however, it is possible that activation of $CD4^+$ T cells by AT2 MHCII antigen presentation contributes to the amplification of this immune pathology. It is also possible that AT2 MHCII can perform both of these tasks under different circumstances, and a switch in these functions contributes to the development of disease. For example, in healthy individuals with no allergy or hypersensitivity, AT2 MHCII tolerization of $CD4^+$ T cells operates unperturbed. However, in situations of allergy, where inappropriate $CD4^+$ T cell responses have been primed and expanded, or in hypersensitivities where large amounts of antigen are present in the alveolar spaces, these tolerance mechanisms may be overridden, with AT2 MHCII presentation to $CD4^+$ T cells instead resulting in disease.

Preliminary data indicates that AT2 MHCII may contribute to protection in the setting of ova-induced murine asthma, in that mice lacking MHCII on AT2s exhibit modestly higher frequencies of Th2-cytokine producing $CD4^+$ T cells and higher numbers of lung eosinophils (**Fig 5.4**); however, additional studies are needed to corroborate this, including those that measure the symptomatic implications of such changes, such as airway hyperresponsiveness.

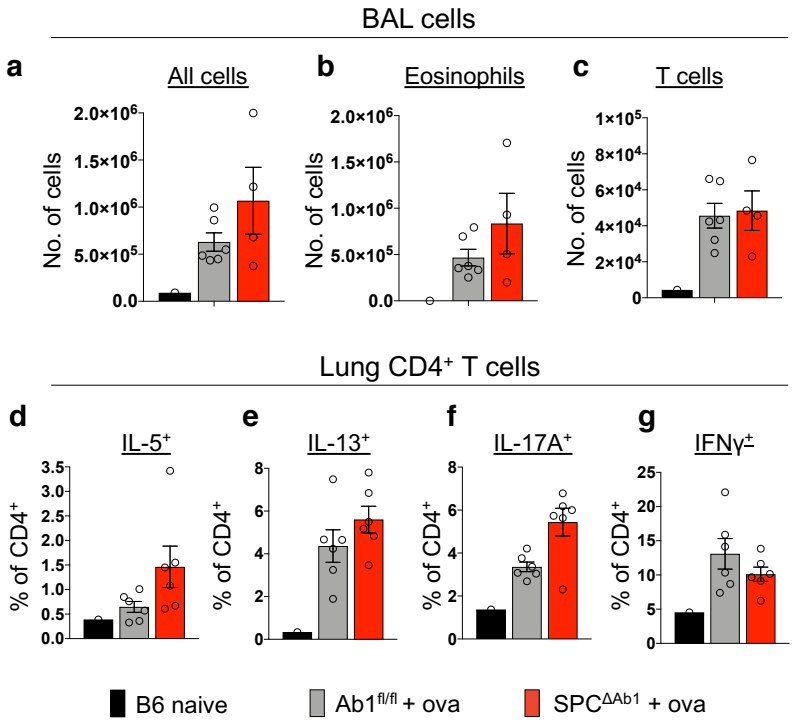

Figure 5.4: $SPC^{\Delta Ah1}$ mice exhibit cellular signs of increased allergic phenotype compared to $Ab1^{fl/fl}$ control mice in an inhaled ova allergy model. a-g, Comparison of $Ab1^{fl/fl}$ and $SPC^{\Delta Ab1}$ mice after ova/alum sensitization followed by intranasal ova challenge. **a-c**, Numbers of all cells (**a**), eosinophils (**b**), and T cells (**c**) in the BAL; n=4-6 mice per strain for $Ab1^{fl/fl}$ and $SPC^{\Delta Ab1}$ mice, with n=1 naïve B6 control mouse control. **d-g**, Proportion of lung $CD4^+$ T cells secreting IL-5 (**d**), IL-13 (**e**), IL-17 (**f**), and IFNγ (**g**), after PMA/Ionomycin restimulation; n=6 mice per strain for $Ab1^{fl/fl}$ and $SPC^{\Delta Ab1}$ mice, with n=1 naïve B6 control mouse control. **a-g**, Data are mean plus SEM from one experiment.

Other disease models of interest stem from previous studies of A/J mice; as AT2s in A/J mice do not express MHCII, they represent another model in which to

assess the outcomes of loss of AT2 MHCII. A/J mice are highly susceptible to developing spontaneous and carcinogen-induced tumors of AT2 cell origin [208], suggesting that the lack of AT2 MHCII may impair cancer-specific immune responses in the lung. AT2s also experience particularly severe respiratory virus disease compared to other conventional mouse strains [209], and of particular interest at this time, they are one of the few strains of inbred mice that are susceptible to pulmonary disease after infection with intranasal murine hepatitis virus-1 (MHV-1), a mouse betacoronavirus in the same family as SARS-CoV2 [210]. As A/J mice also bear other immune-related defects, it is of great interest in future work to determine whether the absence of AT2 MHCII directly contributes to worse coronavirus disease and more facile cancer development in these mice [211].

Finally, it will be an essential avenue of future work will also be to understand how our current and future findings in mice translate to human lung immunity. In particular, I seek to understand whether alterations in AT2 MHCII expression or function contribute to the wide variation in outcome of infectious and immunologic lung diseases in humans. Given the current worldwide Covid-19 pandemic, I am also particularly interested in whether AT2 MHCII contributes to protection or to the outcome of disease in the setting of SARS-CoV-2 infection; as AT2s are the main cell type infected with this virus in the human lung parenchyma [212-214], they may contribute to SARS-CoV-2 specific $CD4^+$ T cell responses via endogenous MHCII antigen presentation.

5.7 Concluding remarks: why do AT2s express MHCII?

A central question underlying this work is, teleologically, why would AT2s "need" to express MHCII? Or framed another way, given the expansive and intricate network of conventional immune cells and specialized immune organs that comprise the formal immune system, why would the lower respiratory tract have evolved to also have its own parenchymal cells constitutively express MHCII?

The most straightforward explanation is that this provides an additional mechanism to further tailor the adaptive immune response based on the structural and functional constraints of the lung. The respiratory tract is a barrier site, and thus is constantly faced with both innocuous and potentially harmful insults. It is also a location where having excessive cellular infiltration and inflammation is particularly dangerous and often has lethal consequences. As most immune cells, in particular T cells, are circulatory, they migrate throughout various organs to exert their effector functions without necessarily intrinsically discriminating based on anatomic location per se. Having a local and lung-specific MHCII-expressing cell that is specifically adapted to regulate these responses, to facilitate rapid infection resolution but spare the delicate gas-exchange surface, would be enormously beneficial. AT2s are highly abundant in the lung parenchyma, and they are poised anatomically at the air/tissue interface, making them uniquely situated to respond to foreign substances that reach the alveolar spaces. Furthermore, they are replete with their own specialized set of intracellular machinery, and they are preferentially infected by a variety of pathogens, endowing them with unique antigen processing and presentation characteristics in comparison to conventional APCs. Thus, AT2s are prime

candidates for contributing to this crucial tissue-specific immune regulation in the lung via MHCII.

Over the last decade or so, the study of immunology in peripheral tissues, rather than in the blood and secondary lymphoid organs, has become more commonplace. Furthermore, the importance of contributions made by stromal and parenchymal cells to shape these immune responses based on organ-specific considerations has been increasingly appreciated [215, 216]. Here I propose that AT2 cells, by virtue of their constitutive MHCII expression and restrained MHCII antigen presentation, contribute to the regulation of local immune responses in the lung. It is our hope that future studies will build upon our initial findings to elucidate roles for AT2 MHCII antigen presentation in other situations of homeostasis and disease, adding to our basic understanding of the exquisite complexities of how adaptive immune responses are regulated *in situ*.

CHAPTER 6:

MATERIALS AND METHODS

Mice

C57Bl/6 wild-type (B6), B6.129S2-*H2*$^{dlAb1\text{-}Ea}$/J (MHCII$^{-/-}$) [217], B6;129S4-*H2-DMa*^{tm1Luc}/J (*H2-DMa*$^{-/-}$) [29], B6.129S7-*Ifng*^{tm1Ts}/J (*Ifng*$^{-/-}$) [218], B6.129S(Cg)-*Stat1*^{tm1Dlv}/J (*Stat1*$^{-/-}$) [219], C.129S2(B6)-*Ciita*^{tm1Ccum}/J (*Ciita*$^{-/-}$) [54, 220], B6.SJL-*Ptprc*^{a} *Pepc*^{b}/BoyJ (CD45.1 B6), B6.129X1-*H2-Ab1*^{tm1Koni}/J (*H2-Ab1*$^{fl/fl}$) [158], as well as C3H, A/J, BALB/c, and CB6F1/J (F1 [BALB/c x C57Bl/6] mice were originally purchased from the Jackson Laboratory. C57Bl/6 *Cd74*$^{-/-}$ mice [20] were originally provided by Guo-Ping Shi (Harvard), and C57Bl/6 *Ciita pIV*$^{-/-}$ mice [146] were provided by S. Hugues (University of Geneva). C57Bl/6 SPC-Cre-ERT2 mice [157] were provided by G.S. Worthen, B6.129S7-*Ifngr1*^{tm1Agt}/J (*Ifngr1*$^{-/-}$) [221], B6(Cg)-*Ifnar1*$^{tm1.2Ees}$/J (*Ifnar1*$^{-/-}$) [222], and B6.Cg-*Ifngr1*^{tm1Agt} *Ifnar1*$^{tm1.2Ees}$/J (*Ifnar1*$^{-/-}$*Ifngr1*$^{-/-}$) mice were provided by E. Behrens, and germ-free mice were provided by M. Silverman (Children's Hospital of Philadelphia). C57Bl/6 B6.129P2(SJL)-*Myd88*$^{tm1.1Defr}$/J (*Myd88*$^{-/-}$) mice [223] were provided by S. Shin, and B6.129S2(C)-*Stat6*^{tm1Gru}/J (*Stat6*$^{-/-}$) mice [224] were provided by C. Hunter (University of Pennsylvania). All mice were maintained in specific pathogen-free facilities at the Children's Hospital of Philadelphia, except for *Myd88*$^{-/-}$ and *Stat6*$^{-/-}$ mice, which were housed in specific pathogen-free facilities at the University of Pennsylvania, and germ-free mice, which were housed in gnotobiotic mouse facilities at the University of Pennsylvania. Mice were age and sex matched for all studies. 8-12 week old mice were used for all experiments except where indicated in the text. All animal procedures were in

compliance with institutional and AAALAC ethical guidelines and were approved by the Institutional Animal Care and Use Committee (IACUC) at the Children's Hospital of Philadelphia.

Cell lines

The B6 primary skin fibroblast cell line was derived in our laboratory and has been described previously [225]; it was maintained in Dulbecco's Modified Eagle Medium (DMEM) containing 5% FBS, Penicillin-Streptomycin, and 2mM L-glutamine. Madin-Darby canine kidney (MDCK) cells were provided by S. Hensley (University of Pennsylvania) and were maintained in MEM with 10% FBS. Monkey kidney LLC-MK2 cells were provided by Carolina Lopez (University of Pennsylvania) and were maintained in DMEM with 10% heat-inactivated FBS, Penicillin-Streptomycin, 2 mM L-glutamine, and 1 mM sodium pyruvate. T cell hybridoma lines were derived in our laboratory and have been described previously [46, 178]; these were maintained in "complete RPMI" media: RPMI media containing 10% FBS, 50 μM 2-mercaptoethanol, Penicillin-Streptomycin, 2mM L-glutamine.

Viruses

Mouse lung-adapted H1N1 influenza A virus, A/Puerto Rico/8/1934 (IAV PR8), was originally provided by C. Lopez (University of Pennsylvania), and then expanded in 10-day-old embryonated chicken eggs. IAV PR8 viral titer was determined by standard focus-forming unit (FFU) assay in MDCK cells. Sendai virus, strain 52 (SeV 52), was also a generous gift of C. Lopez (University of Pennsylvania). SeV 52 viral

titer was determined using a tissue culture infectious dose ($TCID_{50}$) standard infectivity assay in LLC-MK2 cells.

Synthetic peptides

The following synthetic peptides were used: HA^{91-107} (RSWSYIVETPNSENGIC), $NA^{161-175}$ (SVAWSASACHDGMGW), $HA^{302-313}$ (CPKYVRSAKLRM), $HA^{107-119}$ (SVSSFERFEIFPK), NA^{79-93} (IRGWAIYSKDNSIRI). All peptides were obtained at >85% purity from Genscript.

Tissue isolation for *in vitro* analysis and flow cytometry

For isolation of AT2 cells, the lung vasculature was first perfused with 5 mL PBS by injecting into the cardiac right ventricle. Lungs were then inflated via intratracheal instillation of 0.9 mL AT2 digest media [5 U/mL Dispase (354235, Corning), 1.66 mg/mL Collagenase A (10103586001, Sigma), 0.33 mg/mL DNase I (10104159001, Sigma) in PBS]. The trachea was then tied with suture to keep the lungs inflated while they were excised en bloc and then placed in an additional 1 mL digest media, then incubated at 37°C. After 45 minutes, 5 mL 20% FBS in PBS was added, and the parenchymal lung lobes were removed from the large airways with forceps, then dissociated by vigorous pipetting. Digested lungs were passed through a 70 μm strainer, incubated in ACK lysis buffer to remove RBCs, then passed through a 40 μm strainer to obtain a single cell suspension.

For isolation of lung T cells, the lung vasculature was first perfused with 5 mL 1% FBS in PBS by injecting into the cardiac right ventricle. Individual parenchymal lung lobes were removed from the chest cavity and placed into gentleMACS C tubes

containing 2 mL 1% FBS in PBS. Lymphocyte digest media was then added to the lungs (1% FBS, 2.25 mg/mL Collagenase D (11088866001, Sigma), 0.15 mg/mL DNase I in PBS in 4 mL final volume), which were then gently disrupted using gentleMACS homogenizer program m_spleen_01.01, then incubated for 45 minutes at 37C with shaking. Complete RPMI media was then added to each tube, followed by further dissociation using gentleMACS homogenizer program m_lung_02.01. Digested lungs were then passed through a 70 μm strainer, incubated in ACK lysis buffer to remove RBCs, then passed through a 40 μm strainer to obtain a single cell suspension.

AT2s could not be recovered from the T cell digest; likewise, the AT2 digest was not optimal for T cell isolation as it resulted in the degradation of surface CD4 and CD8 from T cells. In some T cell isolation experiments, a small sample of AT2s was also needed for the purposes of confirmation phenotyping to assess deletion or presence of MHCII. In these cases, prior to the addition of lymphocyte digest media to the lungs, a small ([<2mm]^3) portion of lung was removed, and then incubated for 1 hour at 37C in 0.4 mL AT2 digest media. Next, 0.1 mL of FBS was added, and the sample was then homogenized through a 40 μm cell strainer using the flat end of a 1 mL syringe plunger, to obtain a single cell suspension.

To harvest lungs for virus titering, lung lobes were removed directly from the thoracic cavity (with no perfusion or instillation) and placed in gentleMACS M tubes containing 1 mL PBS. Additional PBS was then added to each M tube to produce a final 10% weight/volume solution of lungs/PBS. Lungs were then homogenized using gentleMACS dissociator program RNA_01.01. Cellular debris was removed by

centrifugation at 600xg for 10” at 4°C, and the clarified supernatant was then used for virus titering.

For isolation of splenocytes, spleens were removed from the abdominal cavity and placed directly in PBS. Spleens were then homogenized through a 70 μm cell strainer using the blunt end of a 3 mL syringe plunger. The splenocytes were then incubated in ACK lysis buffer to remove RBCs, then passed through a 40 μm strainer to obtain a single cell suspension.

For isolation of immune cells from peripheral blood, blood was collected via cheek bleed or IVC puncture into PBS containing 25 mM EDTA. Samples were centrifuged at 300xg for 10”, followed by ACK lysis of the cell pellet to remove RBCs.

For isolation of bone marrow cells, whole bones of the hindlimb were removed from mice. In a sterile manner, the ends of the bones were cut and the interior cavity was flushed with PBS.

For isolation of BAL cells, the trachea was cannulated and flushed three times with 0.7 mL of PBS containing 5% BSA, 2 mM EDTA, and complete Mini, EDTA-free protease inhibitor cocktail (11873580001, Sigma). Each flush was collected separately and kept on ice, then centrifuged at 6800xg at 4°C for 2 minutes. The supernatant was removed and the cell pellets from all three flushes were combined, then incubated in ACK lysis buffer to remove RBCs.

For isolation of human distal lung cells, healthy human lungs were obtained with informed consent from the Prospective Registry of Outcomes in Patients Electing Lung Transplant Study approved by University of Pennsylvania Institutional Review Board in accordance with institutional ethical procedures and guidelines. The donor used in this study had the following characteristics: 36 y.o. M, no smoking history, no

evidence of active infection, P/F ratio of 346. Lungs were digested as described previously by Zacharias and Morrisey [226]. Briefly, a 2x2 cm piece of distal lung tissue (pleura and airways removed) was minced then processed in the same AT2 digest media as above using a gentleMACS dissociator at 37°C for 35 minutes. Digested lungs were washed, passed through 70 μm and 40 μm strainers, and then incubated in ACK lysis buffer to remove RBCs and generate a single cell suspension.

Cell type identification via flow cytometry and cell sorting

All flow cytometry antibodies used are listed in **Table 6.1**. For all flow cytometry experiments, unless otherwise stated, single cell suspensions were first stained for dead-cell exclusion with Live/Dead Aqua (L34957, Thermo Fisher) in PBS, followed by Fc-receptor blockade with anti-CD16/CD32 (553141, BD) for mouse cells or Human TruStain FcX (422301, Biolegend) for human cells, in 0.1% BSA in PBS. Cells were then stained with surface antibodies diluted in 0.1% BSA in PBS for 30” in the dark at 4°C. If necessary, cells were then fixed and permeabilized for intracellular staining using the BD Cytofix/Cytoperm kit (554714, BD) or for intranuclear staining using the eBioscience Foxp3/Transcription Factor Staining kit (00-5523-00, Thermo Fisher). Intracellular and intranuclear stains were diluted in the corresponding kit wash buffer and were incubated for 30” at room temperature. Flow cytometry data were acquired on the following analyzers: LSRII and LSRFortessa (BD), CytoFLEX LX and CytoFLEX S (Beckman Coulter). Cell sorting was performed on the following sorters: FACSAria Fusion and FACSJazz (BD), and MoFlo Astrios (Beckman Coulter). All flow cytometry analyses were conducted using FlowJo software (FlowJo LLC).

Murine AT2s were identified by flow cytometry as detailed in **Fig 6.1** [105]. In studies where MHCII expression was evaluated, AT2s were identified using the gating strategy without MHCII as a selection marker, as CD45$^-$, CD31$^-$, EpCAM^{int} cells (**Fig 6.1b**). For all other flow cytometry studies, AT2s were identified as CD45$^-$, CD31$^-$, EpCAM$^+$ MHCII$^+$ cells (**Fig 6.1a**). Both gating strategies were validating by intracellular staining for pro-SPC (**Fig 6.1c**). Human AT2s were identified by flow cytometry as detailed in **Fig 6.2** as HT2-280$^+$ lung cells [145], by staining with unlabeled anti-HT2-280 followed by an anti-mouse IgM fluorophore-conjugated secondary antibody.

Other cell types were identified via flow cytometry as follows: Lung endothelial cells (CD45$^-$, CD31$^+$), Lung CD103$^+$ DCs (CD45$^+$, CD11c$^+$, CD103$^+$), Lung alveolar macrophages (CD45$^+$, CD11c$^+$, CD103$^-$, CD11b$^-$, CD64$^+$), Splenic CD8$^+$ DCs (CD45$^+$, CD11c$^+$, CD3$^-$, CD8$^+$), B cells (FSC-A^{low}, CD45$^+$, CD11c$^-$, CD19$^+$ or B220$^+$), T cells (CD45$^+$ CD3$^+$), CD4$^+$ T cells (CD45$^+$, CD3$^+$, CD4$^+$, CD8$^-$), CD8$^+$ T cells (CD45$^+$, CD3$^+$, CD8$^+$, CD4$^-$), NK cells (CD45$^+$, CD3$^-$, NK1.1$^+$), $\gamma\delta$ T cells (CD45$^+$, CD3$^+$, TCRδ^+), neutrophils (CD45$^+$, CD11c$^-$, CD11b$^+$, Ly6G$^+$), and eosinophils (CD45$^+$, CD11c$^-$, CD11b$^+$, Ly6G$^-$, SiglecF$^+$).

For cell sorting experiments, samples were not stained with the Live/Dead viability dye or Fc-receptor blockade to minimize sample processing time and preserve cell viability. The following professional APC populations were sorted: qPCR DCs (CD45$^+$,CD11c$^+$,MHCII^{hi}); DQ-ova assay DCs (CD45$^+$, CD11c$^+$, MHCII^{hi}) and B cells (CD45$^+$, B220$^+$, MHCII$^+$); C57Bl/6 hybridoma assay CD11c$^+$/CD19$^+$ APCs (CD45$^+$, MHCII$^+$, CD11c$^+$ or CD19$^+$); Balb/c hybridoma assay CD11c$^+$ APCs (CD45$^+$, MHCII$^+$, CD11c$^+$); ELISpot CD103$^+$ DCs (CD45$^+$, CD11c$^+$, CD103$^+$). The following AT2 populations were sorted: DQ-ova assay, qPCR, C57Bl/6 hybridoma assay and Balb/c

hybridoma assay AT2s (CD45$^-$, CD31$^-$, EpCAM$^+$, MHCII$^+$), ELISpot AT2s (CD45$^-$, CD31$^-$, EpCAM$^+$), and AT2s for organoid culture (CD45$^-$, CD31$^-$, Podoplanin$^-$, CD34$^-$, Sca1$^-$, EpCAM^{int}). Lung fibroblasts were sorted for organoid culture as Pdgfrα^+ cells.

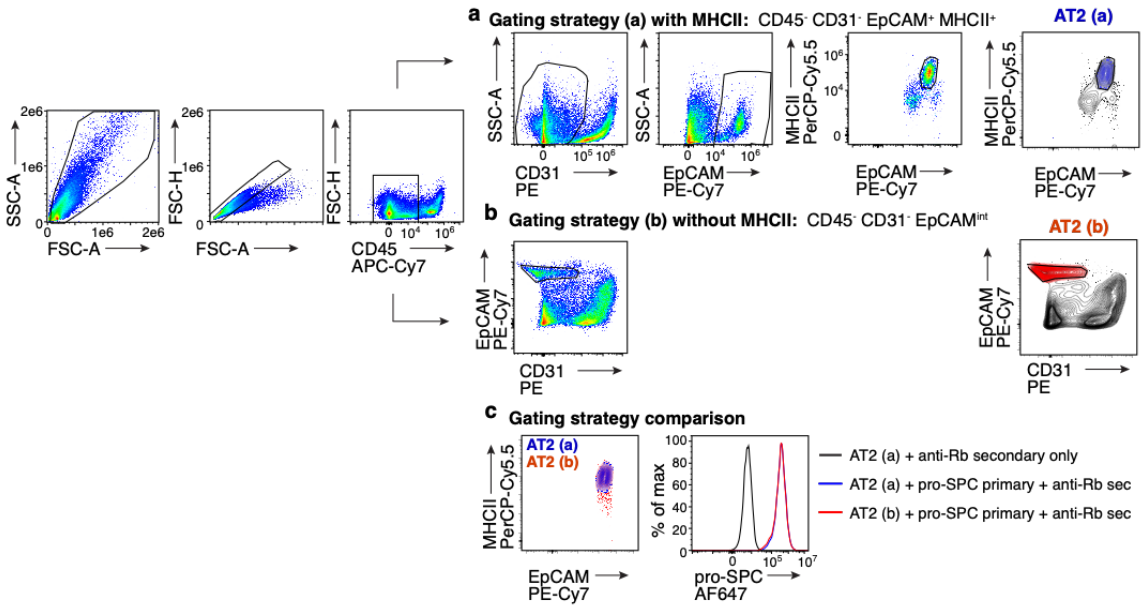

Figure 6.1: Murine AT2s gating strategies. a,b, Flow cytometry gating strategy for murine AT2s using MHCII as a positive marker (**a**) or without using MHCII as a positive marker (**b**). The right column contour plots are the same as the final pseudocolor plots in the corresponding gating strategies, and they are shown to highlight the final AT2 population defined from each strategy. **c**, Comparison of the two populations of AT2s identified by the two gating strategies in terms of MHCII expression (contour plot, left) or pro-SPC expression (histogram, right).

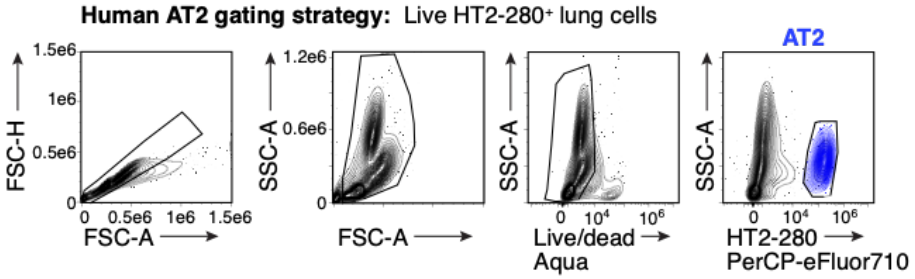

Figure 6.2: Human AT2s gating strategy. Flow cytometry gating strategy for human AT2s. The right-most contour plot highlights in blue the final AT2 population defined by HT2-280$^+$ staining.

Flow cytometric detection of MHCII, peptide/MHCII complexes, and associated machinery

To assess total surface MHCII expression in wild-type and knockout mice, cells were stained with a pan I-A/I-E anti-MHCII antibody. Human MHCII was detected using an anti-HLA-DR antibody. For detection of specific MHCII alleles in YAe presentation assays, cells were surface stained with anti-I-A^b and anti-I-E^d antibodies. Mouse invariant chain and H2M expression were detected by staining intracellularly with anti-mouse CD74 and anti-H2M$\alpha\beta$2 antibodies, respectively. Two different fluorophore-conjugated versions of the anti-H2M$\alpha\beta$2 antibody were labeled in house, with the Pacific Blue and Alexa Fluor 647 labeling kits (P30013 or A20186, Thermo Fisher). Human invariant chain was detected using an anti-human CD74 antibody, and HLA-DM was detected using an anti-HLA-DM antibody [227] provided by L. Denzin (Rutgers). CLIP-loaded MHCII molecules were detected on the cell surface by using an CLIP/I-A^b complex specific antibody [227] provided by L. Denzin (Rutgers). To detect $E\alpha^{52-68}$/I-A^b complexes, lung cells were surface stained with a biotinylated Y-Ae antibody followed by APC-Streptavidin (405207, Biolegend).

Costimulatory molecule expression analysis

To generate bone marrow-derived dendritic cells (BMDCs), bone marrow cells were grown in complete RPMI media supplemented with 20 ng/mL mouse recombinant granulocyte-macrophage colony-stimulating factor ("GM-CSF"; 10822-026, Shenandoah Biotechnology). Fresh media was added on days 3 and 6 after plating, and the floating fraction of cells was harvested on day 7-10.

Mice were infected intranasally with 60 FFU IAV PR8 diluted in 20 μL PBS under isoflurane anesthesia. Lungs were harvested from mice 5 days after infection or from naïve mice.

To evaluate the expression of costimulatory molecules, BMDCs, bulk splenocytes, and lung cells were surface stained with anti-CD80, anti-CD86, and anti-CD54 (ICAM1) antibodies.

DQ-ovalbumin assay

0.75-1.25x10^5 AT2s, DCs, and B cells were incubated with either 0 or 10 μg/mL DQ-ovalbumin (D12053, Thermo Fisher) in complete RPMI media at either 37°C or 4°C for 2 hours. Cells were then washed 3x with PBS and stained with Live/Dead Aqua; cells were maintained at 4°C during these steps. Fluorescence was then immediately assessed by flow cytometry.

RNA isolation and quantitative PCR

Total RNA was extracted and purified using the Qiaqen RNeasy Plus Mini Kit (74134, Qiagen), and cDNA was then prepared using the SuperScript III First-Strand Synthesis System with random hexamers (18080051, Thermo Fisher). Quantitative PCR was performed using the Power SYBR Green PCR Master Mix system (4367659, Thermo Fisher) measured using a StepOnePlus Real Time PCR Machine (Applied Biosystems). Expression was quantified relative to the housekeeping gene *Hprt* using the ΔC_T method. The following forward (F) and reverse (R) primer pairs were used. *H2-Aa* F: CTGATTCTGGGGGTCCTCGC and R: CCTACGTGGTCGGCCTCAAT; *H2-Ab1* F: GAGCAAGATGTTGAGCGGCA and R:

GCCTCGAGGTCCTTTCTGACTC; *H2-DMa* F: GGCGGTGCTCGAAGCA and R: TGTGCCGGAATGTGTGGTT; *H2-DMb1* F: CTATCCAGCGGATGTGACCAT and R: TGGGCTGAGCCGTCTTCT; *Hprt* F: TCAGTCAACGGGGGACATAA and R: GGGGCTGTACTGCTTAACCAG.

Bone marrow chimeras

Donor bone marrow was isolated from C57Bl6 MHCII$^{-/-}$ and CD45.1 B6 mice, and T cells were depleted magnetically using Thy1.2 Dynabeads (11443D, Thermo Fisher). $5x10^6$ bone marrow cells were then injected intravenously into lethally irradiated recipient C57Bl6 MHCII$^{-/-}$ and CD45.1 B6 mice 6 hours after irradiation was completed (5.5 Gy x 2 doses, 3 hours apart). Mice were treated with Bactrim for 3 weeks following the transfer and were housed in autoclaved cages.

Full bone marrow chimera reconstitution was confirmed 6 weeks after transfer, by flow cytometry analysis of peripheral blood cells stained with anti-CD45.1 and anti-CD45.2 antibodies. MHCII expression on chimeric mouse lung cells was assessed 8 weeks post-transfer.

Detection of germline MHCII deletion

Consistent with prior reports [228, 229], our Ab1$^{fl/fl}$ mice experienced spontaneous germline disruption of the I-A^b locus at a rate of ~5%, resulting in global loss of MHCII from all cells. Therefore, in addition to standard genotyping all SPC$^{\Delta Ab1}$ and Ab1$^{fl/fl}$ mice were screened at >5 weeks of age for germline deletion of MHCII, by flow cytometric measurement of MHCII on peripheral blood immune cells isolated by cheek bleed. Specifically, cells were stained for surface expression of CD45, CD19,

and MHCII, and mice were excluded from further study if B cells ($CD45^+$ $CD19^+$) lacked MHCII expression. All mice included in experiments discussed here had appropriately intact MHCII expression by peripheral blood screening.

Tamoxifen administration

$SPC^{\Delta Ab1}$, $Ab1^{fl/fl}$, and SPC^{Cre} mice >5 weeks of age were oral gavaged daily with 2 mg tamoxifen for 4 days, by delivering 100 μL of 20 mg/mL solution of tamoxifen (T5648, Sigma) in a 9:1 corn oil:ethanol mixture. Mice were used in experiments ≥5 days after the last dose of tamoxifen.

Histological analysis

To assess MHCII expression in $SPC^{\Delta Ab1}$, $Ab1^{fl/fl}$, and $MHCII^{-/-}$ mice by immunofluorescence, the lung vasculature was first perfused with 5 mL 4% paraformaldehyde in PBS (4% PFA) by injecting into the cardiac right ventricle. Lungs were then inflated via intratracheal instillation of 0.9 mL 4% PFA. The trachea was then tied with suture to keep the lungs inflated while they were excised en bloc and then placed in an additional 30 mL 4% PFA, then incubated for 24 hours at 4°C. Tissue was then processed, paraffin-embedded, sectioned, and stained with DAPI, and the following antibodies: anti-mouse pro-SPC (AB3786, EMD Millipore), anti-mouse MHCII (107601, Biolegend), and anti-mouse E-cadherin (ab76319, Abcam). Images were acquired using an Axio Observer 7 widefield microscope with Axiocam 702 monochrome CMOS camera and Zen blue acquisition software (Zeiss). Composite images were then generated in Fiji.

To assess lung pathology at homeostasis in SPC$^{\Delta Ab1}$ and Ab1$^{fl/fl}$ mice, the lungs were inflated via intratracheal instillation of ~1 mL 10% neutral buffered formalin (NBF), then placed in an additional ~30 mL 10% NBF and incubated for 24 hours at RT. Tissue was then processed, paraffin-embedded, sectioned, and stained with hematoxylin and eosin, and the resulting lung sections were evaluated for signs of disease by a veterinary pathologist. Images were acquired using an Axio Observer 7 widefield microscope with Axiocam 503 color CCD camera and Zen blue acquisition software (Zeiss).

T cell phenotyping analyses

For determination of T cell phenotype as well as activation status, cells were surface stained for the following markers: CD44, CD62L, CD69, CD11a, PD1, and LAG3. Cells were also stained intranuclearly for FoxP3 and Ki67.

Lung organoids

Alveolar organoids were cultured as described previously [115, 143], with the following modifications. Briefly, 5x10^3 AT2s sorted from either SPC$^{\Delta Ab1}$ and Ab1$^{fl/fl}$ mice were cocultured with 5x10^4 Pdgfrα^+ lung fibroblasts sorted from WT C57Bl/6 mice. Cells were suspended in 90μL of a 1:1 mixture of Matrigel:modified SAGM media (CC-3118, Lonza). SAGM media is modified by adding 0.1 μg/mL cholera toxin (C8052, Sigma) and the following SAGM BulletKit components: 10 μg/mL insulin, 5 μg/mL transferrin, 25 ng/mL EGF, 30 μg/mL bovine pituitary extract, 0.01μM retinoic acid, and 5% FBS. The 1:1 mixture containing cells was placed in a cell culture insert (353095, Corning); after solidification of the matrix at 37°C, the insert was placed

inside a well of 24-well plate containing modified SAGM media. For the first two days of culture, 10 μM ROCK inhibitor Y27632 (Y0503, Sigma) was added to the media. The media was changed every 48 hours, and after 21 days organoids were imaged using an EVOS FL Auto. Organoid numbers were quantified in Fiji using the Cell Counter plugin.

Virus infections for weight loss and mortality analysis

For influenza infection weight loss monitoring, mice were infected intranasally with 3 FFU IAV PR8 diluted in 20 μL PBS under isoflurane anesthesia. For influenza infection mortality experiments, mice were infected intranasally with 15 FFU IAV PR8 diluted in 20 μL PBS under isoflurane anesthesia. For both Sendai virus infection weight loss monitoring and mortality analyses, mice were infected intranasally with 3.5-7x10^4 $TCID_{50}$ SeV 52 diluted in 35 μL PBS under ketamine (70 mg/kg) + xylazine (5 mg/kg) anesthesia. For all weight loss experiments, mice were weighed on the days indicated. For all mortality studies, mice were monitored daily for death or moribund state as an endpoint.

Lung virus titering

For influenza virus titering, mice were infected intranasally with 3 FFU IAV PR8 diluted in 35 μL PBS under ketamine (70 mg/kg) + xylazine (5 mg/kg) anesthesia. For Sendai virus titering, mice were infected intranasally with 7x10^4 $TCID_{50}$ SeV 52 diluted in 35 μL PBS under ketamine (70 mg/kg) + xylazine (5 mg/kg) anesthesia. Mice were sacrificed at the timepoints indicated for virus titers analysis.

For influenza virus titers determination, MDCK cells were infected with serial 10-fold dilutions of lung homogenates in MEM containing 50μg/mL gentamicin, 5mM HEPES, and 1μg/mLTPCK-treated trypsin (LS003750, Worthington Biochemical) in quadruplicate per lung. After 4 days of incubation at 37°C, the presence of virus at each dilution was determined by visual cytopathic effect, and lung virus titers were determined using the Reed and Muench Calculation.

For Sendai virus titers determination, LLC-MK2 cells were infected with serial 10-fold dilutions of lung homogenates in DMEM containing 50μg/mL gentamicin, 0.35% BSA, 0.12% NaHCO3, and 2 μg/mL TPCK-treated trypsin in triplicate per lung. After 3 days of incubation at 37°C, the presence of virus was determined by assessing the capacity of 25μL of supernatant at each dilution to hemagglutinate 0.25% chicken red blood cells (cRBCs) in a 100μL final volume after a 30" incubation at room temperature. Lung virus titers were then determined using the Reed and Muench Calculation.

Influenza LAG3$^+$ T cell expansion analysis

Mice were infected intranasally with 3 FFU IAV PR8 diluted in 20 μL PBS under isoflurane anesthesia. Mice were sacrificed 9 days after infection and lungs were stained *ex vivo* for T cell surface markers and LAG3.

Hybridoma assay

NFAT-*lacZ*-inducible T cell hybridomas recognizing MHCII-restricted influenza-derived epitopes have been described previously [46, 178]. Hybridoma recognition of

cognate peptide/MHCII complexes results in β-galactosidase production, which was detected using a fluorometric β-galactosidase substrate 4-methyl-umbelliferyl-β-D-galactopyranoside ("MUG"; M1633, Sigma).

$1x10^4$ APCs were treated with media only, 20 μg/mL peptide, or $1x10^6$ FFU influenza virus in complete RPMI media for 45" at 37°C, 6% CO_2 in a 384 well plate; for AT2 conditions, wells were pre-coated with a thin layer of 9:1 RPMI:Matrigel (356231, Corning) mixture. After 45", $2x10^4$ hybridomas were directly added, and cells were then cocultured for 14-18 hours at 37°C, 6% CO_2. MUG substrate solution (33 μg/mL MUG in PBS containing 38.5 μM 2-mercaptoethanol, 9 mM MgCl2, and 1.25% NP40) was then added to the co-culture at a ratio of 1:5 MUG solution:co-culture, then incubated for 3 hours at 37°C, 6% CO_2. Fluorescence (excitation: 365 nm, emission: 445nm) was detected on Tecan Infinite M200 Pro Plate Reader.

IFNγ ELISpot assay

For isolation of influenza-infected APCs, WT and $MHCII^{-/-}$ mice were infected intranasally with $1.2x10^6$ FFU IAV PR8 diluted in 35 μL PBS under ketamine (70 mg/kg) + xylazine (5 mg/kg) anesthesia. Lungs were harvested from mice 4 days after infection or from naïve mice. APCs were isolated via cell sorting, as above.

For isolation of influenza-experienced effector T cells, WT mice were infected intranasally with 3 FFU IAV PR8 diluted in 35 μL PBS under ketamine (70 mg/kg) + xylazine (5 mg/kg) anesthesia. Spleens were harvested from mice 10 days after infection. $CD4^+$ and $CD8^+$ T cells were isolated from bulk splenocytes using

Dynabeads Untouched Kits for mouse CD4 cells and CD8 cells, respectively, per the manufacturer's protocol (11415D and 11417D, Thermo Fisher).

96-well MultiScreen$_{HTS}$ IP 0.45 μm filter plates (MSIPS4W10, Millipore-Sigma) were coated with mouse IFNγ capture antibody (551881, BD) and incubated at 4°C for 20 hours prior to the assay. Plates were blocked with complete RPMI media for >1 hour at 37°C, after which $5x10^4$ APCs and $1x10^5$ T cells were co-cultured for 14-18 hours in the presence of 2μg/mL anti-CD28 (40-0281-M001, Tonbo Biosciences). T cell IFNγ production was detected via biotinylated IFNγ detection antibody (551881, BD), followed by HRP-Streptavidin (557630, BD) and chromogenic 3-Amino-9-ethylcarbazole (AEC) substrate (551951). IFNγ spots were imaged and counted using a CTL ImmunoSpot S6 Universal Analyzer.

Detection of influenza-infected cells

For quantification of influenza virus infection in hybridoma and ELISpot assays, at assay endpoint cells were stained for surface hemagglutinin (HA) protein expression or intracellular nucleoprotein (NP) protein expression. Two different fluorophore-conjugated versions of the anti-HA antibody were labeled in house, with the Alexa Fluor 488 and Alexa Fluor 647 labeling kits (A20181 or A20186, Thermo Fisher).

IFNγ treatment of mice

Mice were injected intravenously under isoflurane anesthesia once daily with $1x10^5$ U recombinant mouse IFNγ (575306, Biolegend) in 150 μL PBS, or PBS only, for 3 days in a row.

Inhaled Ova allergy model

Mice were injected intraperitoneally with 10μg ova (A5503, Sigma) and 2.25mg Alum (77161, Thermo Fisher) in 200μL on days 0 and 14. 10μg ova protein in 20μL PBS was then administered to mice intranasally under isoflurane anesthesia once daily on days 28, 29, and 30. BAL cells and lung T cells were harvested on day 31, as described above.

Intracellular cytokine staining

For intracellular cytokine staining, lung cells from ova-immunized mice were incubated in R10 media containing 2μg/mL anti-CD28, 50 ng/mL phorbol 12-myristate 13-acetate (PMA), 1μg/mL ionomycin, and 1X brefeldin-A (420601; Biolegend) for 5 hours at 37°C. Cells were then surface stained with anti-mouse CD8, and intracellularly with antibodies against mouse CD3, CD4, IL5, IL13, IL17, and IFNγ.

Analysis of publicly available RNA-sequencing data

For analysis of H2Mβ1 and H2Mβ2 expression by B cell, dendritic cell, and macrophage subsets, bulk RNA-sequencing data was obtained using the Immunological Genome Project [153] Gene Skyline RNA-seq Data Browser, available at (http://rstats.immgen.org/Skyline/skyline.html).

For analysis of AT2 cells by bulk RNA-sequencing and single cell RNA-sequencing, data were obtained from the LungMAP consortium, which is funded by 1U01HL122638. The bulk RNA-sequencing dataset was contributed by Jeffrey A. Whitsett (CCHMC) and Yan Xu (CCHMC), and is available at

(https://www.lungmap.net/breath-omics-experiment-page/?experimentTypeId=LMXT0000000018&experimentId=LMEX0000001223&analysisId=LMAN0000000225&view=allEntities). The single cell RNA-sequencing dataset was contributed by Jeffrey A. Whitsett (CCHMC), Bruce Aronow (CCHMC), and S. Stephen Potter (CCHMC), and is available at: (https://www.lungmap.net/breath-omics-experiment-page/?experimentTypeId=LMXT0000000016&experimentId=LMEX0000001602&analysisId=LMAN0000000107&view=allEntities).

Statistical analysis

All statistical analyses were performed using Prism 8 software (GraphPad). The statistical tests used are indicated in the figure legend corresponding to each specific experiment. Unpaired two-tailed Student's *t*-test was used to compare means between two groups if they had similar variances by F-test, and if they passed all four of the following normality of residuals tests: Anderson-Darling, D'Agostino-Pearson omnibus, Shapiro-Wilk, and Kolmogorov-Smirnov. If variances were significantly different, unpaired two-tailed Welch's *t*-test was used, and if the samples failed at least one normality test then two-tailed Mann-Whitney test was used. For weight loss analysis, a mixed model, which uses a compound symmetry covariance matrix and is fit using Restricted Maximum Likelihood (REML), with Geisser-Greenhouse correction was used, followed by post-hoc multiple comparisons with Sidak's correction; this was used instead of repeated-measures ANOVA, as it can handle missing values. For mortality analysis, the Log-rank (Mantel-cox) test was used to compare survival curves. Two-way ANOVA followed by post-hoc multiple comparisons with Tukey's or

Sidak's correction was used to compare means between groups with 2 contributing independent variables; Tukey's correction was used when all possible means were compared, and Sidak's correction was used when means were compared across one factor only. Three-way ANOVA followed by post-hoc multiple comparisons with Sidak's correction was used to compare means between groups with 3 contributing independent variables.

Flow cytometry antibodies used		
Target	**Clone or Catalog #**	**Source**
mouse CD45	30-F11	Biolegend
mouse CD31	390	Biolegend
mouse EpCAM (CD326)	G8.8	Biolegend
mouse I-A/I-E (MHCII)	M5/114.15.2	Biolegend
mouse proSP-C	AB3786	Sigma Aldrich
human HT2-280	TB-27AHT2-280	Terrace Biotech
mouse IgM	II/41	Thermo Fisher
mouse CD11c	N418	Biolegend
mouse CD103	2E7	Biolegend
mouse CD11b	M1/70	BD
mouse CD64	X54-5/7.1	Biolegend
mouse CD3	145-2C11 or 17A2	BD or Biolegend
mouse CD8	53-6.7	BD
mouse CD19	6D5	Biolegend
mouse B220	RA3-6B2	Biolegend
mouse CD4	RM4-5 or GK1.5	Biolegend
mouse NK1.1	PK136	Thermo Fisher
mouse TCRδ	GL3	Biolegend
mouse Ly6G	1A8	BD
mouse SiglecF	E50-2440	BD
mouse Podoplanin	8.1.1	Thermo Fisher or Biolegend
mouse Sca-1	D7	Thermo Fisher
mouse CD34	MEC14.7	Biolegend
mouse Pdgfrα (CD140a)	APA5	Thermo Fisher
human HLA-DR	G46-6	BD
mouse I-A^b	AF-120.1	Thermo Fisher
mouse I-E^d	14-4-4S	Biolegend
mouse invariant chain (CD74)	In-1	BD
mouse H2M$\alpha\beta$2	2E5A	BD
human invariant chain (CD74)	Pin.1	Biolegend
human HLA-DM	Map.DM1	L. Denzin
mouse CLIP/I-A^b	15G4	L. Denzin
mouse Eα^{52-68}/I-A^b	YAe	Thermo Fisher
mouse CD80	16-10A1	BD
mouse CD86	GL1	BD
mouse ICAM-1 (CD54)	YN1/1.7.4	Biolegend
mouse CD45.1	A20	Biolegend
mouse CD45.2	104	Biolegend
influenza hemagglutinin (HA)	IC5-4F8	BEI
influenza nucleoprotein (NP)	D67J	Thermo Fisher
mouse CD44	IM7	Biolegend
mouse CD62L	MEL-14	Biolegend
mouse CD69	H1.2F3	Biolegend
mouse CD11a	M17/4	Biolegend
mouse PD1	RMP1-30	Biolegend
mouse LAG3	C9B7W	Biolegend
mouse Foxp3	FJK-16s	Thermo Fisher
mouse Ki67	16A8	Biolegend
mouse IL5	TRFK5	Biolegend
mouse IL13	eBio13A	Thermo Fisher
mouse IL17	TC11-18H10.1	Biolegend
mouse IFNγ	XMG1.2	Biolegend

Table 6.1: Flow cytometry antibodies used for all studies.

REFERENCES

1. Murphy, K., et al., *Janeway's Immunobiology*. 8th ed. 2012, New York: Garland Science.

2. Zhu, J., H. Yamane, and W.E. Paul, *Differentiation of effector CD4 T cell populations.* Annu Rev Immunol, 2010. **28**: p. 445-89.

3. Swain, S.L., K.K. McKinstry, and T.M. Strutt, *Expanding roles for CD4(+) T cells in immunity to viruses.* Nat Rev Immunol, 2012. **12**(2): p. 136-48.

4. Graham, M.B., V.L. Braciale, and T.J. Braciale, *Influenza virus-specific CD4+ T helper type 2 T lymphocytes do not promote recovery from experimental virus infection.* J Exp Med, 1994. **180**(4): p. 1273-82.

5. Alwan, W.H., W.J. Kozlowska, and P.J. Openshaw, *Distinct types of lung disease caused by functional subsets of antiviral T cells.* J Exp Med, 1994. **179**(1): p. 81-9.

6. Braciale, T.J., J. Sun, and T.S. Kim, *Regulating the adaptive immune response to respiratory virus infection.* Nat Rev Immunol, 2012. **12**(4): p. 295-305.

7. Chen, L. and D.B. Flies, *Molecular mechanisms of T cell co-stimulation and co-inhibition.* Nat Rev Immunol, 2013. **13**(4): p. 227-42.

8. Greenwald, R.J., G.J. Freeman, and A.H. Sharpe, *The B7 family revisited.* Annu Rev Immunol, 2005. **23**: p. 515-48.

9. Schwartz, R.H., *T cell anergy.* Annu Rev Immunol, 2003. **21**: p. 305-34.

10. Tubo, N.J. and M.K. Jenkins, *TCR signal quantity and quality in CD4(+) T cell differentiation.* Trends Immunol, 2014. **35**(12): p. 591-596.

11. Itoh, Y. and R.N. Germain, *Single Cell Analysis Reveals Regulated Hierarchical T Cell Antigen Receptor Signaling Thresholds and Intraclonal Heterogeneity for Individual Cytokine Responses of CD4+T Cells.* The Journal of Experimental Medicine, 1997. **186**(5): p. 757-766.

12. Keir, M.E., et al., *PD-1 and its ligands in tolerance and immunity.* Annu Rev Immunol, 2008. **26**: p. 677-704.

13. Sharpe, A.H., *Mechanisms of costimulation.* Immunol Rev, 2009. **229**(1): p. 5-11.

14. Crawford, A. and E.J. Wherry, *The diversity of costimulatory and inhibitory receptor pathways and the regulation of antiviral T cell responses.* Curr Opin Immunol, 2009. **21**(2): p. 179-86.

15. Murphy, K.M. and B. Stockinger, *Effector T cell plasticity: flexibility in the face of changing circumstances.* Nat Immunol, 2010. **11**(8): p. 674-80.

16. Magombedze, G., et al., *Cellular and population plasticity of helper CD4(+) T cell responses.* Front Physiol, 2013. **4**: p. 206.

17. Roche, P.A. and K. Furuta, *The ins and outs of MHC class II-mediated antigen processing and presentation.* Nat Rev Immunol, 2015. **15**(4): p. 203-16.

18. Blum, J.S., P.A. Wearsch, and P. Cresswell, *Pathways of antigen processing.* Annu Rev Immunol, 2013. **31**: p. 443-73.

19. Bakke, O. and B. Dobberstein, *MHC class II-associated invariant chain contains a sorting signal for endosomal compartments.* Cell, 1990. **63**(4): p. 707-16.

20. Bikoff, E.K., et al., *Defective major histocompatibility complex class II assembly, transport, peptide acquisition, and CD4+ T cell selection in mice lacking invariant chain expression.* J Exp Med, 1993. **177**(6): p. 1699-712.

21. Cresswell, P., *Invariant chain structure and MHC class II function.* Cell, 1996. **84**(4): p. 505-7.

22. Riberdy, J.M., et al., *HLA-DR molecules from an antigen-processing mutant cell line are associated with invariant chain peptides.* Nature, 1992. **360**(6403): p. 474-7.

23. Roche, P.A. and P. Cresswell, *Invariant chain association with HLA-DR molecules inhibits immunogenic peptide binding.* Nature, 1990. **345**(6276): p. 615-8.

24. Riese, R.J., et al., *Essential role for cathepsin S in MHC class II-associated invariant chain processing and peptide loading.* Immunity, 1996. **4**(4): p. 357-66.

25. Shi, G.P., et al., *Cathepsin S required for normal MHC class II peptide loading and germinal center development.* Immunity, 1999. **10**(2): p. 197-206.

26. Nakagawa, T., et al., *Cathepsin L: critical role in Ii degradation and CD4 T cell selection in the thymus.* Science, 1998. **280**(5362): p. 450-3.

27. Fling, S.P., B. Arp, and D. Pious, *HLA-DMA and -DMB genes are both required for MHC class II/peptide complex formation in antigen-presenting cells.* Nature, 1994. **368**(6471): p. 554-8.

28. Morris, P., et al., *An essential role for HLA-DM in antigen presentation by class II major histocompatibility molecules.* Nature, 1994. **368**(6471): p. 551-4.

29. Martin, W.D., et al., *H2-M mutant mice are defective in the peptide loading of class II molecules, antigen presentation, and T cell repertoire selection.* Cell, 1996. **84**(4): p. 543-50.

30. Alfonso, C. and L. Karlsson, *Nonclassical MHC class II molecules.* Annu Rev Immunol, 2000. **18**: p. 113-42.

31. Pinet, V., et al., *Antigen presentation mediated by recycling of surface HLA-DR molecules.* Nature, 1995. **375**(6532): p. 603-6.

32. Pinet, V.M. and E.O. Long, *Peptide loading onto recycling HLA-DR molecules occurs in early endosomes.* Eur J Immunol, 1998. **28**(3): p. 799-804.

33. Sinnathamby, G. and L.C. Eisenlohr, *Presentation by recycling MHC class II molecules of an influenza hemagglutinin-derived epitope that is revealed in the early endosome by acidification.* J Immunol, 2003. **170**(7): p. 3504-13.

34. Pathak, S.S., J.D. Lich, and J.S. Blum, *Cutting edge: editing of recycling class II:peptide complexes by HLA-DM.* J Immunol, 2001. **167**(2): p. 632-5.

35. Miller, M.A., A.P. Ganesan, and L.C. Eisenlohr, *Toward a Network Model of MHC Class II-Restricted Antigen Processing.* Front Immunol, 2013. **4**: p. 464.

36. Accapezzato, D., et al., *Generation of an MHC class II-restricted T cell epitope by extracellular processing of hepatitis delta antigen.* J Immunol, 1998. **160**(11): p. 5262-6.

37. Santambrogio, L., et al., *Extracellular antigen processing and presentation by immature dendritic cells.* Proc Natl Acad Sci U S A, 1999. **96**(26): p. 15056-61.

38. Santambrogio, L., et al., *Abundant empty class II MHC molecules on the surface of immature dendritic cells.* Proc Natl Acad Sci U S A, 1999. **96**(26): p. 15050-5.

39. Vacchino, J.F. and H.M. McConnell, *Peptide binding to active class II MHC protein on the cell surface.* J Immunol, 2001. **166**(11): p. 6680-5.

40. Pathak, S.S. and J.S. Blum, *Endocytic recycling is required for the presentation of an exogenous peptide via MHC class II molecules.* Traffic, 2000. **1**(7): p. 561-9.

41. Eisenlohr, L.C. and C.J. Hackett, *Class II major histocompatibility complex-restricted T cells specific for a virion structural protein that do not recognize exogenous influenza virus. Evidence that presentation of labile T cell determinants is favored by endogenous antigen synthesis.* J Exp Med, 1989. **169**(3): p. 921-31.

42. Bikoff, E. and B.K. Birshtein, *T cell clones specific for IgG2a of the a allotype: direct evidence for presentation of endogenous antigen.* J Immunol, 1986. **137**(1): p. 28-34.

43. Weiss, S. and B. Bogen, *B-lymphoma cells process and present their endogenous immunoglobulin to major histocompatibility complex-restricted T cells.* Proc Natl Acad Sci U S A, 1989. **86**(1): p. 282-6.

44. Jacobson, S., et al., *Recognition of intracellular measles virus antigens by HLA class II restricted measles virus-specific cytotoxic T lymphocytes.* Ann N Y Acad Sci, 1988. **540**: p. 352-3.

45. Nuchtern, J.G., W.E. Biddison, and R.D. Klausner, *Class II MHC molecules can use the endogenous pathway of antigen presentation.* Nature, 1990. **343**(6253): p. 74-6.

46. Miller, M.A., et al., *Endogenous antigen processing drives the primary CD4+ T cell response to influenza.* Nat Med, 2015. **21**(10): p. 1216-22.

47. Gannage, M. and C. Munz, *Autophagy in MHC class II presentation of endogenous antigens.* Curr Top Microbiol Immunol, 2009. **335**: p. 123-40.

48. Jaraquemada, D., M. Marti, and E.O. Long, *An endogenous processing pathway in vaccinia virus-infected cells for presentation of cytoplasmic antigens to class II-restricted T cells.* J Exp Med, 1990. **172**(3): p. 947-54.

49. Leung, C.S., *Endogenous Antigen Presentation of MHC Class II Epitopes through Non-Autophagic Pathways.* Front Immunol, 2015. **6**: p. 464.

50. Lich, J.D., J.F. Elliott, and J.S. Blum, *Cytoplasmic processing is a prerequisite for presentation of an endogenous antigen by major histocompatibility complex class II proteins.* J Exp Med, 2000. **191**(9): p. 1513-24.

51. Dani, A., et al., *The pathway for MHCII-mediated presentation of endogenous proteins involves peptide transport to the endo-lysosomal compartment.* J Cell Sci, 2004. **117**(Pt 18): p. 4219-30.

52. van den Elsen, P.J., *Expression regulation of major histocompatibility complex class I and class II encoding genes.* Front Immunol, 2011. **2**: p. 48.

53. Reith, W., et al., *Regulation of MHC class II gene expression.* Immunobiology, 1995. **193**(2-4): p. 248-53.

54. Chang, C.-H., et al., *Mice Lacking the MHC Class II Transactivator (CIITA) Show Tissue-Specific Impairment of MHC Class II Expression.* Immunity, 1996. **4**(2): p. 167-178.

55. Wong, D., et al., *Genomic mapping of the MHC transactivator CIITA using an integrated ChIP-seq and genetical genomics approach.* Genome Biol, 2014. **15**(10): p. 494.

56. Krawczyk, M., et al., *Identification of CIITA regulated genetic module dedicated for antigen presentation.* PLoS Genet, 2008. **4**(4): p. e1000058.

57. Scharer, C.D., et al., *Genome-wide CIITA-binding profile identifies sequence preferences that dictate function versus recruitment.* Nucleic Acids Res, 2015. **43**(6): p. 3128-42.

58. Reith, W., S. LeibundGut-Landmann, and J.M. Waldburger, *Regulation of MHC class II gene expression by the class II transactivator.* Nat Rev Immunol, 2005. **5**(10): p. 793-806.

59. Campana, S., et al., *Cross-dressing: an alternative mechanism for antigen presentation.* Immunol Lett, 2015. **168**(2): p. 349-54.

60. Joly, E. and D. Hudrisier, *What is trogocytosis and what is its purpose?* Nat Immunol, 2003. **4**(9): p. 815.

61. Miyake, K., et al., *Trogocytosis of peptide-MHC class II complexes from dendritic cells confers antigen-presenting ability on basophils.* Proc Natl Acad Sci U S A, 2017. **114**(5): p. 1111-1116.

62. Thery, C., L. Zitvogel, and S. Amigorena, *Exosomes: composition, biogenesis and function.* Nat Rev Immunol, 2002. **2**(8): p. 569-79.

63. Thery, C., et al., *Indirect activation of naive CD4+ T cells by dendritic cell-derived exosomes.* Nat Immunol, 2002. **3**(12): p. 1156-62.

64. Gerdes, H.H. and R.N. Carvalho, *Intercellular transfer mediated by tunneling nanotubes.* Curr Opin Cell Biol, 2008. **20**(4): p. 470-5.

65. Schiller, C., et al., *Tunneling nanotubes enable intercellular transfer of MHC class I molecules.* Hum Immunol, 2013. **74**(4): p. 412-6.

66. Sallusto, F., et al., *Dendritic cells use macropinocytosis and the mannose receptor to concentrate macromolecules in the major histocompatibility complex class II compartment: downregulation by cytokines and bacterial products.* J Exp Med, 1995. **182**(2): p. 389-400.

67. Stuart, L.M. and R.A. Ezekowitz, *Phagocytosis: elegant complexity.* Immunity, 2005. **22**(5): p. 539-50.

68. Rock, K.L., B. Benacerraf, and A.K. Abbas, *Antigen presentation by hapten-specific B lymphocytes. I. Role of surface immunoglobulin receptors.* J Exp Med, 1984. **160**(4): p. 1102-13.

69. Adler, L.N., et al., *The Other Function: Class II-Restricted Antigen Presentation by B Cells.* Front Immunol, 2017. **8**: p. 319.

70. Lanzavecchia, A., *Receptor-mediated antigen uptake and its effect on antigen presentation to class II-restricted T lymphocytes.* Annu Rev Immunol, 1990. **8**: p. 773-93.

71. Avalos, A.M. and H.L. Ploegh, *Early BCR Events and Antigen Capture, Processing, and Loading on MHC Class II on B Cells.* Front Immunol, 2014. **5**: p. 92.

72. Cella, M., et al., *Inflammatory stimuli induce accumulation of MHC class II complexes on dendritic cells.* Nature, 1997. **388**(6644): p. 782-7.

73. Chow, A., et al., *Dendritic cell maturation triggers retrograde MHC class II transport from lysosomes to the plasma membrane.* Nature, 2002. **418**(6901): p. 988-94.

74. West, M.A., et al., *Enhanced dendritic cell antigen capture via toll-like receptor-induced actin remodeling.* Science, 2004. **305**(5687): p. 1153-7.

75. Delamarre, L., et al., *Differential lysosomal proteolysis in antigen-presenting cells determines antigen fate.* Science, 2005. **307**(5715): p. 1630-4.

76. Manoury, B., *Proteases: essential actors in processing antigens and intracellular toll-like receptors.* Front Immunol, 2013. **4**: p. 299.

77. Manoury, B., et al., *Destructive processing by asparagine endopeptidase limits presentation of a dominant T cell epitope in MBP.* Nat Immunol, 2002. **3**(2): p. 169-74.

78. Leroux, L.P., et al., *Parasite Manipulation of the Invariant Chain and the Peptide Editor H2-DM Affects Major Histocompatibility Complex Class II Antigen Presentation during Toxoplasma gondii Infection.* Infect Immun, 2015. **83**(10): p. 3865-80.

79. Long, E.O., et al., *Invariant chain prevents the HLA-DR-restricted presentation of a cytosolic peptide.* J Immunol, 1994. **153**(4): p. 1487-94.

80. Tourne, S., et al., *Selection of a broad repertoire of CD4+ T cells in H-2Ma0/0 mice.* Immunity, 1997. **7**(2): p. 187-95.

81. Stebbins, C.C., et al., *The requirement for DM in class II-restricted antigen presentation and SDS-stable dimer formation is allele and species dependent.* J Exp Med, 1995. **181**(1): p. 223-34.

82. Ma, C. and J.S. Blum, *Receptor-mediated endocytosis of antigens overcomes the requirement for HLA-DM in class II-restricted antigen presentation.* J Immunol, 1997. **158**(1): p. 1-4.

83. Yin, L., et al., *HLA-DM constrains epitope selection in the human CD4 T cell response to vaccinia virus by favoring the presentation of peptides with longer HLA-DM-mediated half-lives.* J Immunol, 2012. **189**(8): p. 3983-94.

84. Hung, S.C., et al., *Epitope Selection for HLA-DQ2 Presentation: Implications for Celiac Disease and Viral Defense.* J Immunol, 2019. **202**(9): p. 2558-2569.

85. Honey, K., et al., *Effect of decreasing the affinity of the class II-associated invariant chain peptide on the MHC class II peptide repertoire in the presence or absence of H-2M.* J Immunol, 2004. **172**(7): p. 4142-50.

86. Van Seventer, G.A., et al., *The LFA-1 ligand ICAM-1 provides an important costimulatory signal for T cell receptor-mediated activation of resting T cells.* J Immunol, 1990. **144**(12): p. 4579-86.

87. Waldburger, J.M., et al., *Promoter IV of the class II transactivator gene is essential for positive selection of CD4+ T cells.* Blood, 2003. **101**(9): p. 3550-9.

88. Abramson, J. and G. Anderson, *Thymic Epithelial Cells.* Annu Rev Immunol, 2017. **35**: p. 85-118.

89. Hepworth, M.R., et al., *Group 3 innate lymphoid cells mediate intestinal selection of commensal bacteria-specific CD4(+) T cells.* Science, 2015. **348**(6238): p. 1031-5.

90. Hepworth, M.R., et al., *Innate lymphoid cells regulate CD4+ T-cell responses to intestinal commensal bacteria.* Nature, 2013. **498**(7452): p. 113-7.

91. Dubrot, J., et al., *Lymph node stromal cells acquire peptide-MHCII complexes from dendritic cells and induce antigen-specific CD4(+) T cell tolerance.* J Exp Med, 2014. **211**(6): p. 1153-66.

92. Dubrot, J., et al., *Absence of MHC-II expression by lymph node stromal cells results in autoimmunity.* Life Sci Alliance, 2018. **1**(6): p. e201800164.

93. Rouhani, S.J., et al., *Roles of lymphatic endothelial cells expressing peripheral tissue antigens in CD4 T-cell tolerance induction.* Nat Commun, 2015. **6**: p. 6771.

94. Nadafi, R., et al., *Lymph Node Stromal Cells Generate Antigen-Specific Regulatory T Cells and Control Autoreactive T and B Cell Responses.* Cell Rep, 2020. **30**(12): p. 4110-4123 e4.

95. Koyama, M., et al., *MHC Class II Antigen Presentation by the Intestinal Epithelium Initiates Graft-versus-Host Disease and Is Influenced by the Microbiota.* Immunity, 2019. **51**(5): p. 885-898 e7.

96. Thelemann, C., et al., *Interferon-gamma induces expression of MHC class II on intestinal epithelial cells and protects mice from colitis.* PLoS One, 2014. **9**(1): p. e86844.

97. Kreisel, D., et al., *Cutting edge: MHC class II expression by pulmonary nonhematopoietic cells plays a critical role in controlling local inflammatory responses.* J Immunol, 2010. **185**(7): p. 3809-13.

98. Carman, C.V. and R. Martinelli, *T Lymphocyte-Endothelial Interactions: Emerging Understanding of Trafficking and Antigen-Specific Immunity.* Front Immunol, 2015. **6**: p. 603.

99. Pober, J.S., et al., *Antigen Presentation by Vascular Cells.* Front Immunol, 2017. **8**: p. 1907.

100. Krupnick, A.S., et al., *Cutting Edge: Murine Vascular Endothelium Activates and Induces the Generation of Allogeneic CD4+25+Foxp3+ Regulatory T Cells.* The Journal of Immunology, 2005. **175**(10): p. 6265-6270.

101. van den Elsen, P.J., et al., *Lack of CIITA expression is central to the absence of antigen presentation functions of trophoblast cells and is caused by methylation*

of the IFN-gamma inducible promoter (PIV) of CIITA. Hum Immunol, 2000. **61**(9): p. 850-62.

102. Kambayashi, T. and T.M. Laufer, *Atypical MHC class II-expressing antigen-presenting cells: can anything replace a dendritic cell?* Nat Rev Immunol, 2014. **14**(11): p. 719-30.

103. Duraes, F.V., et al., *Role of major histocompatibility complex class II expression by non-hematopoietic cells in autoimmune and inflammatory disorders: facts and fiction.* Tissue Antigens, 2013. **82**(1): p. 1-15.

104. DiPiazza, A., et al., *Pandemic 2009 H1N1 Influenza Venus reporter virus reveals broad diversity of MHC class II-positive antigen-bearing cells following infection in vivo.* Sci Rep, 2017. **7**(1): p. 10857.

105. Hasegawa, K., et al., *Fraction of MHCII and EpCAM expression characterizes distal lung epithelial cells for alveolar type 2 cell isolation.* Respir Res, 2017. **18**(1): p. 150.

106. Debbabi, H., et al., *Primary type II alveolar epithelial cells present microbial antigens to antigen-specific CD4+ T cells.* Am J Physiol Lung Cell Mol Physiol, 2005. **289**(2): p. L274-9.

107. Gereke, M., et al., *Alveolar type II epithelial cells present antigen to CD4(+) T cells and induce Foxp3(+) regulatory T cells.* Am J Respir Crit Care Med, 2009. **179**(5): p. 344-55.

108. Lo, B., et al., *Alveolar Epithelial Type II Cells Induce T Cell Tolerance to Specific Antigen.* The Journal of Immunology, 2008. **180**(2): p. 881-888.

109. Corbiere, V., et al., *Phenotypic characteristics of human type II alveolar epithelial cells suitable for antigen presentation to T lymphocytes.* Respir Res, 2011. **12**: p. 15.

110. Cunningham, A.C., et al., *A comparison of the antigen-presenting capabilities of class II MHC-expressing human lung epithelial and endothelial cells.* Immunology, 1997. **91**(3): p. 458-63.

111. Fehrenbach, H., *Alveolar epithelial type II cell: defender of the alveolus revisited.* Respir Res, 2001. **2**(1): p. 33-46.

112. Mason, R.J., *Biology of alveolar type II cells.* Respirology, 2006. **11 Suppl**: p. S12-5.

113. Han, S. and R.K. Mallampalli, *The Role of Surfactant in Lung Disease and Host Defense against Pulmonary Infections.* Ann Am Thorac Soc, 2015. **12**(5): p. 765-74.

114. Beers, M.F. and S. Mulugeta, *Surfactant protein C biosynthesis and its emerging role in conformational lung disease.* Annu Rev Physiol, 2005. **67**: p. 663-96.

115. Zacharias, W.J., et al., *Regeneration of the lung alveolus by an evolutionarily conserved epithelial progenitor.* Nature, 2018. **555**(7695): p. 251-255.

116. Vaughan, A.E., et al., *Lineage-negative progenitors mobilize to regenerate lung epithelium after major injury.* Nature, 2015. **517**(7536): p. 621-5.

117. Holt, P.G., et al., *Regulation of immunological homeostasis in the respiratory tract.* Nat Rev Immunol, 2008. **8**(2): p. 142-52.

118. Iwasaki, A., E.F. Foxman, and R.D. Molony, *Early local immune defences in the respiratory tract.* Nat Rev Immunol, 2017. **17**(1): p. 7-20.

119. Brown, D.M., et al., *Multifunctional CD4 cells expressing gamma interferon and perforin mediate protection against lethal influenza virus infection.* J Virol, 2012. **86**(12): p. 6792-803.

120. Bautista, B.L., et al., *Short-Lived Antigen Recognition but Not Viral Infection at a Defined Checkpoint Programs Effector CD4 T Cells To Become Protective Memory.* J Immunol, 2016. **197**(10): p. 3936-3949.

121. Hufford, M.M., et al., *The effector T cell response to influenza infection.* Curr Top Microbiol Immunol, 2015. **386**: p. 423-55.

122. Hufford, M.M., et al., *Antiviral CD8+ T cell effector activities in situ are regulated by target cell type.* J Exp Med, 2011. **208**(1): p. 167-80.

123. Lawrence, C.W., R.M. Ream, and T.J. Braciale, *Frequency, specificity, and sites of expansion of CD8+ T cells during primary pulmonary influenza virus infection.* J Immunol, 2005. **174**(9): p. 5332-40.

124. McKinstry, K.K., et al., *Effector CD4 T-cell transition to memory requires late cognate interactions that induce autocrine IL-2.* Nat Commun, 2014. **5**: p. 5377.

125. McGill, J., N. Van Rooijen, and K.L. Legge, *Protective influenza-specific CD8 T cell responses require interactions with dendritic cells in the lungs.* J Exp Med, 2008. **205**(7): p. 1635-46.

126. Damjanovic, D., et al., *Immunopathology in influenza virus infection: uncoupling the friend from foe.* Clin Immunol, 2012. **144**(1): p. 57-69.

127. Wright, J.R., *Immunoregulatory functions of surfactant proteins.* Nat Rev Immunol, 2005. **5**(1): p. 58-68.

128. Singh, G., et al., *Pulmonary lysozyme--a secretory protein of type II pneumocytes in the rat.* Am Rev Respir Dis, 1988. **138**(5): p. 1261-7.

129. Strunk, R.C., D.M. Eidlen, and R.J. Mason, *Pulmonary alveolar type II epithelial cells synthesize and secrete proteins of the classical and alternative complement pathways.* J Clin Invest, 1988. **81**(5): p. 1419-26.

130. Stegemann-Koniszewski, S., et al., *Alveolar Type II Epithelial Cells Contribute to the Anti-Influenza A Virus Response in the Lung by Integrating Pathogen- and Microenvironment-Derived Signals.* MBio, 2016. **7**(3).

131. Armstrong, L., et al., *Expression of functional toll-like receptor-2 and -4 on alveolar epithelial cells.* Am J Respir Cell Mol Biol, 2004. **31**(2): p. 241-5.

132. Ito, Y., et al., *Influenza induces IL-8 and GM-CSF secretion by human alveolar epithelial cells through HGF/c-Met and TGF-alpha/EGFR signaling.* Am J Physiol Lung Cell Mol Physiol, 2015. **308**(11): p. L1178-88.

133. Blau, H., et al., *Secretion of cytokines by rat alveolar epithelial cells: possible regulatory role for SP-A.* Am J Physiol, 1994. **266**(2 Pt 1): p. L148-55.

134. Finkelstein, J.N., et al., *Particulate-cell interactions and pulmonary cytokine expression.* Environ Health Perspect, 1997. **105 Suppl 5**: p. 1179-82.

135. Wallace, W.A. and S.E. Howie, *Immunoreactive interleukin 4 and interferon-gamma expression by type II alveolar epithelial cells in interstitial lung disease.* J Pathol, 1999. **187**(4): p. 475-80.

136. Yu, W.C., et al., *Viral replication and innate host responses in primary human alveolar epithelial cells and alveolar macrophages infected with influenza H5N1 and H1N1 viruses.* J Virol, 2011. **85**(14): p. 6844-55.

137. Harbeck, R.J., et al., *Class II molecules on rat alveolar type II epithelial cells.* Cell Immunol, 1988. **111**(1): p. 139-47.

138. Glanville, A.R., et al., *The distribution of MHC class I and II antigens on bronchial epithelium.* Am Rev Respir Dis, 1989. **139**(2): p. 330-4.

139. Cunningham, A.C., et al., *Constitutive expression of MHC and adhesion molecules by alveolar epithelial cells (type II pneumocytes) isolated from human lung and comparison with immunocytochemical findings.* J Cell Sci, 1994. **107 (Pt 2)**: p. 443-9.

140. Peters, U., T. Papadopoulos, and H.K. Muller-Hermelink, *MHC class II antigens on lung epithelial of human fetuses and neonates. Ontogeny and expression in lungs with histologic evidence of infection.* Lab Invest, 1990. **63**(1): p. 38-43.

141. Steiniger, B. and E. Sickel, *Class II MHC molecules and monocytes/macrophages in the respiratory system of conventional, germ-free and interferon-gamma-treated rats.* Immunobiology, 1992. **184**(4-5): p. 295-310.

142. Wosen, J.E., et al., *Epithelial MHC Class II Expression and Its Role in Antigen Presentation in the Gastrointestinal and Respiratory Tracts.* Front Immunol, 2018. **9**: p. 2144.

143. Barkauskas, C.E., et al., *Type 2 alveolar cells are stem cells in adult lung.* J Clin Invest, 2013. **123**(7): p. 3025-36.

144. Beers, M.F. and Y. Moodley, *When Is an Alveolar Type 2 Cell an Alveolar Type 2 Cell? A Conundrum for Lung Stem Cell Biology and Regenerative Medicine.* Am J Respir Cell Mol Biol, 2017. **57**(1): p. 18-27.

145. Gonzalez, R.F., et al., *HTII-280, a biomarker specific to the apical plasma membrane of human lung alveolar type II cells.* J Histochem Cytochem, 2010. **58**(10): p. 891-901.

146. Waldburger, J.M., et al., *Selective abrogation of major histocompatibility complex class II expression on extrahematopoietic cells in mice lacking promoter IV of the class II transactivator gene.* J Exp Med, 2001. **194**(4): p. 393-406.

147. Neefjes, J., et al., *Towards a systems understanding of MHC class I and MHC class II antigen presentation.* Nat Rev Immunol, 2011. **11**(12): p. 823-36.

148. Ma, J.Z., et al., *Unique Transcriptional Architecture in Airway Epithelial Cells and Macrophages Shapes Distinct Responses following Influenza Virus Infection Ex Vivo.* J Virol, 2019. **93**(6).

149. Walter, W., et al., *H2-Mbeta 1 and H2-Mbeta 2 heterodimers equally promote clip removal in I-A(q) molecules from autoimmune-prone DBA/1 mice.* J Biol Chem, 2001. **276**(14): p. 11086-91.

150. Walter, W., et al., *MHC class II antigen presentation pathway in murine tumours: tumour evasion from immunosurveillance?* Br J Cancer, 2000. **83**(9): p. 1192-201.

151. Dubey, C., M. Croft, and S.L. Swain, *Naive and effector CD4 T cells differ in their requirements for T cell receptor versus costimulatory signals.* J Immunol, 1996. **157**(8): p. 3280-9.

152. Cose, S., et al., *Evidence that a significant number of naive T cells enter non-lymphoid organs as part of a normal migratory pathway.* Eur J Immunol, 2006. **36**(6): p. 1423-33.

153. Heng, T.S., M.W. Painter, and C. Immunological Genome Project, *The Immunological Genome Project: networks of gene expression in immune cells.* Nat Immunol, 2008. **9**(10): p. 1091-4.

154. Alvaro-Benito, M., et al., *Distinct editing functions of natural HLA-DM allotypes impact antigen presentation and CD4(+) T cell activation.* Cell Mol Immunol, 2018.

155. Alvaro-Benito, M., et al., *Human leukocyte Antigen-DM polymorphisms in autoimmune diseases.* Open Biol, 2016. **6**(8).

156. Andrews, L.P., et al., *LAG3 (CD223) as a cancer immunotherapy target.* Immunol Rev, 2017. **276**(1): p. 80-96.

157. Chapman, H.A., et al., *Integrin alpha6beta4 identifies an adult distal lung epithelial population with regenerative potential in mice.* J Clin Invest, 2011. **121**(7): p. 2855-62.

158. Hashimoto, K., S.K. Joshi, and P.A. Koni, *A conditional null allele of the major histocompatibility IA-beta chain gene.* Genesis, 2002. **32**(2): p. 152-3.

159. Zens, K.D., et al., *Reduced generation of lung tissue-resident memory T cells during infancy.* J Exp Med, 2017. **214**(10): p. 2915-2932.

160. Strutt, T.M., et al., *Memory CD4+ T-cell-mediated protection depends on secondary effectors that are distinct from and superior to primary effectors.* Proc Natl Acad Sci U S A, 2012. **109**(38): p. E2551-60.

161. Workman, C.J., et al., *Lymphocyte activation gene-3 (CD223) regulates the size of the expanding T cell population following antigen activation in vivo.* J Immunol, 2004. **172**(9): p. 5450-5.

162. Shedlock, D.J. and H. Shen, *Requirement for CD4 T cell help in generating functional CD8 T cell memory.* Science, 2003. **300**(5617): p. 337-9.

163. Sun, J.C. and M.J. Bevan, *Defective CD8 T cell memory following acute infection without CD4 T cell help.* Science, 2003. **300**(5617): p. 339-42.

164. Laidlaw, B.J., et al., *CD4+ T cell help guides formation of CD103+ lung-resident memory CD8+ T cells during influenza viral infection.* Immunity, 2014. **41**(4): p. 633-45.

165. Eichelberger, M., et al., *Clearance of influenza virus respiratory infection in mice lacking class I major histocompatibility complex-restricted CD8+ T cells.* J Exp Med, 1991. **174**(4): p. 875-80.

166. Hou, S., et al., *Delayed clearance of Sendai virus in mice lacking class I MHC-restricted CD8+ T cells.* J Immunol, 1992. **149**(4): p. 1319-25.

167. Topham, D.J., et al., *Immune CD4+ T cells promote the clearance of influenza virus from major histocompatibility complex class II -/- respiratory epithelium.* J Virol, 1996. **70**(2): p. 1288-91.

168. Bodmer, H., et al., *Environmental modulation of the autonomy of cytotoxic T lymphocytes.* Eur J Immunol, 1993. **23**(7): p. 1649-54.

169. Tripp, R.A., S.R. Sarawar, and P.C. Doherty, *Characteristics of the influenza virus-specific CD8+ T cell response in mice homozygous for disruption of the H-2lAb gene.* J Immunol, 1995. **155**(6): p. 2955-9.

170. Allan, W., et al., *Cellular events in the lymph node and lung of mice with influenza. Consequences of depleting CD4+ T cells.* J Immunol, 1990. **144**(10): p. 3980-6.

171. Hou, S., et al., *Host response to Sendai virus in mice lacking class II major histocompatibility complex glycoproteins.* J Virol, 1995. **69**(3): p. 1429-34.

172. Crowe, C.R., et al., *Critical role of IL-17RA in immunopathology of influenza infection.* J Immunol, 2009. **183**(8): p. 5301-10.

173. Dial, C.F., et al., *Foxp3(+) Regulatory T Cell Expression of Keratinocyte Growth Factor Enhances Lung Epithelial Proliferation.* Am J Respir Cell Mol Biol, 2017. **57**(2): p. 162-173.

174. Mock, J.R., et al., *Foxp3+ regulatory T cells promote lung epithelial proliferation.* Mucosal Immunol, 2014. **7**(6): p. 1440-51.

175. Kudo, E., et al., *Low ambient humidity impairs barrier function and innate resistance against influenza infection.* Proc Natl Acad Sci U S A, 2019. **116**(22): p. 10905-10910.

176. Dickson, R.P., et al., *The Lung Microbiota of Healthy Mice Are Highly Variable, Cluster by Environment, and Reflect Variation in Baseline Lung Innate Immunity.* Am J Respir Crit Care Med, 2018. **198**(4): p. 497-508.

177. Rosshart, S.P., et al., *Wild Mouse Gut Microbiota Promotes Host Fitness and Improves Disease Resistance.* Cell, 2017. **171**(5): p. 1015-1028 e13.

178. Tewari, M.K., et al., *A cytosolic pathway for MHC class II-restricted antigen processing that is proteasome and TAP dependent.* Nat Immunol, 2005. **6**(3): p. 287-94.

179. Dobbs, L.G., *Isolation and culture of alveolar type II cells.* Am J Physiol, 1990. **258**(4 Pt 1): p. L134-47.

180. Dobbs, L.G., et al., *Maintenance of the differentiated type II cell phenotype by culture with an apical air surface.* Am J Physiol, 1997. **273**(2 Pt 1): p. L347-54.

181. Murphy, D.B., et al., *A novel MHC class II epitope expressed in thymic medulla but not cortex.* Nature, 1989. **338**(6218): p. 765-8.

182. Weinheimer, V.K., et al., *Influenza A viruses target type II pneumocytes in the human lung.* J Infect Dis, 2012. **206**(11): p. 1685-94.

183. Rockx, B., et al., *Comparative pathogenesis of COVID-19, MERS, and SARS in a nonhuman primate model.* Science, 2020. **368**(6494): p. 1012-1015.

184. Brasch, F., et al., *Involvement of cathepsin H in the processing of the hydrophobic surfactant-associated protein C in type II pneumocytes.* Am J Respir Cell Mol Biol, 2002. **26**(6): p. 659-70.

185. Hsieh, C.S., et al., *A role for cathepsin L and cathepsin S in peptide generation for MHC class II presentation.* J Immunol, 2002. **168**(6): p. 2618-25.

186. Watts, C., et al., *Roles for asparagine endopeptidase in class II MHC-restricted antigen processing.* Biochem Soc Symp, 2003(70): p. 31-8.

187. Manoury, B., et al., *Asparagine endopeptidase can initiate the removal of the MHC class II invariant chain chaperone.* Immunity, 2003. **18**(4): p. 489-98.

188. Maric, M., et al., *Defective antigen processing in GILT-free mice.* Science, 2001. **294**(5545): p. 1361-5.

189. Hastings, K.T., *GILT: Shaping the MHC Class II-Restricted Peptidome and CD4(+) T Cell-Mediated Immunity.* Front Immunol, 2013. **4**: p. 429.

190. Schroder, B., *The multifaceted roles of the invariant chain CD74--More than just a chaperone.* Biochim Biophys Acta, 2016. **1863**(6 Pt A): p. 1269-81.

191. Marsh, L.M., et al., *Surface expression of CD74 by type II alveolar epithelial cells: a potential mechanism for macrophage migration inhibitory factor-induced epithelial repair.* Am J Physiol Lung Cell Mol Physiol, 2009. **296**(3): p. L442-52.

192. Gil-Yarom, N., et al., *CD74 is a novel transcription regulator.* Proc Natl Acad Sci U S A, 2017. **114**(3): p. 562-567.

193. Yun, Y., et al., *Environmentally determined differences in the murine lung microbiota and their relation to alveolar architecture.* PLoS One, 2014. **9**(12): p. e113466.

194. Abolins, S., et al., *The comparative immunology of wild and laboratory mice, Mus musculus domesticus.* Nat Commun, 2017. **8**: p. 14811.

195. Rosshart, S.P., et al., *Laboratory mice born to wild mice have natural microbiota and model human immune responses.* Science, 2019. **365**(6452).

196. Belz, G.T., et al., *Compromised Influenza Virus-Specific CD8+-T-Cell Memory in CD4+-T-Cell-Deficient Mice.* Journal of Virology, 2002. **76**(23): p. 12388-12393.

197. Sangster, M.Y., et al., *An early CD4+ T cell-dependent immunoglobulin A response to influenza infection in the absence of key cognate T-B interactions.* J Exp Med, 2003. **198**(7): p. 1011-21.

198. Wilkinson, T.M., et al., *Preexisting influenza-specific CD4+ T cells correlate with disease protection against influenza challenge in humans.* Nat Med, 2012. **18**(2): p. 274-80.

199. Devarajan, P., et al., *New Insights into the Generation of CD4 Memory May Shape Future Vaccine Strategies for Influenza.* Front Immunol, 2016. **7**: p. 136.

200. Chiu, C. and P.J. Openshaw, *Antiviral B cell and T cell immunity in the lungs.* Nat Immunol, 2015. **16**(1): p. 18-26.

201. Ogongo, P., J.Z. Porterfield, and A. Leslie, *Lung Tissue Resident Memory T-Cells in the Immune Response to Mycobacterium tuberculosis.* Front Immunol, 2019. **10**: p. 992.

202. Schreiner, D. and C.G. King, *CD4+ Memory T Cells at Home in the Tissue: Mechanisms for Health and Disease.* Front Immunol, 2018. **9**: p. 2394.

203. Teijaro, J.R., et al., *Cutting edge: Tissue-retentive lung memory CD4 T cells mediate optimal protection to respiratory virus infection.* J Immunol, 2011. **187**(11): p. 5510-4.

204. Lambrecht, B.N. and H. Hammad, *The immunology of asthma.* Nat Immunol, 2015. **16**(1): p. 45-56.

205. Riario Sforza, G.G. and A. Marinou, *Hypersensitivity pneumonitis: a complex lung disease.* Clin Mol Allergy, 2017. **15**: p. 6.

206. Selman, M., A. Pardo, and T.E. King, Jr., *Hypersensitivity pneumonitis: insights in diagnosis and pathobiology.* Am J Respir Crit Care Med, 2012. **186**(4): p. 314-24.

207. Simonian, P.L., et al., *Th17-polarized immune response in a murine model of hypersensitivity pneumonitis and lung fibrosis.* J Immunol, 2009. **182**(1): p. 657-65.

208. Meuwissen, R. and A. Berns, *Mouse models for human lung cancer.* Genes Dev, 2005. **19**(6): p. 643-64.

209. Srivastava, B., et al., *Host genetic background strongly influences the response to influenza a virus infections.* PLoS One, 2009. **4**(3): p. e4857.

210. De Albuquerque, N., et al., *Murine hepatitis virus strain 1 produces a clinically relevant model of severe acute respiratory syndrome in A/J mice.* J Virol, 2006. **80**(21): p. 10382-94.

211. Sellers, R.S., et al., *Immunological variation between inbred laboratory mouse strains: points to consider in phenotyping genetically immunomodified mice.* Vet Pathol, 2012. **49**(1): p. 32-43.

212. Zou, X., et al., *Single-cell RNA-seq data analysis on the receptor ACE2 expression reveals the potential risk of different human organs vulnerable to 2019-nCoV infection.* Front Med, 2020. **14**(2): p. 185-192.

213. Sungnak, W., et al., *SARS-CoV-2 entry factors are highly expressed in nasal epithelial cells together with innate immune genes.* Nat Med, 2020. **26**(5): p. 681-687.

214. Ziegler, C.G.K., et al., *SARS-CoV-2 Receptor ACE2 Is an Interferon-Stimulated Gene in Human Airway Epithelial Cells and Is Detected in Specific Cell Subsets across Tissues.* Cell, 2020. **181**(5): p. 1016-1035 e19.

215. Krausgruber, T., et al., *Structural cells are key regulators of organ-specific immune responses.* Nature, 2020. **583**(7815): p. 296-302.

216. Nowarski, R., R. Jackson, and R.A. Flavell, *The Stromal Intervention: Regulation of Immunity and Inflammation at the Epithelial-Mesenchymal Barrier.* Cell, 2017. **168**(3): p. 362-375.

217. Madsen, L., et al., *Mice lacking all conventional MHC class II genes.* Proc Natl Acad Sci U S A, 1999. **96**(18): p. 10338-43.

218. Dalton, D.K., et al., *Multiple defects of immune cell function in mice with disrupted interferon-gamma genes.* Science, 1993. **259**(5102): p. 1739-42.

219. Durbin, J.E., et al., *Targeted disruption of the mouse Stat1 gene results in compromised innate immunity to viral disease.* Cell, 1996. **84**(3): p. 443-50.

220. Fikrig, E., et al., *Protective antibodies develop, and murine Lyme arthritis regresses, in the absence of MHC class II and CD4+ T cells.* J Immunol, 1997. **159**(11): p. 5682-6.

221. Huang, S., et al., *Immune response in mice that lack the interferon-gamma receptor.* Science, 1993. **259**(5102): p. 1742-5.

222. Prigge, J.R., et al., *Type I IFNs Act upon Hematopoietic Progenitors To Protect and Maintain Hematopoiesis during Pneumocystis Lung Infection in Mice.* J Immunol, 2015. **195**(11): p. 5347-57.

223. Hou, B., B. Reizis, and A.L. DeFranco, *Toll-like receptors activate innate and adaptive immunity by using dendritic cell-intrinsic and -extrinsic mechanisms.* Immunity, 2008. **29**(2): p. 272-82.

224. Kaplan, M.H., et al., *Stat6 Is Required for Mediating Responses to IL-4 and for the Development of Th2 Cells.* Immunity, 1996. **4**(3): p. 313-319.

225. Sinnathamby, G., et al., *Differential requirements for endosomal reduction in the presentation of two H2-E(d)-restricted epitopes from influenza hemagglutinin.* J Immunol, 2004. **172**(11): p. 6607-14.

226. Zacharias, W. and E. Morrisey, *Isolation and culture of human alveolar epithelial progenitor cells.* Protocol Exchange, 2018.

227. Denzin, L.K., et al., *Neutralizing Antibody Responses to Viral Infections Are Linked to the Non-classical MHC Class II Gene H2-Ob.* Immunity, 2017. **47**(2): p. 310-322 e7.

228. Wohn, C., et al., *Absence of MHC class II on cDC1 dendritic cells triggers fatal autoimmunity to a cross-presented self-antigen.* Sci Immunol, 2020. **5**(45).

229. Mundt, S., et al., *Conventional DCs sample and present myelin antigens in the healthy CNS and allow parenchymal T cell entry to initiate neuroinflammation.* Sci Immunol, 2019. **4**(31).